# VARIATION IN THERMAL SENSITIVITY AMONG CORAL GENOTYPES, SPECIES, AND HABITATS: IMPLICATIONS FOR IMPROVED RESTORATION

Katelyn J. Gould

A dissertation submitted to the faculty at the University of North Carolina at Chapel Hill in partial fulfillment of the requirements for the degree of Doctor of Philosophy in the Evolution, Ecology, and Organismal Biology program in the department of Biology in the College of Arts and Sciences.

Chapel Hill
2023

Approved by:

John F. Bruno

Karl D. Castillo

Gretchen Goodbody-Gringley

Joel G. Kingsolver

Kenneth J. Lohmann

## ABSTRACT

Katelyn J. Gould: Characterizing Thermal Influences on Metabolism: Impacts on Coral Restoration and Resilience in a Changing World
(Under the direction of John F. Bruno)

Global climate change has rapidly altered marine systems, resulting in negative impacts on tropical reef-building corals around the globe. As the leading driver of coral bleaching, ocean warming disrupts the mutualistic relationship between reef-building corals and their algal symbionts (*Symbiodinaceae*) in a process known as coral bleaching. During periods of elevated sea temperatures corals expel their symbionts causing declines in metabolic and physiological function. Mass bleaching events deteriorate coral reefs, reducing the ecosystem services they provide including foundational habitat which host 32 of 34 recognized marine phyla of the ocean's biodiversity, impacts on reef fisheries, physically protecting coasts from storms by reducing erosion, and elevates economic income of coastal communities. To reduce the impacts of warming, conservationists are attempting to protect and revitalize these systems by identifying resilient reefs. The goal is then to enhance coral abundance and preserve coral genetic variation with coral farming, and related restoration efforts. These activities are relatively new and identifying resilient corals and refining coral restoration techniques are only just beginning. Identifying how different coral species respond to restoration activities and their responses to temperature in general is critical in understanding coral persistence in the future.

This dissertation examines the effect temperature has on coral survival, metabolism, and physiology from three conservation perspectives to enhance restoration methodologies in Caribbean and north Atlantic coral ecosystems. In Chapter 1, I identified a potential thermal

refuge habitat in Bermuda by comparing thermal tolerance, optima, and sensitivities of four coral species from shallow and upper-mesophotic reef habitats. In Chapter 2, I used metabolic thermal performance curves (respiration and gross photosynthesis) to assess the effectiveness of stress-mediating interventions to alter thermal performance during heat stress, for use in coral farming. The results from this work highlight how variation in genotypes can influence metabolic and physiological responses (*Acropora cervicornis*) to thermal stress. In Chapter 3, I showed how genotypic variation (*Orbicella annularis*), and environmental interactions are necessary in planning and understanding the success of coral restoration across environmental gradients. Overall, investigating how corals respond to temperature stress and restoration methodologies are important in predicting the future persistence of corals and identifying successful procedures to enhance coral conservation.

To Lyndie Gould (aka Minty) for being the most supportive sister and hype-woman anyone could ask for and to my lovie, Julie Koenig and our future sailing adventures.

## ACKNOWLEDGEMENTS

I could never have arrived here without the love and support of so many people. Thank you, John Bruno for being the most welcoming, understanding, and encouraging advisor. You made me feel more like a colleague than a student. You recognized and respected my learning style, and you were there for me as a friend and mentor when I was overwhelmed with theory and statistics. Thank you, Colleen Bove, I can't say enough good things about you, you are truly an amazing person, genius R statistician, and a wonderful friend, thank you. Gretchen Goodbody-Gingley, you are what I hope to be like when I grow up. Additionally, thank you to my committee member Karl Castillo for hosting me in your marine science laboratory and letting me take it over for a full semester.

To all my colleagues and friends who have helped me on this scientific journey, starting at Chris Martin's lab, you all have helped shape me into the scientist I am today. Michelle St. John and Emily Richards, I wish we could have seen it through together in the same place, but I am so proud of you and thankful to you both. To Joe Mcgirr and Bryan Reatini my first grad school roommates, you both were always there for me, and always made it fun (TEN!). To my amazing lab mates, Esteban Agudo, Savannah Ryburn, Isa Silva Romero, Haley Capone, and Salomé Jaramillo Gil, you make coming into school worth it. To the Affectionates who made NC my music home. To my family who love to remind my dad who the real doctor is now. And finally, to Julie for being my foundation and making me laugh every single day and always down for the next adventure.  I wouldn't be here without y'all.

## TABLE OF CONTENTS

## LIST OF TABLES

## LIST OF FIGURES

## LIST OF ABBREVIATIONS

| | |
|---|---|
| ACER | *Acropora cervicornis* |
| AGRRA | Atlantic and Gulf Rapid Reef Assessment |
| AIC | Akaike's information criterion |
| BCA | Bicinchoninic Acid |
| BIOS | Bermuda Institute of Ocean Science |
| ℃ | Degrees Celsius |
| CISME | Community *In Situ* MEtabolism |
| CPH | Cox Proportional Hazard |
| CREMP | Coral Reef Evaluation and Monitoring Program |
| CRF | Coral Restoration Foundation |
| $CT_{max}$ | Thermal maximum |
| $CT_{min}$ | Thermal minimum |
| DO | Dissolved oxygen |
| $E$ | Activation energy |
| $Eh$ | Deactivation energy |
| eV | Electron volt |
| FGBNMS | Flower Garden Banks National Marine Sanctuary |
| FKNMS | Florida Keys National Marine Sanctuary |
| FRT | Florida Reef Tract |
| FSW | Filtered salt water |
| GLM | Generalized linear models |
| $GP$ | Gross photosynthesis |
| GxE | Genotype by environmental interaction |
| HR | Hazard Ratio |
| $I_k$ | Saturating irradiance |
| Kd | Diffuse Attenuation Coefficient |
| LED | Light-emitting diode |

| | |
|---|---|
| *lnc* | Average performance |
| MCEs | Mesophotic Coral Ecosystems |
| MHWs | Marine heat waves |
| MMM | Mean monthly maximum |
| *NP* | Net photosynthesis |
| OANN | *Orbicella annularis* |
| P:R | Photosynthesis Respiration ratio |
| PAR | Photosynthetically active radiation |
| PCA | Principal Component Analysis |
| PI | Photosynthesis irradiance |
| $P_{max}$ | Performance maximum |
| *R* | Respiration |
| SD | Standard deviation |
| SE | Standard error |
| SERC | Southeast Environmental Research Center |
| SNP | Single Nucleotide Polymorphism |
| spp. | Species |
| $T_{br}$ | Thermal breadth |
| *Th* | Enzyme deactivation temperature |
| TN | Total nitrogen |
| TN:TP | Total nitrogen total phosphorus ratios |
| TOC | Total organic carbon |
| $T_{opt}$ | Thermal optimum |
| TP | Total phosphorus |
| TPC | Thermal performance curve |
| µmol | micromole |

# INTRODUCTION

While coral reefs are one of the most diverse marine ecosystems and provide innumerable services to millions globally, they are under threat of collapse due to stressors caused by anthropogenic activities (Gil et al., 2020; Kennedy et al., 2013; Sweet & Brown, 2016). Despite a myriad of perturbations (pollution, overfishing, destructive tourism, disease, sedimentation, ocean acidification, and tropical storms), ocean warming and associated marine heat waves (MHWs) are the primary drivers of coral loss (Alves et al., 2022; Aronson & Precht, 2006; Gardner et al., 2003; Manzello, 2015; van Woesik & Kratochwill, 2022). The continued accumulation of greenhouse gases is projected to result in annual bleaching events globally by 2050 (Board, 2019).

Ocean warming is a significant concern for marine organisms, especially reef-building corals as they currently live within a degree of their thermal maxima (Jokiel & Coles, 1977; Kleypas et al., 1999). When exposed to temperatures above its thermal threshold, the symbiosis between corals and their endosymbiotic algae (*Symbiodiniaceae*) breaks down in a process called coral bleaching (Glynn, 1991; Brown, 1997). Coral reefs are a dynamic ecosystem and have an inherent capacity to resist and recover from disturbances. Yet, the frequency, intensity, and severity of mass bleaching events are increasing, and recovery time between events is declining (Cheal et al., 2017; Emanuel, 2005; Gouezo et al., 2019; Montefalcone et al., 2018; Oliver et al., 2018). The impacts to and responses of coral ecosystems from ocean warming are highly variable and contingent on species and location (Hoegh-Guldberg, 1999; Tanzil et al., 2013).

Adaptation to warming has been documented in corals (Bairos-Novak et al., 2021; Coles et al., 2018; Padilla-Gamiño et al., 2019; Smith et al., 2022), however, the rate of adaptation needed to prevent global extinction would need to average ~0.2–0.3℃ each decade and in some regions a rate of 0.5–1.0℃ is required (Bay et al., 2017; Császár et al., 2010; Donner et al., 2005). Due to decadal generation times in corals, a population-level recovery driven by thermal selection would take centuries. The capacity for corals to attain this rate of adaptation and/or acclimatization potential is unknown (Hoegh-Guldberg, 1999; Smith et al., 2022).

The most recent global bleaching analyses by van Woesik and Kratochwill (2022) reports thermal stress events are increasing in frequency and intensity. Rising ocean temperatures can no longer be disregarded as non-causal, but a precise understanding of coral susceptibility and their responses to warming is crucial. Coral bleaching has been documented across the globe since the 1982–83 El Niño warming event (Glynn, 1984). By using thermal performance curves (TPC), which quantify physiological and metabolic function over a range of temperatures, we can predict coral bleaching thresholds under shifting thermal conditions (Angilletta, 2009). Only recently has the use of thermal performance curves in corals gained popularity in the field however (Aichelman et al., 2019; Anton et al., 2020; Becker et al., 2021; Castillo et al., 2014; Gould et al., 2021; Jiang et al., 2021; Jurriaans & Hoogenboom 2019; Jurriaans & Hoogenboom 2020; Jurriaans & Hoogenboom 2021; Rodolfo-Metalpa et al., 2014; Silbiger et al., 2019).

The mounting threats to coral survival have driven increased application of interventions that in theory could enhance resilience[1], persistence, genetic preservation, and restores structural complexity and ecosystem function (Anthony et al., 2017; Schmidt-Roach et al., 2020; van

[1]**Resilience**: The ability to survive and/or tolerate stress and if impacted by these stressors, corals capacity to recover from that stress event

Oppen et al., 2017). Active interventions such as restoration practices are aimed at protecting biodiversity, increasing rare and endangered species population sizes (e.g., *Acropora cervicornis, Acropora palmata*), and growing environmental stewardship and community involvement in the short-term while climate change mitigation takes effect. Despite the numerous organizations and ongoing restoration projects globally, many are inadequately designed and do not integrate science-based knowledge and/or research that can inform local decision-making, which will ultimately determine the failure or success of projects (Boström-Einarsson et al., 2020). Passive interventions, such as instating marine protected areas (MPAs), aim to protect habitats by limiting tourism and restoring fishing communities, thereby reducing fishing pressures and in turn positively influencing coral reef community structure (Agardy, 1994; Kelleher, 1999). The establishment of MPAs however, does not lessen the effects of ocean warming on declining coral cover and by extension community function (Aronson & Precht, 2006; Bruno et al., 2019; Cox et al., 2017; Selig et al., 2010; Selig et al., 2012). For example, Bates et al. (2019) assessed the role of MPAs in increasing thermal resilience in marine ecosystems and found that current protection from MPAs is insufficient at mitigating climate change.

A hallmark of coral bleaching is the striking variability in bleaching susceptibility among locations, habitat types, species, and individual colonies (van Woesik & Kratochwill, 2022). The goal of my dissertation is to take advantage of this variation to improve the protection and restoration of reef-building corals. Using a variety of approaches to address the disconnect between restoration practices with limited understanding of coral thermal sensitivities, this work emphasizes identifying species, genotypes, and/or individuals for these activities with a greater capacity to resist thermal stress and acclimate to local environments and associated temperature increases. In Chapter 1, I characterize respiration and gross photosynthesis TPCs across four

species to compare thermally unique reef corals to identify a potential refuge environment in Bermuda. Chapter 2 quantifies TPCs for three genotypes from an active coral restoration organization (Coral Restoration Foundation, CRF) under stress-mitigation interventions in an 82-day mesocosom experiment to test the efficacy of these interventions. Additionally, assessing multiple genotypes allows for identification of stress tolerant genotypes, which can aid in restoration efforts at thermally variable reef sites. Chapter 3 evaluates restoration success in a framework building coral species currently used in restoration (CRF) to identify genotypes that outperform others at specific reef sites across an environmental gradient in the Florida Reef Tract (FRT). This research will allow the CRF to rapidly adapt my findings into their methodologies to ensure their approaches consider local environmental conditions and corals' physiological response limits within the wider context of ocean warming.

My findings will expand the scope of current restoration practices and enhance our understanding of techniques that promote coral resilience and persistence when mitigated by human intervention. My work can be directly applied to the CRF's current restoration strategies by focusing on propagating and transplanting the thermally tolerant genotypes I identified. My research can lead to future work improving intervention techniques and implementing them locally *in situ,* including targeted restoration efforts on site. This will enable coral conservationists to initiate a more comprehensive science-driven approach to current restoration methodologies to enhance coral thermal resilience, persistence, community structure and ecosystem function.

# CHAPTER 1: UPPER-MESOPHOTIC AND SHALLOW REEF CORALS EXHIBIT SIMILAR THERMAL TOLERANCE, SENSITIVITY, AND OPTIMA

## Introduction

Metabolic rates of ectotherms are driven by their internal body temperatures and determined by the thermal environment they inhabit. Marine ectotherms become vulnerable to external conditions when temperatures increase above their localized thermal thresholds (Huey & Kingsolver, 2019). Ocean warming results in decreased rates of biological processes such as enzymatic functioning, whole organism metabolism, reproduction, and behavior, which vary across individuals and populations. Measuring biological rates over a range of temperatures enables researchers to compare thermal sensitivities of individuals and populations among locations and across environmentally heterogenous landscapes or seascapes (Angilletta, 2009). Differences in thermal ranges and sensitivities among habitats can be caused in part by local adaptation/ acclimatization (Angilletta, 2009), phenotypic plasticity (Sawall et al., 2015), and/or inherited thermal tolerance through epigenetics (Dixon et al., 2015). Evolutionary thermal biology predicts that individuals in colder environments should have lower thermal optimum ($T_{opt}$) and thermal performance maximums ($P_{max}$), and higher sensitivities ($E$ & $Eh$) when compared to individuals in warmer environments (Angilletta et al., 2006; Schult et al., 2011). As a notable example, Silbiger et al. (2019) found evidence of local adaptation and/or acclimatization in the coral *Orbicella franksi*, where corals from cooler Bermuda sites had lower

performance rates and optimal temperature requirements compared to their warm-water conspecifics in Panama.

Shallow water corals live at or close to their thermal maximum and an increase in seawater temperature of 1℃ can result in large-scale bleaching and mortality (Sheppard et al., 2020). Globally, approximately 30% of coral reefs are categorized as severely damaged, while 50−75% of live coral cover has declined in the last 30−40 years (Schutte et al., 2010; De'ath et al., 2012; Jackson et al., 2014; Precht et al., 2020). In the Caribbean, shallow coral reef systems have been disproportionately impacted by anthropogenic stressors, leading to substantial decline in living coral cover, e.g., from ~50% to ~10% from 1977 to 2001 (Gardner et al., 2003; Precht et al., 2020) and from ~33% prior to 1984 to ~16% in 2006 (Bruno & Selig, 2007; Bruno et al., 2009; Schutte et al., 2010). Impacts to corals are expected to escalate as exposure to thermal stress continues to increase annually (Muñiz-Castillo et al., 2019).

Mesophotic Coral Ecosystems (MCEs), generally found between depths of 30−100m may be buffered from anthropogenic and natural stressors compared to shallower reefs in some regions (Lesser et al., 2009; Bongaerts et al., 2010; Kahng et al., 2014; Holstein et al., 2016; Prasetia et al., 2017; Kahng et al., 2016; Frade et al., 2018; Pinheiro et al., 2019). MCEs are characterized as light-dependent communities in subtropical and tropical waters beginning at 30m and can extend to the depth at which photosynthesis can no longer be sustained (~150m) (Hinderstein et al., 2010; Lesser et al., 2009; Loya et al., 2016). Laverick et al. (2020) defines the upper-mesophotic zone as lying between ~36−62m based on preferred light conditions of shallow and mesophotic corals. Many species of scleractinian corals have a broad depth distribution ranging from shallow to mesophotic depths. For example, Carpenter et al. (2008) found that out of the 845 species of corals globally, 704 were assigned conservation status and

40% of those threatened are found within the first 20m, while the remaining 60% survive at depths greater than 20m. Kramer et al. (2020) found corals across 14 families and 45 genera were more abundant in mesophotic (55.6%) compared to shallow depths (44.4%), in the Gulf of Eilat/Aqaba.

Due to relative proximity to the surface and the coastline, it has been suggested that thermal anomalies, bleaching, disease, pollution, and storms may have greater impacts to shallow reefs compared to MCEs (West & Salm, 2003; Lesser et al., 2009; Kahng et al., 2012; Kahng et al., 2016). For example, shallow reef temperatures are driven by atmospheric thermal dynamics and wind, and due to their depth can experience aggressive heat accumulation leading to water stratification. Once stratified, mixing of thermal layers can occur via internal waves, upwelling, or high winds, however this depends on the stratification depth, tidal forcing, and reef-slope angle (Wyatt et al., 2019). Heat accumulation with a high residence time (average time reef is exposed to heat) can trigger extreme thermal anomalies leading to coral bleaching (Wyatt et al., 2019; Baird & Guest, 2009). However, as depth increases heat accumulation decreases leading to generally cooler and more stable temperatures on MCEs (Turner et al., 2019).

Rocha et al. (2018) observed coral bleaching at mesophotic depths in the Pacific and Caribbean as well as sediment coverage and physical damage in both shallow and mesophotic (135m) reefs in the Bahamas following Hurricane Matthew in 2016. Likewise, Smith et al. (2016) documented multiple occurrences of bleaching and disease on MCEs in the US Virgin Islands. In addition, MCEs may disproportionately suffer from upwelling and low temperature stress events leading to cold water bleaching due to their position at greater depths (Kobluk & Lysenko, 1994; Bak et al., 2005; Menza et al., 2007; Studivan, 2018). Thus, MCEs are not immune to the impacts of environmental stress. Rather, stable and cooler temperatures in MCEs

are suggested to result in lower thermal thresholds for coral bleaching (Smith et al., 2016), which affect the resilience of MCEs and their capacity to serve as a coral refuge under future climate scenarios. However, whether MCEs are measurably more protected from environmental and anthropogenic stressors than shallow reefs, and if locational biases play a role in this variation, remains unclear (Rocha et al., 2018; Turner et al., 2018).

The purpose of this study was to measure thermal sensitivities among four Western Atlantic coral species to (1) compare performance responses between depth-zones (shallow vs. upper-mesophotic), and (2) among species (*Diploria labyrinthiformis, Montastraea cavernosa, Orbicella franksi,* and *Porites astreoides*) to determine whether coral populations exhibit depth-specific thermal sensitivities relative to their unique temperature exposures. Specifically, we compared TPC metrics during both gross photosynthesis and respiration responses in corals from a shallow (5–10m) and upper-mesophotic (30–35m) reef site in Bermuda. If upper-mesophotic corals are locally adapted to cooler, stable temperature ranges, we expected to see lower thermal optimums compared to shallow reef corals adapted to warmer, highly variable temperatures. As such, we hypothesized that upper-mesophotic corals would be less heat-tolerant than shallow corals resulting in lower thermal optimum ($T_{opt}$) and increased thermal sensitivities (high $E$ and $Eh$ values), and shallow corals would exhibit a higher $T_{opt}$ with reduced thermal sensitivity.

## Materials and Methods

### Site Selection

This study was performed on the North Atlantic Bermuda platform across two reef sites which vary by depth and environmental conditions (Fig. 1.1): a shallow rim reef (Hog Beacon; 8−10m depth; 32°27’26’N, 64°50’05’W) and an upper-mesophotic reef (Deep Baby; 30−35m

depth; 32°29’18’N, 64°51’18’W). On November 26th, 2018, three colonies (~40cm diameter) from each of the following four coral species; *D. labyrinthiformis, M. cavernosa, O. franksi,* and *P. astreoides* were collected by hammer and chisel with a minimum of 5m distance between colonies to ensure collection of distinct genotypes. The four coral species were chosen due to their abundance across depth and their varied thermal sensitivities and ecological strategies (Darling et al., 2012). Immediately upon returning to the Bermuda Institute of Ocean Sciences (BIOS) mesocosm facility, coral colonies were fragmented into 8 individual ramet nubbins using a wet table saw. Ramets were on average 20.7 $cm^2$ (SD= 4.2 $cm^2$) and all metabolic rates were standardized to individual’s surface area and volume. Ramets were maintained in common garden conditions with depth-specific light (upper-mesophotic coral’s light reduced by 37%) and ambient seawater temperature (measured *in situ* on collection day, 22℃) in one 380-gallon flow-through filtered seawater (FSW) system for 24hrs to acclimate. A short acclimation period was selected in order to minimize confounding effects of the common garden environment to experimental responses while minimizing measuring a stress response due to removal and fragmenting. However, potential impacts of the recovery time as well as the low sample size (n=3 genotype per species) should be considered when interpreting our results.

Maximum PAR measurements reflected values taken at daily peak irradiance on the day of collection (283.90 μmol photons $m^{-2}\,s^{-1}$ on the shallow reef and 97.32 μmol photons $m^{-2}\,s^{-1}$ on the upper-mesophotic site). Mesocosm tank mimicked average seasonal *in situ* light readings collected with paired HOBO pendant temperature loggers from September–October 2018. Temperature and salinity were quantified in the wet lab holding totes to mimic the ambient temperature of the BIOS mesocosm facility to 22℃, controlled by an Apex Aquacontroller (Neptune Systems to ±0.1℃). Filtered seawater (5μm filter) was replenished daily and stored in

three large 20-gallon Rubbermaid (BRUTE tote storage) containers, two holding totes and one experimental tote. Water was recirculated and controlled for temperature in each individual tote with a chiller (AquaEuroUSA Max Chill-1/13 HP Chiller) and heaters (AccuTherm Heater 300W) controlled to ±0.1℃ by the Apex Aquacontroller.

*In situ* temperature data was collected from September 3rd, 2018 −August 13th, 2019, at Hog Beacon, and September 7th, 2018 −August 21st, 2019, at Deep Baby with paired ProV2 temperature loggers, and HOBO pendant temperature and light loggers (lux converted to photosynthetically active radiation; PAR). Loggers sampled at 30min intervals, and data values were averaged across paired loggers (Fig. 1.1). Similarly, an additional temperature data deployment occurred with two HOBO pendant temperature and light loggers (lux) from September 3rd, 2018 –October 15th, 2018, at Hog Beacon, and at Deep Baby from September 7th –November 18th, 2018 to provide supplementary temperature and irradiance. These pendant loggers were removed from the sites and used to convert lux light levels to PAR in the mesocosm. Used in combination with an underwater cosine corrected sensor (MQ-510 quantum meter Apogee Instruments, spectral range of 389−692 nm ± 5nm) corresponding lux values were converted to PAR. We achieved this by taking simultaneous measurements every hour for a week to identify the PAR values from equivalent lux measurements. This allowed us to use the PAR sensor during the experimental procedure (real-time measurements) while still accounting for the lux measurements taken *in situ*. Common garden irradiance exposure was modified for upper-mesophotic corals by placing shade cloths over the flow-through system, reducing ambient light levels by 37% thus mimicking *in situ* PAR measurements (283.90 μmol photons $m^{-2}$ $s^{-1}$ on the shallow reef; 97.32 μmol photons $m^{-2}$ $s^{-1}$ on upper-mesophotic).

Metabolic Responses

Characterization of thermal sensitivities and ranges in organisms can be achieved by constructing thermal performance curves (TPC), which define the relationship between performance rates (in this study, gross photosynthesis and respiration) of an individual/species and temperature. TPC have a characteristic shape (see Fig. 1 and Table 1 in Silbiger et al., 2019), where performance rates (metabolic, behavioral, or physiological) rapidly rise from zero (thermal minimum, $CT_{min}$) with increasing temperature (activation energy, $E$) and peak at the thermal optimum ($T_{opt}$) and performance maximum ($P_{max}$). Following the peak is typically a rapid decline in performance (deactivation energy, $Eh$), culminating where organismal performance is zero ($CT_{max}$). The temperature at which enzymatic activity halts lies along the $Eh$ slope and is termed the enzyme deactivation temperature ($Th$) and the overall mean performance rate across all temperatures is defined as $lnc$. Thermal minimum and maximum ($CT_{min}$ & $CT_{max}$) demarcate an individuals or species thermal range, while performance maximum represents the peak performance rate at their ideal temperature ($T_{opt}$) (Huey & Kingsolver, 1989, 1993; Angilletta et al., 2002; Angilletta, 2009). TPC with steep $E$ and $Eh$ slopes (higher values) will be more thermally sensitive due to thermal conditions rapidly shifting from optimal to suboptimal. High thermal sensitivity implies that a small change in temperature causes dramatic physiological responses, while low thermal sensitivity indicates a large change in temperature is required to cause a similar response. Among-population variations in TPC shape (i.e., shifts in the height of the curve, position of $T_{opt}$, or the breadth of the curve) can be indicative of localized phenotypic plasticity and/or adaptation (Huey & Kingsolver, 1989; Knies et al., 2009).

One of 8 ramets from each genet and species (n= 3 ramets/species/site) was randomly assigned to one of eight temperature treatments (19, 21, 23, 26, 29, 32, 34, or 36 °C). Assay temperatures were randomized by day, and each temperature trial consisted of 3 forty-minute

incubation's (continuous 20-minute dark and light trial). Each temperature incubation measured 8 individual ramets and one empty control chamber (FSW only). Individuals were randomized into a trial and incubation chamber. The control chamber accounted for oxygen consumption and production of microorganisms and bacteria within seawater. The metabolic rate from each incubation's control chamber was subtracted from each corresponding experimental chamber to correct for background metabolic activity.

The eight assay temperatures were chosen to capture Bermudian corals natural thermal range of 17−30°C (yearly sea surface average of 23°C, Locarnini et al., 2006, & yearly maximum of 29°C, Coates et al., 2013), and above (31−36°C), to quantify TPC parameters. Due to collection restrictions on coral size and number of individuals, each genotype produced 9−10 nubbins after fragmentation. Therefore, we chose eight assay temperatures to reflect cooler minimum temperatures found in the upper-mesophotic zone based on the missing lower end of the thermal range used in Silbiger et al. (2019) (24, 26, 27, 29, 31, 32, 34, 36 °C). Assay temperatures were concentrated around the lower and upper limits (2°C gap compared to 3°C gap around thermal maximum) of the performance ranges estimated in Silbiger et al. (2019) to refine performance metrics (thermal sensitivities, *E* & *Eh*) at the boundaries of their thermal range and to ensure upper-mesophotic thermal optima was represented (shallow *O. franksi* predicted to be <31°C, see Fig. 3 in Silbiger et al., 2019).

To avoid synergistic effects of temperature treatments over time (i.e., thermal stress loading), we tested one individual at each temperature to measure instantaneous thermal stress, allowing relative parameter estimate comparisons at each temperature level (n=192). Individual coral fragments were transferred to the experimental indoor wet laboratory at approximately 8:00 AM daily, kept in complete darkness to dark acclimate for at least 30 minutes and then tested for

20-minutes in the dark followed by a 20-minute light incubation (583.5 ± 3 µmol photon $m^{-2}$ $s^{-1}$). After each temperature trial, corals were immediately frozen and maintained in a –80°C freezer at BIOS for subsequent analyses.

To determine thermal sensitivities, discrete measurements of temperature dependent metabolism, net photosynthetic (*NP*) and respiration (*R*) rates were collected via respirometry. Nine, 650mL closed acrylic incubation chambers with a fiber-optic oxygen probe sensor (Presens dipping probes [DP-PSt-7-10-L2.5-ST10-YP]) measured oxygen evolution in both dark *R* and light *NP* trials sequentially. All chambers were equipped with a magnetic stir bar and locked into a custom-built motor powered magnetic stirring table as in Silbiger et al. (2019). This set up ensured continuous water circulation in each chamber to prevent oxygen super-saturation. Respirometry chambers were submerged in temperature controlled FSW in the experimental tote and covered with a tarp to ensure complete darkness for the first twenty-minute trial to estimate dark respiration rates.

To estimate photosynthetic rates, a full spectrum aquarium light (MARS AQUA 300W LED) was suspended above the chambers and set at an average of 583.5 µmol $m^{-2}$ $s^{-1}$. The irradiance value used for the light incubations was derived from photosynthesis-irradiance (PI) curves and based on saturating irradiances ($I_k$) and the point of photoinhibition for all species. Prior to experimental trials, we tested eight corals, two from each species and across depth (n=1 per genotype) in respirometry chambers held at ambient temperature (22°C). We ran 20-minute incubations under eleven light intensities averaging: 0, 105, 218, 272, 408, 506, 538, 710, 802, 902, and 1003 µmol photon $m^{-2}$ $s^{-1}$. Due to differences in irradiance experienced at depth (~37% reduction) we expected upper-mesophotic corals to be photoinhibited at lower light levels (Kahng et al., 2019), however there was no evidence of photoinhibition at either depth. We

selected 580 µmol photon $m^{-2}$ $s^{-1}$ (583.5 ± 3 µmol photon $m^{-2}$ $s^{-1}$, mean ± SE, n=10) as the experimental light level to reflect a value below the point of photoinhibition and above the saturating irradiances found at both depths, $I_k$ of 141.5 µmol photon $m^{-2}$ $s^{-1}$ for shallow and 94.6 µmol photon $m^{-2}$ $s^{-1}$ for the upper-mesophotic (Appendix 1: Figure S1.1).

PAR measurements for each chamber were quantified before each experimental light trial with an underwater cosine corrected sensor. Metabolic rates were extracted from oxygen concentrations recorded by the Pre-Sens Measurement Studio 2 software (v. 2.1.0.443) from the raw change in oxygen over the dark and light trials in base R v. 3.5.2 (R Core Team, 2018) using repeated local linear regressions in the package *LoLinR* (Olito et al., 2017). Following protocols outlined in Silbiger et al. (2019), raw metabolic rates were normalized to chamber volume and surface area using a planar tracing approach as outlined in Naumann et al. (2009). Surface area was quantified (in $cm^2$) from pictures (n=3) taken immediately before each trial and estimated with image analysis software ImageJ v1.

Statistical Analysis

Oxygen rates used in the PI curve were extracted and fit to a non-linear least squares regression of a non-rectangular hyperbola (Marshall & Biscoe, 1980) and analyzed using the methods described by Silbiger et al. (2019) to extract curve parameters: area-based net and maximum gross photosynthetic (*GP*) rates, *NP*, and *R*. Thermal sensitivities were characterized by constructing TPC following the Sharpe-Schoolfield model (Sharpe & DeMichele, 1977; Schoolfield et al., 1981).

Metabolic rates were calculated from absolute values of *NP* plus dark *R* to obtain gross photosynthesis (*GP*) (Hoogenboom et al., 2006; Lyndby et al., 2018). Log transformed oxygen concentrations (*GP* & *R*) were averaged for each coral species and site, fit to a non-linear least squares regression using the statistical program base R, and run through *nls.multstart* (Padfield et

al., 2016). Uncertainty around each curve was accounted for with bootstrapping calculating ±95% confidence bands around predictions. Metabolic processes were separated into gross photosynthesis and respiration and thermal performance parameters *E, Eh, Th, lnc*, $T_{opt}$, and $P_{max}$ were estimated for each genotype. Parameter outliers were identified and removed using Cook's distance (values 4 times greater than the mean were considered outliers). ANOVA assumptions were tested with the Levene's test for homogeneity of variance, and the Shapiro-Wilk's test for normality of residuals. Variables that violated ANOVA assumptions (Th parameter during respiration; Sharipo-Wilk's test: $p = 0.0104$) were log-transformed prior to subsequent analyses.

Linear regression models were run for each performance metric using the *lm* function in R statistical software including interactions between the fixed effects, depth and species. This was followed by a one-way ANOVA testing the effect of depth within each species. We performed a mixed model with genotype as a random effect, however it was found to show collinearity to both depth and species and subsequently removed from the model. Post-hoc Tukey's HSD tests were performed to reveal significant effects between variables. Similarly, gross photosynthesis measurements for each species at each temperature tested was divided by the corresponding *R* values and used to construct and compare photosynthesis and respiration ratios (*P:R*). A linear model was run using the *lm* function in R to assess the interaction between fixed effects depth and species.

Temperature data collected during September 2018 –August 2019 was compared using a paired *t* test in *ggpubr*. Subsequently, we tested the average daily temperature with a linear *lm* model and 0.05 alpha between sites to determine significant effects. To identify seasonal differences, summer and winter months were tested using the same methodology.

**Results**

The *in situ* temperature data show patterns consistent with previous thermal descriptions in Bermuda (Goodbody-Gringley et al., 2015). The shallow rim reef (Hog Beacon) experienced a yearly mean temperature of 23.3℃ ± 3.05 (mean ± SD) fluctuating between 18.5℃ to 30.2℃ (Δ11.7℃). The upper-mesophotic reef (Deep Baby) had a mean temperature of 23.4℃ ± 2.4 (mean ± SD) varying from 19℃ to 28.7℃ (Δ9.7℃) during an annual cycle (Fig. 1.1). Temperatures across depth fluctuated differentially seasonally, showing an overlap in mean temperatures, while highlighting broader fluctuations in shallow maximum and minimums throughout the year. Comparison of average daily temperature between sites further confirmed different thermal environments (*t* test*; p*= 8.1e–08 & linear model; *p*= 3.058e–07, df= 35.810, F= 26.22). During the winter months (November − April) sites experienced equivalent average temperatures (deep= 21.6℃, shallow= 21.3℃; *t* test*; p*= 0.4825 & linear model; *p*= 0.4824, df= 58, F= 0.4999), while during summer months (May − October) there was a significant difference in temperatures where Hog Beacon was 1.6℃ warmer than Deep Baby (deep= 24.7℃, shallow= 26.3℃; *t* test; *p*= 0.0047 & linear model; *p*= 0.0046, df= 54, F= 8.719).

Thermal performance curves for each species show overlap between shallow and upper-mesophotic corals in both gross photosynthesis and respiration rates (Fig. 1.2). No significant interactive effects between depth and species were found for any gross photosynthesis or respiration thermal performance parameters (Table 1.1)

Gross photosynthetic performance parameters *E, Eh, Th,* $T_{opt}$ *, lnc,* and $P_{max}$ did not differ significantly by depth when assessing across all species (see Fig. 1.3 and Appendix 1; Figure S1.2; *p*= 0.170, *p*= 0.0799, *p*= 0.152, *p*= 0.106, *p*= 0.4339, and *p*= 0.774 respectively). Photosynthesis metric *Eh* (deactivation energy) was significantly different between depths for *D. labyrinthiformis* only (see Appendix 1; Figure S1.3; one-way ANOVA; *p*= 0.0435). Gross

respiration performance parameters did not differ significantly by depth for any species (Fig. 1.4 and Appendix 1; Figure S1.4; *E*: $p$= 0.22, *Eh*: $p$= 0.785, log *Th*: $p$= 0.666, $T_{opt}$: $p$= 0.762, *lnc*: $p$= 0.088, & $P_{max}$: $p$= 0.449).

Overall, gross photosynthetic parameters *E*, *Eh*, *Th* and $T_{opt}$, did not differ significantly by species (see Appendix 1: Figure S1.5; $p$= 0.362, $p$= 0.504, $p$= 0.133, and $p$= 0.159 respectively), however, $P_{max}$ and *lnc* did differ ($p$= 4.02e$^{-06}$, df= 18 , F= 21.11, and $p$= 0.0031, df= 19 , F= 6.592). Subsequent Tukey's HSD tests were performed to identify pairwise differences between species, significant *p*-values are listed in Table 1.2 Further, comparisons among species for thermal performance parameters for gross respiration performance rates were not significant (see Appendix 1: Figure S1.6; *E*: $p$= 0.228, *Eh*: $p$= 0.48, log *Th*: $p$= 0.293, $T_{opt}$: $p$= 0.438, *lnc*: $p$= 0.231, and $P_{max}$: $p$= 0.0511).

Photosynthesis to respiration (*P:R*) ratios remained constant from 19 to 30℃ but declined rapidly from 31 to 36℃ (Fig. 1.5 & Appendix 1: Figure S1.7). Upper-mesophotic and shallow reef corals showed similar *P:R* curves with a non-significant linear regression for the interaction of species and depth (species; $p$= 0.066 , df= 3, F= 2.44, depth; $p$= 0.796, df= 1, F= 0.0673, and interaction; $p$= 0.75, df= 3, F= 0.403).

Similar to *P:R* curves, *GP* thermal optimums (temperature at peak performance) did not differ between depths. In fact, when comparing between depths all upper-mesophotic corals had larger $T_{opt}$ values than shallow; *D. labyrinthiformis* (31.05℃ ± 0.204 & 29.34℃ ± 1.96), *M. cavernosa* (31.76℃ ± 3.28 & 31.27℃ ± 0.732), *O. franksi* (29.61℃ ± 0.488 & 28.91℃ ± 1.62), and *P. astreoides* (30.24℃ ± 1.656 & 26.92℃ ± 3.41) respectively.

## Discussion

Contemporary views on depth-dependent coral thermal sensitivity are that deeper, cooler, more thermally stable environments should result in lower bleaching thresholds for corals (Howells et al., 2012; Smith et al., 2016). Given the statistically cooler temperatures documented on MCEs in Bermuda (Goodbody-Gringley et al., 2015), we predicted that upper-mesophotic corals would have lower thermal optima and higher thermal sensitivities compared to shallow water populations. Instead, we found similar thermal optima and sensitivities between depths for all species examined, suggesting that local adaptation and/or acclimatization to temperature has not occurred in these populations. Our findings show nearly identical gross photosynthesis and respiration TPC between depths, and notably all but one upper-mesophotic coral species (*O. franksi*) had *GP* thermal optimums above the mean shallow water yearly maximum (30.2℃). These results illustrate the potential role of upper-mesophotic reefs in Bermuda as thermal refuge for these four species under future climate change scenarios and warrant further investigation.

Differences in annual reef temperature between the shallow and upper-mesophotic sites documented in this study conform with previous studies, showing cooler more stable thermal environments in MCEs due to thermoclines, upwelling, and decreased heat attenuation at depth (Leichter et al., 2006; Smith et al., 2008; Lesser et al., 2009; Leichter et al., 2012; Brandt et al., 2013; Smith et al., 2013a; Goodbody-Gringley et al., 2015: Bongaerts et al., 2015; Smith et al., 2016; Kahng et al., 2019). While thermal variation between our reef sites was significantly different over a 1-year period, concordant with findings in previous studies at similar depths, (Goodbody-Gringley et al., 2015, 2018), the latitudinal position of Bermuda makes these reefs unique. Being the northern-most subtropical reef in the Atlantic, Bermuda's juxtaposition of the warm Gulf Stream current and cool temperatures found at high latitudes leads to temperature fluctuations. The temperature variation in Bermuda is generally cooler than typical Caribbean

reefs but is strikingly variable and skewed towards the low end of the average range in tropical reef ecosystems. For instance, Bermudian corals can experience yearly minimums of 15°C while corals at lower latitudinal reef locations experience minimum temperatures of roughly 25°C in Panama (2016−2018) (Silbiger et al., 2019), 21°C in the Florida Keys National Marine Sanctuary (FKNMS), and 20°C in the Flower Garden Banks National Marine Sanctuary (FGBNMS) (both 2005−2009) (Haslun et al., 2011). Similarly, average summer maximums of 31°C in Panama (Randall et al., 2020), 30.5−31°C in FKNMS (Haslun et al., 2011; Manzello, 2015), and 30−30.5°C in FGBNMS (Precht et al., 2008; Haslun et al., 2011) are common. Yet, the average maximum summer temperature in Bermuda is 30.2°C in shallow reefs and 28.7°C in the mesophotic, which is 0.2−1.2°C lower than the former.

Our results indicate that when temperatures are separated by season (summer and winter), there is no difference in daily winter temperatures between depth, suggesting both shallow and upper-mesophotic reefs are exposed to the same extreme minimum temperatures (shallow; 18.5°C and upper-mesophotic; 19°C). Extreme thermal exposure (cold or warm) is known to contribute to similarities in thermal tolerances, despite differences in daily mean temperatures (Buckley & Huey, 2016). Therefore, the similar extreme minimum temperatures experienced at both sites may be more significant in determining thermal sensitivities than the differences in mean daily temperatures during the summer months (shallow; 26.3°C and upper-mesophotic; 24.7°C), despite the shallow being on average 1.6°C higher than upper-mesophotic.

Past research on corals has shown temperature fluctuations can substantially contribute to thermal tolerance (Oliver & Palumbi, 2011; Guest et al., 2012; Kenkel et al., 2015; Schoepf et al., 2015; Cziesielski et al., 2019), however, the effect of "thermal stability" found in upper-mesophotic reefs may be eclipsed by the overall latitudinal position and broad temperature

exposure typical of this subtropical system. While dramatic temperature fluctuations are not uncommon in tropical reefs (Ofu, American Samoa; 24.5−35℃ and 25−32℃, and 14.7−32.4℃ in Tung Ping Chau, China) Bermuda's propensity toward a lower yet tapered thermal range compared to Ofu & Tung Ping Chau may explain the unique thermal stability and persistence between depth in Bermuda (Thomas et al., 2018; McIlroy et al., 2019). Specifically, McIlroy et al. (2019) found that corals in Tung Ping Chau persisted during low temperature exposure while seasonal variation negatively impacted coral productivity and metabolism. The low temperatures experienced at both depths in Bermuda may outweigh the impacts of localized thermal fluctuation on thermal sensitivities.

Our results provide evidence that upper-mesophotic habitats in Bermuda may serve as thermal refuge for some coral species, addressing a larger theory regarding roles of MCEs in the survival of shallow reefs. Evidence for this theory has been mixed, however (Bongaerts et al., 2010; Goodbody-Gringley et al., 2015; Holstein et al., 2016; Loya et al., 2016; Semmler et al., 2016; Smith et al., 2016; Bongaerts et al., 2017; Goodbody-Gringley et al., 2018; Kim et al., 2019; Pinheiro et al., 2019). A thermal refuge is defined as a reef that is thermally buffered, with the potential to provide viable offspring for adjacent damaged reef following a disturbance (Bongaerts et al., 2010). Smith et al. (2016) argues that to be a thermal refuge mesophotic corals cannot have a lower bleaching threshold than their shallow water conspecifics. Despite the cooler buffered environment of MCEs, an increase in temperature above the mean summer maximum of local conditions can cause thermal stress and bleaching, negating the main premise of the hypothesis (Smith et al., 2016). Thus, for the refuge to function mesophotic corals must have similar thermal sensitivities as their shallow water counterparts. As demonstrated in our results, the upper-mesophotic reef in Bermuda has significantly different yearly temperatures, yet no

difference in associated coral thermal optima, or thermal sensitivities compared to shallow corals. The physiological metrics captured for four common coral species by our study, combined with temperature observation through time (this study, Goodbody-Gringley et al., 2015, Goodbody-Gringley et al., 2018), suggest that Bermudian MCEs meet these criteria to serve as thermal refuge.

Generally, physiological and metabolic stress induced by temperature extremes increase with magnitude and frequency of exposure, and sensitivities can vary throughout ontogeny, among species, and across seasons (Buckley & Huey 2016). Consequently, the interpretation of our results needs to address three caveats; 1) metabolic responses were measured in 4 species of adult Bermudian corals 2) in December via 3) heat-shock methodology. These three experimental limitations have important implications in our overall understanding of thermal sensitivities in shallow and upper-mesophotic corals in Bermuda. To characterize upper-mesophotic reefs as a refuge, thermal sensitivities between depth should be measured at multiple life stages, specifically larval and coral recruits. Previous research by Goodbody-Gringley et al. (2018) has found similarities in fecundity of adult *P. astreoides* from the same reef sites used in our study. Additionally, they found shallow reef larvae were similar in size and *Symbiodinaceae* densities compared to upper-mesophotic larvae, however shallow corals had lower growth, survival and settlement rates. These results suggest heightened recruitment potential and coral resilience in upper-mesophotic reefs and if applied in concert with thermal performance curves for larvae may bring us closer to determining the role of upper-mesophotic reefs in future climate scenarios.

Furthermore, our study was performed in December of 2018, and coral resistance to heat stress is known to differ across seasons. Thermal sensitivities are not fixed but can be modified

throughout an organism's life in response to acute heat shocks resulting in heat hardening or acclimatizing to seasonal conditions (Buckley & Huey, 2016). For example, photosynthesis rates are often higher in the summer, whereas during the winter, corals are more susceptible to photodamage and pigment loss (Scheufen et al., 2017). This winter vulnerability can negatively impact coral responses and lead to cold-water bleaching (Lirman et al., 2011). Although there have not been any reports or evidence of cold-water bleaching in Bermuda since 1902 (Schopmeyer et al., 2012), Hog Beacon did experience a lower average minimum temperature (18.5℃) than Deep Baby (19℃), which could have negatively affected shallow coral metabolic rates. While winter temperatures were statistically similar between shallow and mesophotic depth zones during our study, summer temperatures were on average 1.6℃ higher in shallow versus mesophotic depths.

Just as metabolic responses can differ depending on the season of testing, the methodological approach can also elicit different responses. In this study, we measured coral responses to heat-shock (short-term instantaneous stress) under acute incubation periods (40 mins), which inherently has negative effects on performance due to the lack of an acclimation period. As this methodology is not representative of natural conditions (save marine heat waves), the heat-shock method provides instantaneous stress responses that can be used to identify relative thermal sensitivities, ranges, and limits. The heat-shock method has been demonstrated to estimate thermal responsiveness, but it may overestimate metrics relative to individuals that are acclimatized to (heat-stress experiment) or ramped through all temperatures (Schulte et al., 2011; Sinclair et al., 2016). Further research is needed to delineate the effect of temperature ramping rates and long-term thermal exposure on performance between depths. Supplementary

heat-stress experiments analyzing TPC and *P:R* curves can refine our understanding of coral capacity to sustain long-term survival and persistence.

Generally, *P:R* curves are used to identify differences between coral reliance on autotrophic products from *Symbiodinaceae* and the maintenance needs (respiration) of the coral-algae symbiosis (Coles & Jokiel 1977; Castillo & Helmuth 2005). Consistent with our results, *P:R* curves commonly decline when temperatures surpass the thermal optimum (Castillo and Helmuth 2005; Coles & Jokiel 1977). However, for corals to maintain long-term survival, *P:R* values of 2 or higher are necessary (Coles & Jokiel 1977). In our study, the temperature at which all species *P:R* fell below 2 was ~30℃ (Fig. 1.5), but the capacity to sustain this ratio over time remains unknown, reinforcing the need for long-term heat-stress studies. It appears that shallow reef corals in Bermuda are currently living at or near their thermal maxima, with annual peak temperatures exceeding 30℃. Thus, while bleaching events are historically rare for the island, global temperature increases may cause substantial changes to coral survivability in Bermuda in the near future.

Long-term survival and stability of coral communities have been typical of Bermudian reefs (MEP, 2007, Smith et al., 2013a, b; Courtney et al., 2017, 2020), however, predicted temperature increases (0.01℃ per year down to 400m depth) still pose a threat if temperatures exceed species thermal optimums and *P:R* survival thresholds. To date, Bermuda has experienced one major bleaching event documented in 1988 (Cook et al., 1990) followed by several minor bleaching events recurring annually after 1999 (Smith et al., 2013a, b; Courtney et al., 2017, 2020). Characterized by pale, blotchy, or white tissue, these bleaching events did not exceed 30% of total coral population in the four species in our study, nor was there any significant mortality (up to 25m). The lack of mortality has been attributed to temporal heat

attenuation during July−September caused by the prevailing climatological conditions associated with Bermuda's high latitudinal position (Smith et al., 2013a, b).

Moreover, it has been shown that corals exposed to prior thermal stress events can acclimatize and resist bleaching during future temperature exposures (Brown et al., 2002), including trans-generational acclimatization in offspring of corals exposed to high temperatures (Putnam & Gates, 2015). This is consistent with the 1988 bleaching event having the highest impact on corals while subsequent events were less severe (Smith et al., 2013a, b). Yet neither Cook et al. (1990) nor Courtney et al. (2017) observed or collected corals on upper-mesophotic reefs leaving speculation as to whether impacts were more or less substantial at depth. Due to their depths and inherent oceanic features (cold water upwelling and thermocline depth) lowering heat stress, upper-mesophotic reefs may have additional protection from thermal anomalies up to 1°C (Bridge et al., 2014) negating seasonal bleaching impacts. For example, Frade et al. (2018) found significantly less bleaching and mortality in mesophotic corals (40% bleached, 6% death at 40m) compared to shallow (60−69% bleached, 8−12% death at 5−25m) during the 2016 mass bleaching event in the Great Barrier Reef. Further research analyzing upper-mesophotic coral cores and temperature variation may help disentangle whether long-term acclimation or abiotic factors have influenced the similarities in thermal sensitivities.

The only difference in observed thermal sensitivities between depths occurred in *D. labyrinthiformis* conspecifics (Fig. 1.3 & Appendix 1; Figure S1.3) for the *GP* deactivation rate (*Eh*). Upper-mesophotic *D. labyrinthiformis* had a steeper slope (5.122 ± 0.926 eV; mean ± SD) compared to shallow *D. labyrinthiformis* (3.188 ± 0.681 eV; mean ± SD), indicating higher sensitivity in corals from Deep Baby. The sharp decline in *Eh* suggests photosynthesis drops out more rapidly after surpassing the thermal optimum, indicating coral/algae metabolic costs

outweigh the photosynthetic input. This may have implications for bleaching severity and recovery rates post stress events and may indicate sensitivity in enzymatic machinery (RuBISCo during photosynthesis) in upper-mesophotic *Symbiodinaceae* for this species (Hill et al., 2014).

Although we did not characterize algal symbiont assemblages in this study, previous research in Bermuda (Savage et al., 2002, Yost et al., 2012; Serrano et al., 2014, 2016; Reich et al., 2017) found *Symbiodiniaceae* assemblages and densities did not differ across depth (4−24m) within the four species used in our study (Lajeunesse et al., 2018; Yost et al., 2012). Thus, we do not anticipate *Symbiodiniaceae* variation across our study sites. The uniformity of coral *Symbiodiniaceae* assemblages found between depths is attributed to Bermuda's isolated high-latitudinal location and vertical mixing (Reich et al., 2017), which may also explain the high levels of coral genetic connectivity. Genomic analyses performed across depths (≤10 m, 15–20 m and ≥25 m) for *P. astreoides* and *M. cavernosa* showed no genetic differentiation (Serrano et al., 2014, 2016). While it is unclear how *D. labyrinthiformis* and *O. franksi* populations differ across depth in Bermuda, we expect similar patterns of connectivity due to Bermuda's geographical isolation, identical *Symbiodiniaceae* assemblages found between depths (Yost et al., 2012), and the life-history traits of theses corals (Darling et al., 2012). Therefore, the similarities in thermal sensitivities found between depths may be a consequence of genetic and symbiont similarities.

While bleaching in response to thermal anomalies has been reported for reefs across variable depth gradients (Rocha et al., 2018; Smith et al., 2013a, b; Turner et al., 2018) there is a striking gap in physiological response data (specifically, TPC) for assessing thermal sensitivities in corals. Understanding thermal performance is essential for predicting future responses to changing thermal conditions. Here we advance our understanding of coral thermal sensitivities

and tolerance thresholds and show that, in Bermuda, corals on shallow and upper-mesophotic reefs respond similarly to a wide range of temperatures (19−36°C). Our findings therefore suggest that upper-mesophotic reefs in Bermuda may serve as a thermal refuge for coral survival under future climate change scenarios. Although these results may ultimately be unique to Bermuda, identification of reef systems beyond Bermuda with similar refuge potential is crucial for the effective management and conservation of these critically threatened ecosystems in the face of global coral reef decline.

**Table 1.1 Thermal performance curve parameter metrics model statistics**

Summary statistics for linear regression models with interacting terms (~species*depth) for all gross photosynthesis and respiration thermal performance parameters. *E*= activation energy, *Eh*= deactivation energy, *Th*= temperature enzymatic inactivity, $T_{opt}$= thermal optimum, *lnc*= mean performance rate, $P_{max}$= maximum rate of performance.

| Performance parameter | Performance metric | df | F statistic | *p-value* |
|---|---|---|---|---|
| $P_{max}$ | *GP* | 3 | 0.372 | 0.774 |
| *lnc* | *GP* | 3 | 0.967 | 0.434 |
| $T_{opt}$ | *GP* | 3 | 0.568 | 0.645 |
| *E* | *GP* | 3 | 2.106 | 0.145 |
| *Eh* | *GP* | 3 | 1.379 | 0.080 |
| *Th* | *GP* | 3 | 0.768 | 0.530 |
| $P_{max}$ | *R* | 3 | 0.033 | 0.992 |
| *lnc* | *R* | 3 | 1.170 | 0.352 |
| $T_{opt}$ | *R* | 3 | 0.125 | 0.944 |
| *E* | *R* | 3 | 1.143 | 0.362 |
| *Eh* | *R* | 3 | 1.262 | 0.323 |
| log *Th* | *R* | 3 | 0.787 | 0.520 |

**Table 1.2 Significant pairwise photosynthesis thermal performance curve parameters**

Summary statistics for significantly different post hoc Tukey-HSD pairwise species comparisons for gross photosynthesis metrics, $P_{max}$ and *lnc*. Significant differences are denoted with an asterisk (*p-values* <0.05). DLAB= *Diploria labyrinthiformis*; MCAV= *Montastrea cavernosa*; OFRA= *Orbicella franksi*; and PAST= *Porites astreoides*. $P_{max}$= performance maximum & *lnc*= mean performance rate.

| Performance parameter | Species | Mean ± SD (µmol $O_2$ $cm^{-2}$ $hr^{-1}$) | Pairwise comparison | Difference | *p-value* |
|---|---|---|---|---|---|
| *lnc* | *O. franksi* | 1.4 ± 0.258 | OFRA−MCAV | 0.4511 | 0.008* |
| *lnc* | *D. labyrinthiformis* | 1.38 ± 0.014 | DLAB−MCAV | 0.4245 | 0.013* |
| *lnc* | *M. cavernosa* | 0.95 ± 0.056 | NA | NA | NA |
| $P_{max}$ | *O. franksi* | 1.17 ± 0.053 | OFRA−PAST | 0.1944 | 0.0036* |
| $P_{max}$ | *D. labyrinthiformis* | 1.24 ± 0.046 | DLAB−MCAV | 0.324 | $1.3e^{-5}$* |
| $P_{max}$ | *M. cavernosa* | 0.92 ± 0.078 | MCAV−OFRA | -0.2582 | $1.2e^{-5}$* |
| $P_{max}$ | *P. astreoides* | 0.98 ± 0.121 | PAST −DLAB | -0.26001 | $3.1e^{-5}$* |

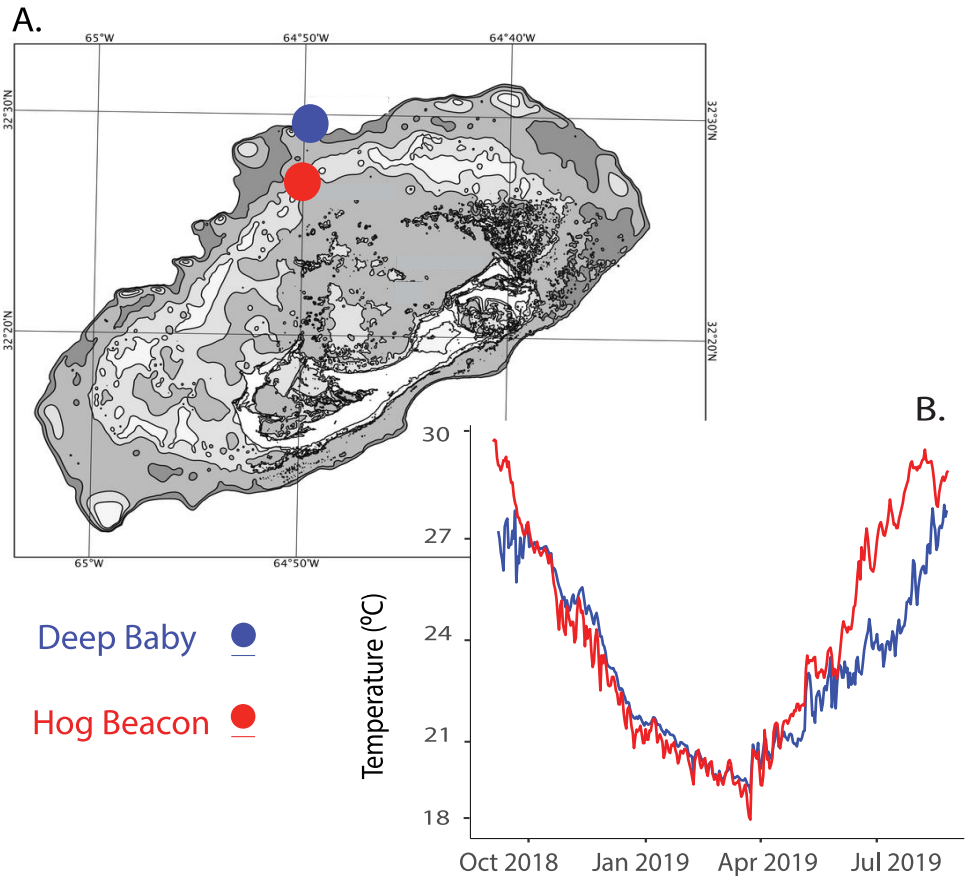


**Figure 1.1 Site locations and thermal histories**

A) Bermuda reef platform designating location of reef sites: Hog Beacon (red circle) and Deep Baby (blue circle), B) Annual *in situ* temperature (°C) data recorded with two HOBO ProV2 loggers from Sept. 2018−Aug. 2019. Daily temperatures were averaged (48 measurements/day) across 2 loggers per site and graphed as values.

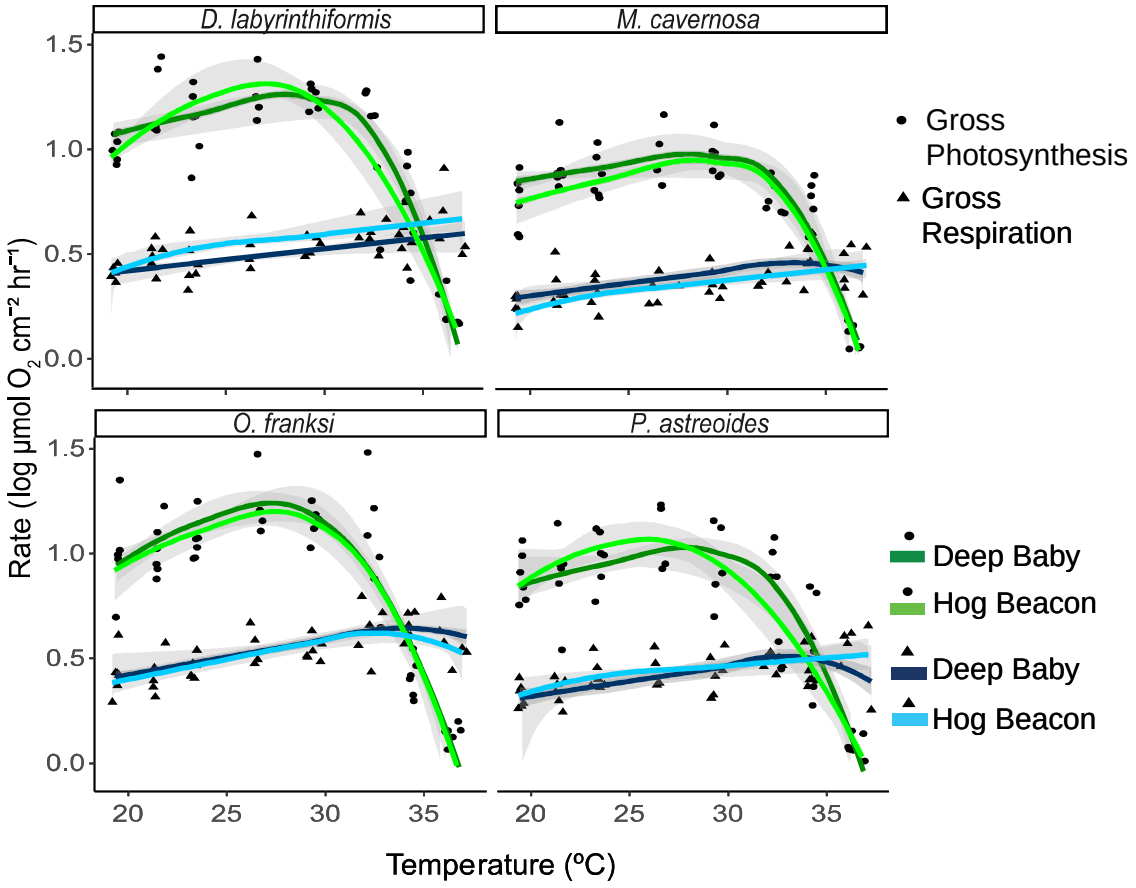


**Figure 1.2 Species-specific thermal performance curves**

Gross photosynthesis (circles) and respiration (triangles) measured in µmol $O_2$ $cm^{-2}hr^{-1}$ across four coral species (n= 192). Fitted lines represent medians from three genotypes per species ± gray 95% bootstrap confidence bands. Upper-mesophotic corals from Deep Baby are dark green (photosynthesis) and dark blue (respiration). Hog Beacon curves are light green (photosynthesis) and light blue (respiration) and depict shallow water coral.

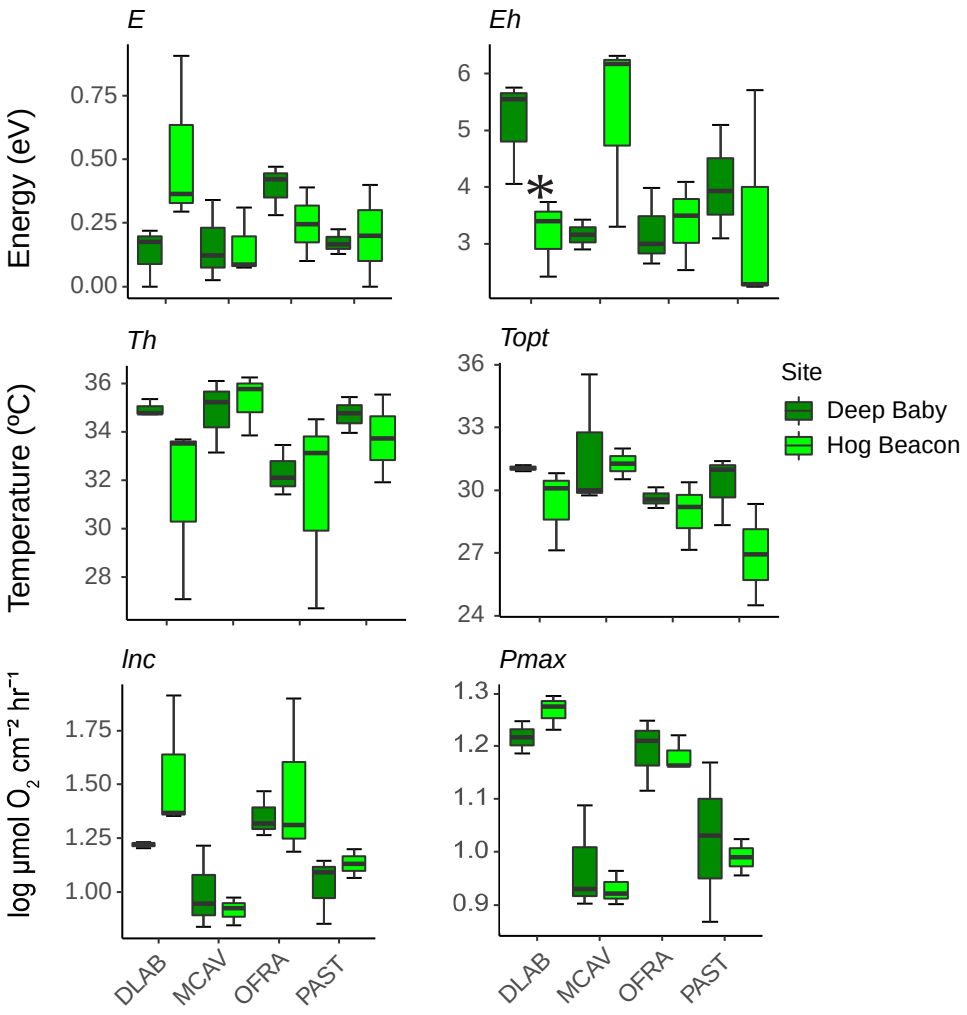


**Figure 1.3 Gross photosynthesis performance parameter comparisons**

Box and whisker plots of thermal performance parameters for gross photosynthesis compared between depths and species (n= 187, 5 unique outliers). The centerlines of boxes are median values and whiskers represent upper and lower 1.58*IQR (inter-quantile range). DLAB= *Diploria labyrinthiformis*; MCAV= *Montastrea cavernosa*; OFRA= *Orbicella franksi*; and PAST= *Porites astreoides*. Upper-mesophotic corals from Deep Baby are represented by dark green, and shallow corals from Hog Beacon are light green. The black asterisk over DLAB for (Eh) denotes a significant one-way ANOVA result ($p$= 0.0435 between depths within *Diploria labyrinthiformis*). *E*= activation energy, *Eh*= deactivation energy, *Th*= temperature enzymatic inactivity, $T_{opt}$= thermal optimum, *lnc*= mean performance rate, $P_{max}$= maximum rate of performance.

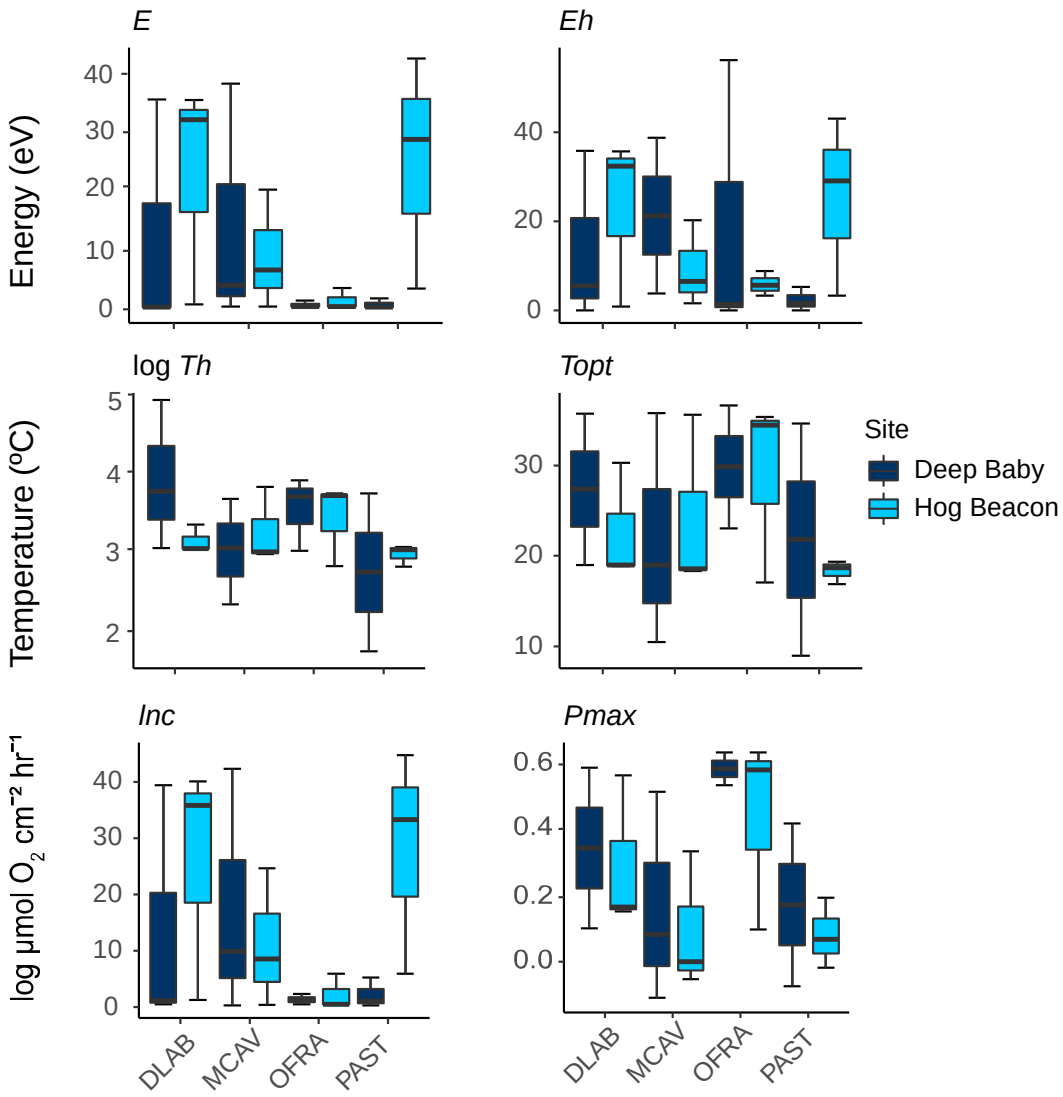


**Figure 1.4 Gross respiration performance parameter comparisons**

Box and whisker plots of thermal performance parameters for respiration compared between depths and species (n= 188, 4 unique outliers). The centerlines of boxes are median values and whiskers represent upper and lower 1.58*IQR (inter-quantile range). DLAB= *Diploria labyrinthiformis*; MCAV= *Montastrea cavernosa*; OFRA= *Orbicella franksi*; and PAST= *Porites astreoides*. Upper-mesophotic corals from Deep Baby are represented by dark blue, and shallow corals from Hog Beacon are light blue. *E*= activation energy, *Eh*= deactivation energy, *Th*= temperature enzymatic inactivity, $T_{opt}$= thermal optimum, *lnc*= mean performance rate, $P_{max}$= maximum rate of performance.

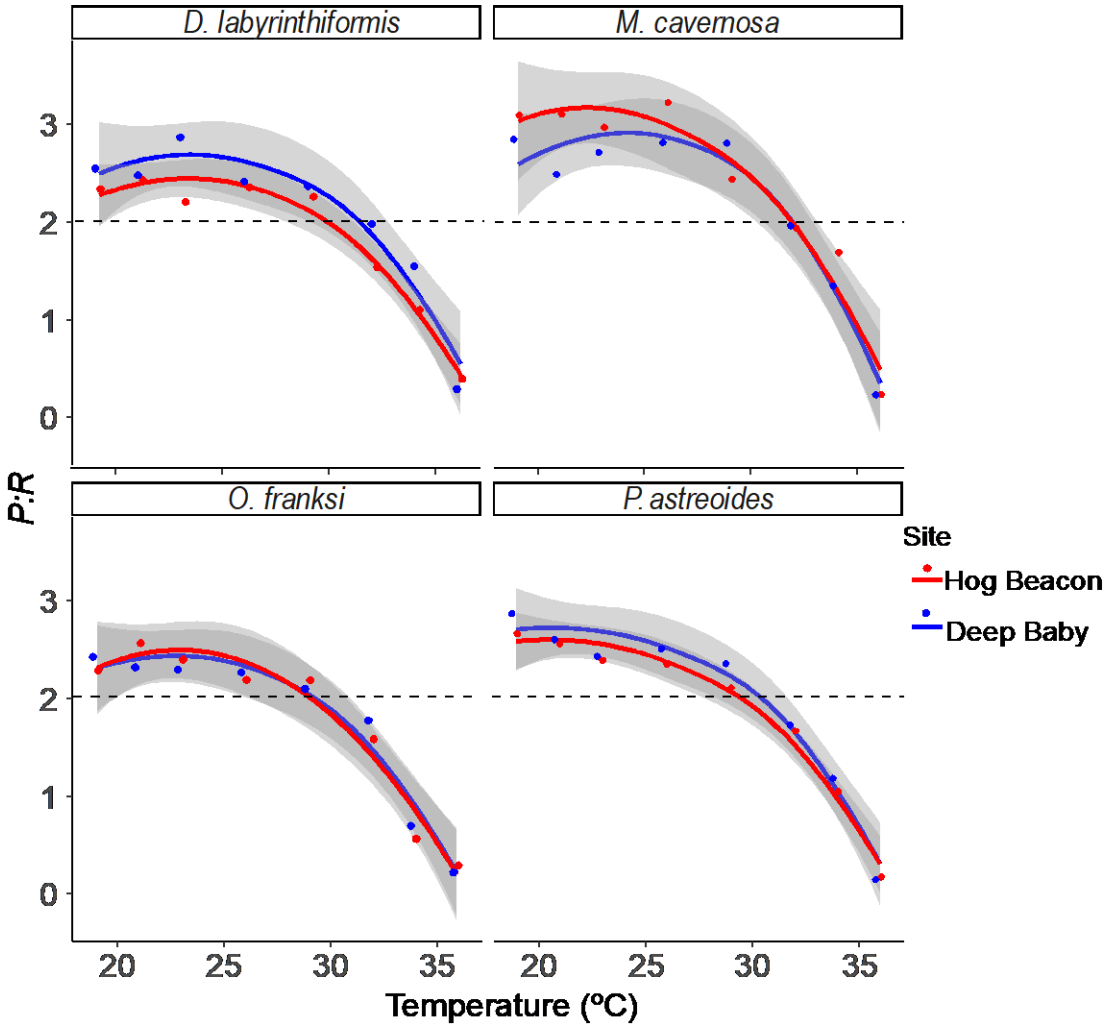


**Figure 1.5 Photosynthesis and respiration ratios**

Photosynthesis respiration ratios for upper-mesophotic (blue) and shallow reef (red) by temperature for each species (n= 192). Solid lines represent the average fitted values and the gray bands are 95% confidence intervals. The black dashed horizontal line is where *P:R*= 2 (i.e., the upper threshold for long-term survival) .

# CHAPTER 2: VARIATION IN CORAL THERMAL PERFORMANCE IN *ACROPORA CERVICORNIS* GENETS UNDER NOVEL STRESS-MEDIATING INTERVENTIONS

## Introduction

Coral reef ecosystems support millions of people worldwide (Woodhead et al., 2019) by providing local income for an estimated global value of US$36 Billion per year from tourism (Cesar, 1996; Dixon et al., 1993; Driml & Great Barrier Reef Marine Park Authority, 1994; Spalding et al., 2017), high-protein food sources (Birekland, 1997; Craik et al., 1990), potential material for the pharmaceutical industry (Birekland, 1997; Carte,1996; Sorokin, 2013) and shoreline protection (Cesar, 1996). Since 1950, however, 50% of global coral cover has declined due to overfishing, pollution, habitat destruction, and climate change, all linked to anthropogenic stresses (Eddy et al., 2021). The rate of change at which these stresses are occurring leave corals little time to adapt or acclimate to their environment, resulting in coral bleaching events, mortality, and reef degradation (Bay et al., 2017; Logan et al., 2021; Muñiz-Castillo & Arias-González, 2021).

Coral bleaching is the abrupt discharge of endosymbiotic algae resulting in a loss of coral pigmentation and subsequent white appearance. The response is primarily caused by sea surface temperatures rising above local mean summer maximums (DeCarlo et al., 2017; Gintert et al., 2018; T. P. Hughes et al., 2017, 2018; McClanahan et al., 2020). While most research on bleaching and coral mortality focuses on temperature, the additive effect of solar radiation also

plays an important role (Board. O.S. & National Academies of Sciences, 2019; Forsman et al., 2012; Kenkel et al., 2011; Masiri et al., 2008). The primary factor driving bleaching in corals occurs when their symbiotic algae (*Symbiodiniaceae*) undergo damage (light-stress) to their photosystem II leading to photoinhibition which can result in expulsion of symbionts from coral tissue (Brown & Dunne, 2015; Coelho et al., 2017; Freeman et al., 2001).

There is a direct correlation between the increased frequency of marine heat waves and coral bleaching events (Moore et al., 2012; Smale et al., 2019; T. B. Smith et al., 2014). MHW severely impact coral reef ecosystems which results in reduced growth rates, health, and increased mass bleaching events leading to coral death (Holbrook et al., 2020; Leggat et al., 2019; sen Gupta et al., 2020). MHW frequency is a major cause for concern because as the time between events shrinks, coral ecosystems are exposed to temperatures beyond their thermal ranges and sensitivities without time to acclimate or adapt causing irrevocable changes in these communities (Holbrook et al., 2019; Oliver et al., 2018; K. E. Smith et al., 2021). Climate change mitigation and policy will be integral to reducing the effects of heatwaves and general ocean warming on coral ecosystem survival. The pace of these strategies, however, leaves marine scientists exploring local mitigation interventions to help reduce the adverse effects of MHW and rising ocean temperatures (Henson et al., 2017; Laufkötter et al., 2020; Leggat et al., 2019).

On calm, clear summer afternoons, increased light-stress can exacerbate photoinhibition and diminish symbiont cellular mechanisms, physiological responses, and increase thermal sensitivity in corals (Cacciapaglia & van Woesik, 2016; DiPerna et al., 2018; Gonzalez-Espinosa & Donner, 2021; Hill et al., 2012). Cloud cover, volcanic clouds, storms, and marine turbidity have been linked to lowered bleaching risk and reduced thermal sensitivity during peak summer

temperatures, triggering interest in applying shading interventions on vulnerable reefs (Baker et al., 2008; Cacciapaglia & van Woesik, 2016; Gonzalez-Espinosa & Donner, 2021; Leahy et al., 2013; Mumby et al., 2001; Oxenford & Vallès, 2016). Reef shading is an engineering mediation that aims to reduce solar radiation, light irradiance, and sea surface temperatures (Board. O.S. & National Academies of Sciences, 2019). Masiri et al. (2008) found that if 30% of solar irradiance is scattered or reflected over a reef at daily peak temperatures, a reduction in total reef system energy of 10Mj $m^{-2}$ $d^{-1}$ can be achieved. This level of solar reduction may cool the water column, lowering the negative impacts of bleaching events.

Shading techniques have been investigated on small scales using a variety of methodologies from knitted black polyethylene fabric that reduces PAR (photosynthetically active radiation) by 50–75% (Coelho et al., 2017), sprinkler irrigation systems removing wave lensing (Veal et al., 2010), and complete shading with black plastic (Rogers, 1979). The results from these studies vary widely from having negative effects on net primary production and respiration of coral communities (Rogers, 1979), to increased coral growth under shaded treatments (Coelho et al., 2017), to no differences in photophysiological responses in corals from the Red Sea (Veal et al., 2010). While this technique cannot directly influence coral adaptation or thermal tolerance, the potential to increase coral persistence by decreasing environmental stresses may be influential on small spatial scales (Atwoli et al., 2021; Board. O.S. & National Academies of Sciences, 2019).

Holobiont health is reliant on the exchange of nutrients between both coral and algae (Frankowiak et al., 2016). The algal symbionts use respiratory $CO_2$ and nitrogen from coral waste products to power photosynthesis. In exchange, the coral receives most of their daily carbon (70%) from algal photosynthates (Muscatine et al., 1981). Current hypotheses suggest

that under increased solar radiation, $CO_2$ demand for photosynthesis is the limiting factor weakening the light reactions in *Symbiodiniaceae* (see Figure 1. In Wooldridge, 2014). Increasing low $CO_2$ levels by maximizing coral respiration rates via heterotrophic feeding may improve the autotrophic capacity of algal symbionts and limit bleaching severity (Becker et al., 2021; Becker & Silbiger, 2020; Ferrier-Pagès et al., 2010).

Similar to the effects irradiance has on thermal sensitivity, rates of heterotrophic feeding and nutrient supply also affects coral responses to temperature. Several studies have found that corals which maintain higher heterotrophic consumption rates decrease their risk of bleaching and have faster recoveries (Baumann et al., 2014; Bessell-Browne et al., 2014; Grottoli et al., 2006; A. D. Hughes & Grottoli, 2013; Sangmanee et al., 2020). When corals consume nutrients heterotrophically, ~80–94% of total daily carbon and ~50–85% of nitrogen needs can be met, but environmental nutrient availability limits heterotrophy (Houlbrèque et al., 2004). Nutrient supplementation before and during peak periods of environmental stress has the potential to aid in coral recovery from thermal-induced bleaching events (Board. O.S. & National Academies of Sciences, 2019), especially if sequestration of nutrients occurs over extended periods of time (A. D. Hughes & Grottoli, 2013). One approach to increasing rates of heterotrophy in corals was explored by Ben-Zvi et al. (2022) in the Red Sea, who found that blue light excited the natural fluorescence in corals which increased predation success significantly. The use of LED lights as a prey-lure system is dependent on prey and coral species which have not been tested in *A. cervicornis*.

The objective of this research was to quantify thermal ranges, sensitivities, and optima in *Acropora cervicornis* genotypes (genets) currently used in coral restoration under three different environmental mitigation scenarios to determine the effect of these intervention treatments on

clone-specific performance responses. Specifically, we tested the efficacy of three proposed interventions; 1) a shading technique (irrigated sprinkler system) which reduced PAR by 25%, 2) a prey-lure treatment (illuminated LED lights during night-time feeding to attract live phytoplankton (*Nannochloropsis oculate*)), and 3) an interactive technique which used both shading and prey-lure approaches (sprinkler and LED systems) to assess the presence of interactive or additive effects of both techniques. We hypothesized that corals under the three stress-mitigation treatments would have improved responses when compared to controls. Specifically, we theorized that corals in the reduced PAR treatment would have higher symbiont densities and chlorophyll a content resulting in higher gross photosynthesis performance maximums, and the LED feeding treatment would have higher protein content and growth rates, which would increase the performance maximum during respiration. we used several physiological parameters including metabolic metrics; thermal optimums ($T_{opt}$), performance maximums ($P_{max}$), thermal sensitivities (activation energy: *E*; deactivation energy: *Eh*; thermal maxima: $CT_{max}$: and thermal breadth; $T_{br}$), and physiological responses; symbiont density, chlorophyll a content, total protein levels, and coral growth rates.

**Materials and Methods**

We compared thermal ranges and sensitivities by measuring thermal performance curves to evaluate the success of these mitigation techniques. TPC are based on measured biological rates (gross photosynthesis (*GP*) and respiration (*R*) in this study) over a range of temperatures (27–34°C) (Angilletta Jr. & Angilletta, 2009; Kingsolver & Woods, 2016; Schulte et al., 2011). The distinctive shape of TPC outlines the rapid increase (activation energy, *E*) in performance (metabolic, behavioral, or physiological) as temperatures increase from zero performance

(thermal minimum, $CT_{min}$) (Fig. 2.1). The peak of the curve represents the thermal optimum ($T_{opt}$) of organisms where their performance is highest (performance maximum, $P_{max}$). The slope decreases (deactivation energy, *Eh*) in performance following $T_{opt}$ and $P_{max}$ and terminates at zero performance (thermal maximum, $CT_{max}$). The thermal breadth ($T_{br}$) of an organism is the range of temperature values over the curve's rate of at least 80% of the peak. Ramets with higher *E* and *Eh* values will be more thermally sensitive as small changes in temperature will cause substantial physiological responses (Angilletta Jr. & Angilletta, 2009; Angilletta et al., 2002; Huey & Kingsolver, 1989; Sinclair et al., 2016).

Coral Acquisition, Transportation, and Maintenance

Forty–eight *Acropora cervicornis* coral fragments (7–10cm in length) from 3 genotypes (K2, M5 & M6. n =16 ramets/genotype) grown on a coral nursery tree (~7.5m) were donated and shipped overnight from the Coral Restoration Foundation (CRF) in Key Largo, Florida. Upon arrival to the University of North Carolina at Chapel Hill's Aquarium Research Center, ramets were glued (Seachem reef glue Cyanoacrylate gel) to Eshopps clear plastic frag plugs. Corals were acclimated to laboratory conditions for 15 days in four 75.7-liter glass aquaria tanks (4 randomly chosen ramets from each genotype, n =12 corals/tank). Each tank had artificial seawater recirculated (Hydor Koralia circulation wave-pumps with 240gph flow rate 3 per tank) through a closed sump system (outflow from each tank was filtered into a shared brute tote bin and re-circulated water was pumped back into each tank). Corals were exposed to a 12h light:12h dark photoperiod under a constant irradiance of 450 ± 3µmol photons $m^{-2}$ $s^{-1}$ (measured with a MQ-510 quantum meter Apogee Instruments, spectral range of 389-692 ± 5nm in 35ppt salinity at 27℃ to acclimate to optimal light conditions (650 µmol photons $m^{-2}$ $s^{-1}$ (O'Neil, 2015)). Additional water quality parameters were maintained and tested weekly, and data can be

accessed on the GitHub repository (https://github.com/GouldKate/TPC_Acropora). Tank temperatures were individually controlled by an Apex Aquacontroller (Neptune systems to ± 0.1℃) using individual tank heaters (AccuTherm Heater 300 W, 1 per tank) and a chiller (AquaEuroUSA Max Chill-1/13 HP Chiller) in the shared 75.7-liter sump system (2-heaters) (Fig. 2.2A). Visual inspection of corals occurred twice daily, and no signs of bleaching or disease was observed.

Irradiance was increased over a ten-day period from 450 ± 3µmol photons $m^{-2}$ $s^{-1}$ to an average of 650 ± 3µmol photons $m^{-2}$ $s^{-1}$ using AC86-264V LED aquarium lights (120W) over each treatment tank. This incremental increase in irradiance was intended to reduce shock associated with high light exposure. PAR was averaged over the 12 coral placement locations on egg crate trays prior to coral arrival using an underwater cosine corrected sensor (MQ-510 quantum meter Apogee Instruments, spectral range of 389-692 ± 5nm). We increased light intensity by 10 ± 3µmol photons $m^{-2}$ $s^{-1}$ daily following coral acclimation. The light exposure to each coral was cast asymmetrically over each tank with an average difference of 260 ± 3µmol photons $m^{-2}$ $s^{-1}$ at the front compared to the back of the tank. To account for this discrepancy corals were rotated to a new position every other day within each treatment tank for the duration of the experiment.

Treatment Exposure

After the acclimation period, two irrigation sprinkler systems (Orbit ½ pattern shrub nozzle) were set above two treatment tanks (sprinkler and interactive, see Fig. 2.2B) and sprayed sump-supplied recirculating artificial seawater (24-hours/day) on the surface water of the tanks which reduced PAR to 450 ± 3µmol photons $m^{-2}$ $s^{-1}$. Temperature and salinity were kept at an average 35.06 ± 0.92ppt salinity and 27.02 ± 0.09℃ in all treatments. Four submersible LED

lights (Whatook submersible remote-controlled LED waterproof lights) were affixed in all tanks to the underside of egg crate trays which kept corals erect. LEDs were activated (white light emitting 60 ± 2µmol photons $m^{-2}$ $s^{-1}$) only in feeding and interactive treatments (6:00pm-7:00pm) once per week during phytoplankton feeding (Fig. 2.2B). Water circulation was paused during feeding intervals. A concentration of 13% *Nannochloropsis oculate* (4–5µm sized) from AlgaGen Phycopure Seapro Functional Algae and 35ppt artificial sea water solution was supplied to all tanks (3.5mls each) weekly. This concentration was adopted from Espinosa and Allam (Espinosa & Allam, 2006) and based on an *Acropora cervicornis* feeding experiment done by Muehllehner (2013). Phytoplankton was chosen for feeding due to *Acropora cervicornis* characteristically small polyps. Most studies to date have used brine shrimp, *Artemia nauplii,* as the main nutritional supply in heterotrophic consumption studies (Al-Moghrabi et al., 1995; Axworthy & Padilla-Gamiño, 2019; Clayton & Lasker, 1982; Conlan et al., 2018; Fong et al., 2021; Forsman et al., 2012; Hii et al., 2009; Krueger et al., 2018; Piniak, 2002; van Os et al., 2011; Wijgerde et al., 2011, 2012). However, we decided to feed *Nannochloropsis oculate* due to its affinity for light and considering *A. cervicornis'* diet is composed primarily of very small particles (<20µm) (Houlbrèque & Ferrier-Pagès, 2009; Muehllehner, 2013). Tanks resumed circulation after 60-min feeding and a whole system water change occurred the following morning at 8:00am. Corals remained under this regimen for over one month (March 2nd, 2018–April 23rd, 2018) with weekly feeding, algae removal, and coral rotations within each tank. The rationale behind the sprinkler irrigation system was to identify how a reduction in PAR during heat stress impacts coral responses and thermal sensitivity. Similarly, the natural affinity for light in phytoplankton species and the nighttime feeding behaviors of *Acropora cervicornis* led us to evaluate the advantages of LED feeding as the second mitigation intervention. To test interactive

or additive effects on coral physiological and metabolic responses we paired the sprinkler and prey-lure LED treatments. The metabolic and physiological responses under these two stress mediation treatments (sprinkler and prey-lure) are unknown and could produce additive or interactive effects depending on the interaction of these interventions.

Heat Stress

The heat stress experiment took place April 9th, 2018–April 23rd, 2018. Temperatures were raised from ambient 27℃ to 34℃ at intervals of 0.5℃/day in each tank. We measured metabolic activity on coral ramets (n = 48) every second day over 8 temperatures; 27, 28, 29, 30, 31, 32, 33, 34℃ (Fig. 2.2). We performed the heat stress experiment to characterize TPC parameter estimates under a heatwave scenario to find how rapidly increasing temperature affects the metabolic responses with thermal stress loading effects. We chose to use 27℃ as the ambient temperature based on the *in-situ* temperature on the day of coral collection at the Tavernier coral nursery (personal communication Amelia Moura, CRF). To ensure corals were set at their average ambient *in situ* temperature, daily temperature data was obtained from the shallow Conch reef CREMP (Coral Reef Evaluation and Monitoring Program) field site (see Appendix 2; Figure S2.1). Daily temperatures were averaged across 4 years (2018-2021) and compared using a linear model with ANOVA and post-hoc Tukey HSD. Average values were 27.3℃ across the four years, and no significant differences were found between years (see Appendix 2; Figure S2.2). We set up an incubation chamber (chambermaid) in a 142-liter Igloo polar cooler with a second Apex Aquacontroller, heater, and chiller. The chambermaid had recirculating water (Hydor Koralia wave-pump) replaced every testing day and a full spectrum aquarium light (MARS AQUA 300 W LED) was set to 650 ± 3µmol photons $m^{-2}$ $s^{-1}$. We chose this light intensity for metabolic responses based on *in-situ* PAR measurements made by CRF at

the coral nursery where corals were collected in February 2018 (personal communication Amelia Moura, CRF).

Metabolic Responses

For each of the eight temperature trials, eight ramets were randomly assigned into one of six incubation trials (n = 48 corals/temperature, n = 6 incubation trials/temperature). We ensured that at least one ramet from each genotype and each treatment were represented in each incubation, which consisted of eight corals and two control chambers (artificial seawater only) for each thirty-minute incubation period (continuous 15-min dark and subsequent light trial). The control chambers accounted for oxygen consumption and production from any bacteria or microorganisms that may have been within the seawater. The averaged metabolic rate of the two control chambers was subtracted from each corresponding experimental chamber to correct for background metabolic noise. Ramets were transferred from their treatment tank into incubation chambers prior to their randomly assigned trial. Each assay temperature comprised 6 incubation trials which occurred every other day from 8am–6pm (Fig. 2.2). At the end of the 34°C temperature trials (April 23rd, 2018) corals were flash frozen in liquid nitrogen and maintained in a –80°C freezer at UNC for subsequent physiological and 3D surface area analysis.

To estimate thermal performance parameters, we used respirometry to measure temperature dependent oxygen levels to calculate net photosynthesis (*NP*) and respiration (*R*) rates. Oxygen evolution was tracked using a fiber-optic oxygen probe sensor (Pre-Sens dipping probes [DP-PSt-7–10-L2.5-ST10-YP]) in ten, 650-ml closed acrylic incubation chambers. Chambers were filled with temperature specific seawater and corals were secured to the coral frag fastening system then locked into a custom-built motor powered magnetic stirring table with a magnetic stir bar in each chamber (Gould et al., 2021). Corals were loaded into their chambers

and the table was submerged in the chambermaid system at the appropriate temperature. To estimate metabolic rates, a large tarp covered the entire chambermaid system to ensure complete darkness during dark respiration trials (15-min). The lights were subsequently turned on for the net photosynthesis trial (15-min). PAR measurements were quantified before each experimental light trial and raw values of oxygen were recorded with the Pre-Sens Measurement Studio 2 Software (v. 1.2.0.443). *NP* and *R* rates were quantified from raw oxygen data in base R v 4.1.0 (R Core Team, 2021) using repeat local linear regressions in *LoLinR* (Olito et al., 2017). Raw metabolic rates were normalized to surface area estimates for each coral from airbrushed skeletal 3D imaging (n = 6 images/coral fragment) using a NextEngine 3D Scanner (Santa Monica, California) and Agisoft Metashape (v.1.7) software.

Growth Rates

Individual corals were buoyantly weighed to quantify growth rates using a Mettler Toledo 4-place balance (XS105 dual range) with an under pan weighing hook (Jokiel & Maragos, 1978). The balance was placed over a 75.7-liter glass aquarium and filled with artificial seawater. Salinity and temperature of the seawater were measured with an YSI 3200 conductivity probe (Yellow Spring Incorporated, Yellow Springs, Ohio). The change in skeletal growth was calculated as the difference between initial weights (April 5$^{th}$, 2018) and final weights taken after the final heat stress (34°C) respirometry incubation on April 23$^{rd}$, 2018.

*Symbiodiniaceae density, chlorophyll a, and total protein*

One ramet from each of the three genets was flash frozen after the acclimation period and used to compare physiological values after the heat-stress experiment to ensure physiological ranges (protein content, symbiont density, and chlorophyll a) did not exceed normal pre-stress ranges (see Appendix 2; Figure S2.6). Corals (n = 51) were removed from the –80°C freezer and

let thaw for 10-min prior to tissue collection. Coral tissue was removed from skeletons using a 110–120V airbrush compressor (Vivohome, model VH174) with artificial seawater using methodology from Wall (2016). Using a Tissue-Tearor® handheld homogenizer (BioSpec), the resulting tissue slurry (blastate) was mixed, and separated into two samples of 1mL for *Symbiodiniaceae* density analysis. Symbiotic algae densities were determined by conducting two 10µL replicate (n = 4–9) cell counts with a hemocytometer and compound microscope. Total density counts were standardized to total surface area of each individual coral.

Chlorophyll a was extracted from two 1.5mL samples of tissue blastate per coral fragment. Samples were centrifuged at 3,450rpm for 3min and subsequently incubated for 36hr in the dark with 5mL of 100% acetone (Fitt et al., 2000; Jeffrey & Humphrey, 1975; C. B. Wall et al., 2014). Using a spectrophotometer (Thermospectronic model 4.1/4), we measured extracted chlorophyll a samples and averaged absorbance values of the two samples per ramet at 663nm (chlorophyll a), and 630nm (chlorophyll $c_2$). Turbidity and solvent absorbances were corrected with readings at 750nm.

Total protein was quantified using a copper-based colorimetric approach with the BCA Protein Assay Kit (Pierce™ Thermoscientific, 23225). Following the BCA test-tube protocol, duplicate measurements were made for each ramet, and values were averaged. Briefly, 0.1mL of standards (n = 2) and samples (n = 48) were added to 2mL of the working reagent (50:1, BCA reagent A and B) and incubated for 30min at 37℃. After cooling to room temperature, absorbance values were measured, and a standard curve was created from the standards.

Statistical Analysis

Metabolic processes were separated into absolute *NP* and dark *R* values and gross photosynthesis (*GP*) was calculated ($GP = NP+R$) (Hoogenboom et al., 2006; Lyndby et al.,

2018). Oxygen concentrations (*GP* & *R*) were log transformed and each individual coral, the genotypic average, and treatment averages were fit to a nonlinear least square regressing using *rTPC* pipelines in the statistical program base R (Padfield et al., 2021). Regression curves were bootstrapped with ± 95% confidence bands around predictions accounting for uncertainty and TPC parameters were estimated. Parameter metrics were approximated for each coral fragment using parameter calculations in *rTPC* for gross photosynthesis and respiration ($P_{max}$ (*GP*), $R_{max}$ (*R*), *E, Eh,* $CT_{max}$, $T_{Br}$, and $T_{opt}$). Parameter outliers were identified and removed using Cook's distance and no more than 4 individual corals per parameter (n = 48) were removed from subsequent analyses.

ANOVA assumptions were tested with the Bartlett, Levene, and Fligner-Killeen tests for homogeneity of variance and the Shapiro–Wilk's test for normality of residuals. Variables that violated ANOVA assumptions were log transformed and assumptions were tested again. Physiological and parameter data that did not meet assumptions of ANOVA were tested with the non-parametric test Kruskal-Wallis followed by a Bonferroni adjusted post-hoc Dunn test to control familywise error (total protein & chlorophyll a; *GP*-$T_{opt}$, $T_{Br}$, and $CT_{max}$; *R*-$R_{max}$, $T_{Br}$, and $CT_{max}$). Linear regression models were run for each performance metric and raw physiological data that did not violate ANOVA assumptions (*GP*-$P_{max}$, *E, Eh*; *R-Topt*, *E, Eh;* logged symbiont density, and logged percent growth) using the *lm* function in R statistical software including interactions between fixed effects, genotype and treatment. Post-hoc Tukey's HSD tests were performed to reveal significant effects between variables. All raw data and code done in the analyses are presented in a GitHub repository (https://github.com/GouldKate/TPC_Acropora). All analyses were performed using R version 4.0.1 (R Core Team 2017).

## Results

Thermal Performance Curves

Thermal performance curves varied among genotypes and between treatments, (Fig. 2.3). For example, in the prey-lure LED treatment K2 ramets had the highest peak in gross photosynthesis (average $P_{max}$ = 0.764, n =4), but in the control, M5 had the highest peak (average $P_{max}$ = 0.804, n =3) (Fig. 2.3B & D). In the sprinkler treatment, averaged genotypic gross photosynthesis curves (Fig. 2.3A) were tightly associated with abundant overlap, whereas in the control there is wider variation in GP curves across the three genets (Fig. 2.3D). Differences in all (~treatments*genotype) *GP* curvature were analyzed and performance parameters were estimated. We found significant differences for $P_{max}$ (ANOVA $p$ = 0.0082) and $CT_{max}$ (Kruskal-Wallis $p$ = 0.021, K2–M5) (see Appendix 2; Figure S2.4). Performance maximums differed across *GP* treatments between the sprinkler treatment and both the LED (Tukey $p$ = 0.045) and interactive (Tukey $p$ = 0.007) treatments (Fig. 2.4A), however there was no difference between the sprinkler and the control. Overall, gross photosynthesis performance parameters (*E*, *Eh*, $T_{opt}$, and $T_{Br}$) did not differ significantly by treatment, genotype, or the interactive effects between treatment and genotype (see Appendix 2; Table S2.1).

For gross respiration (GR), all thermal performance parameters were significantly different among treatments, genotype, and/or their interaction except for $CT_{max}$ and *E* (see Appendix 2; Table S2.2). Significant differences (GR) were found between the sprinkler and interactive treatment for the $T_{opt}$ performance parameter (Tukey $p$ = 0.028, Fig. 2.4B). We found three performance parameters differed significantly in the interactive effect of treatment and genotype (treatment*genotype; $R_{max}$, $T_{opt}$, and $T_{Br}$), confirming most differences occurred among genotypes. Significant genotypic differences were found across four of the six *GR* parameters with $R_{max}$ differing between genotype M5 and M6 (Dunn $p$ = 0.0064), $T_{opt}$ differed between M6

and K2 (Tukey $p = 0.0065$), and amongst M5 and K2 (Tukey $p = 0.0124$). Thermal breadth ($T_{Br}$) was highest in K2 and differed from the M5 genet (Dunn $p = 0.0234$) and thermal sensitivity *Eh* differed significantly in M5 and K2 (Tukey $p = 0.030$) (see Appendix 2; Figure S2.3).

Physiological data

Physiological data (growth rates, symbiont density, chlorophyll a, and total protein content) was compared between all treatments and genet groupings, which showed a similar pattern to TPC where the greatest differences occurred among genotypes rather than treatments (Fig. 2.5 & Fig. 2.6). The sprinkler treatment had the highest symbiont density (1.90 log cell density ($10^5$ cells $cm^{-2}$) ± 0.563 SD) and differed significantly from the LED treatment (Tukey $p = 0.0119$). While the control and sprinkler did not differ, the latter had the second highest symbiont density (1.89 log cell density ($10^5$ cells $cm^{-2}$) ± 0.557 SD) and varied significantly from the LED treatment (Tukey $p = 0.014$). Genotypic differences followed the same trend where the K2 genotype outperformed either the M5 or M6 genet with significantly higher chlorophyll a content (Dunn $p = 0.0359$, K2–M6) and faster growth rates (Tukey $p = 8.2^{e-05}$, K2–M5 & $p = 0.0084$, M5–M6).

**Discussion**

Our results demonstrate that differences among genotypes were the most prevalent, with five statistically significant metabolic variables among genotypes and two physiological responses. This indicates that the three *Acropora cervicornis* genets used extensively in restoration activity by the CRF vary in their thermal sensitivities and performance under thermal stress and in varying environmental conditions. While coral restoration activities do not currently employ the stress-mediating interventions tested here, the broad responses identified among

genets warrant further investigation into the varied responses during environmental stresses and the benefit of characterizing thermal tolerances and sensitivities.

While our data did not characterize replicate baseline thermal performance curves (control treatment), we believe that all treatment curves provide a basis of understanding genet variability and could benefit restoration practitioners if expanded upon. For example, genets differed significantly for gross photosynthesis parameters $CT_{max}$, and respiration parameters $R_{max}$, $T_{opt}$, $T_{br}$, and *Eh* (see Appendix 2; Figure S2.3 & Figure S2.4), and in chlorophyll a and growth rates (Fig. 2.5 & 2.6). Understanding trait variation in response to warming can help practitioners evaluate evolutionary, biological, and ecological processes which can enhance persistence in coral restoration efforts by addressing the adaptive potential of genets and their responses to changing environments (Baums et al., 2019; Drury et al., 2017).

To fully understand the adaptive potential of corals used in restoration, subsequent research should investigate and identify the endosymbiont community across genets at nursery locations and post-transplantation sites. Although symbiont identity was not determined in this study, past research on these genotypes from the Tavernier nursery tree have found that the M5 and the M6 genotype both house different species of *Symbiodiniaceae* (*Symbiodinium* '*fitti'* A3 and *Cladocopium* respectively) (Yetsko et al., 2020). This may explain the significant differences in respiration performance maximums and growth rates (Tukey $p = 0.0064$ M6–M5 & Tukey $p = 0.00084$ M5–M6), where M6's high respiration rates could indicate less carbon translocation from symbionts reducing growth rate significantly. The K2 genotype's endosymbiont community has not been previously verified, however past studies have found that this genet exhibits significantly faster growth rates and higher bleaching tolerance as found in our study (Baer et al., 2017; Lohr & Patterson, 2017; Ware, 2015).

It has been shown that the dominant *Symbiodiniaceae* species housed within coral tissue can influence physiological expression in corals including thermal tolerance (Berkelmans & van Oppen, 2006; Howells et al., 2011; Jones et al., 2008). However, symbiont identification can be expensive, time consuming, and necessitates genetic analyses, all of which are rare among restoration agencies (Boström-Einarsson et al., 2020). Regardless of the current dominating species of symbiont in nursery genets, restoration activities and environmental stresses on restored reef sites will influence coral survival (Baums et al., 2010). Current bleaching thresholds are dependent on the established coral-algae complex, therefore, understanding coral responses to thermal stress can provide insight into the overall success nursery ready genets have when facing increasing temperatures post transplantation. To improve our knowledge of coral performance after transplantation, thermal performance characterization should be compared at nursery and transplantation sites in addition to symbiont identity to disentangle the effects the environment, genotype, and symbiont have on thermal responses.

The data demonstrates thermal tolerances and sensitivities do differ amongst genets in ambient and treatment conditions (Fig. 2.3) and this information can be utilized immediately by the Coral Restoration Foundation to ensure K2 genotypes are represented in transplantation sites with elevated thermal risk, and to ensure diverse genetic material is available for selection to act on at all sites (Baums et al., 2019; Boström-Einarsson et al., 2020; Drury et al., 2017). It is important to stress the limitations of this study as we had access to only three of the 60 *A. cervicornis* genotypes used by CRF. However, these genotypes are outplanted by CRF yearly and are among the oldest collected genets with K2 (Acer-008) being the first collected genotype in June of 2005, and M5 (Acer-031) and M6 (Acer-032) collected in April of 2008. The three genotypes have also shown consistent spawning in the Tavernier nursery and have been verified

by SNP chip as unique genotypes within the nursery population (personal communication with Amelia Moura, CRF).

In addition to selecting thermally resilient corals, we found that one of our stress-mitigation treatments, use of an irrigated sprinkler system, bolstered coral responses during heat stress. To combat environmental stress (irradiance), reduce bleaching and coral death of newly transplanted corals, we suggest further research exploring the feasibility and potential benefits of using irrigated sprinkler systems at shallow transplantation sites and nurseries during above average heat exposures. Our results indicate an increase in metabolic and physiological functioning under the sprinkler treatment (with nutrient supplementation, i.e., weekly feeding without LED), demonstrating potential benefits if used as a conservation tool, specifically if PAR reduction is increased to or above 50% (Coelho et al., 2017). For instance, the sprinkler treatment had the highest mean symbiont density (mean = 1.90 log $10^5$ cells $cm^{-2}$, SD = 0.563, $p$ = 0.005), which differed significantly from the LED feeding treatment (Fig 2.5A.). While not significant, the sprinkler treatment showed trends in coral physiology with the highest protein content (mean = 1.13mg $cm^{-2}$, SD = 0.326), and growth rates (mean = 1.68 log (%), SD = 0.307). Thermal performance was also significantly different for photosynthetic performance maximum (mean = 0.77 log µmol $O_2$ $cm^{-2}$ $hr^{-1}$, SD = 0.041, $p$ = 0.0115). A prevailing trend in our data was the similarity in thermal performance and physiological responses between the sprinkler and control treatments. No significant differences were identified, however, when compared side by side (see Appendix 2; Figure S2.5). The gross photosynthesis and respiration curves of the corals subjected to the sprinkler treatment were slightly elevated. We believe the sprinkler treatment has the potential to shift coral TPC marginally to the right (higher thermal optimum) if our methodology is revised, enhanced, and prototypes are tested *in situ*.

Due to laboratory restrictions, we could not trigger the sprinkler heads to short bursts of activity, instead corals were exposed to consistently low PAR conditions (25% reduction) for a month prior and during heat stress (Warner et al., 1999). While the reduction in PAR may have been beneficial for our thermal exposure methodology, we believe the overall trends in responses (elevated symbiont densities and increased thermal tolerance at high temperatures) will continue to contribute positively to coral resilience if irradiance is reduced to ~50–70% at daily peak light exposure, and only when temperatures exceed the monthly mean maximum (MMM) (Coelho et al., 2017; Takahashi et al., 2004; Warner et al., 1999). There is a limit to shading however, as Titlyanov et al. (2004) found, exposure to consistently low PAR levels (0.8% of ambient PAR) can cause significant loss of *Symbiodiniaceae* and impact the coral-dinoflagellate symbiosis. Conversely, during periods of low winds and high temperatures, summertime irradiance penetration increases significantly impacting coral bleaching prevalence (Zepp et al., 2008). Based on our results, we believe if this sprinkler mitigation technique is used more precisely (i.e., limited to times of high temperature exposure at daily peak irradiance), the trend in positive responses will continue and this intervention should enhance coral persistence (Cacciapaglia & van Woesik, 2016; Coelho et al., 2017).

While the sprinkler treatment shows potential for altering thermal performance, there are additional considerations associated with the LED feeding treatment and the interactive treatment. For example, the interactive treatment with both an irrigated sprinkler system and LED submersible lights were predicted to result in higher protein content, growth rates, symbiont density, and $P_{max}$ (Wooldridge, 2014). Surprisingly, the interactive treatment differed significantly from the sprinkler treatment in two variables $P_{max}$ (ANOVA $p = 0.007$) and $GR\text{-}T_{opt}$ (ANOVA $p = 0.028$) suggesting photosynthetic rates were elevated and the temperature optimum

during respiration was higher in the sprinkler treatment. This contradicts our assumption that LED lights would contribute to increased protein content (via prey-lure) and respiration rates by extension (Houlbrèque et al., 2004; Rodolfo-Metalpa et al., 2008). There were no differences found between the interactive treatment and the LED treatment for physiological or metabolic responses, except for one interaction across genotypes in growth rate between the M6 genet in the interactive treatment and M5 in the LED (Tukey $p = 0.0375$). The similarities between the interactive and LED treatments show that the effects of both sprinkler and LED do not have an interactive or additive effect on thermal responses.

Further, the LED feeding treatment had significantly lower photosynthetic maximum (ANOVA $p = 0.045$, see Appendix 2; Figure S2.4A) than the sprinkler treatment and symbiont density in both the sprinkler and control respectively (ANOVA $p = 0.0119$, $p = 0.014$, Fig. 2.4A). Although the submersible lights were shown to attract *Nannochloropsis oculate* (personal observations) closer to the lights and corals, heterotrophic consumption was not assessed, and protein content was not significantly altered. Instead, the LED lights may have disrupted the symbiont's nighttime cellular repair processes which are essential for photosynthetic machinery operation (Hill et al., 2011) Following the completion of this study, multiple reports were published showing the negative impacts of LED lights on the coral-algae symbiosis, ranging from loss of symbionts and chlorophyl content to overproduction of reactive oxygen species (Ayalon et al., 2019; Levy et al., 2020). These studies exposed corals to LED lights from sunset to sunrise (~12 hours) which explained the significant effects on photoinhibition. Our study had minimal exposure to LEDs (1 hour weekly) but still produced the lowest density of symbionts compared to the other treatments (Fig. 2.5A). Additionally, it was found by Ayalon et al. (2019) that white LED lights when compared to blue and yellow, showed the greatest alteration in

performance, which could explain the loss of symbionts in our LED treatment. Further exploration into the use of lights as a prey-luring mechanism should explore the use of blue LED collimated lights as an attractant. The most recent study into prey-luring systems was by Ben-Zvi and colleagues (2022) who found that plankton prey prefers fluorescent cues, and the use of blue lights enhanced coral's natural fluorescent cues which resulted in higher rates of coral predation. Additional research into the "light trap hypothesis" (Ben-Zvi et al., 2022) should develop methodologies that use blue collimated LED cues rather than white LED signals, which may have contributed to the pattern observed in this study.

Overall, estimating thermal sensitivities of genets is worthwhile, potentially driving conservation tactics. This information could, in theory, improve conservation outcomes especially when planning and implementing programs such as assisted gene flow, migration, and/or relocation initiatives. Understanding which genet performs best in certain environments (temperature range limits) could hypothetically maximize success. Similarly, knowing the thermal sensitivities of genotypes can be helpful in interventions such as assisted breeding, outcrossing, hybridization, and cryopreservation techniques by choosing genets with large thermal ranges and low thermal sensitivities for breeding (Baums, 2008; Boström-Einarsson et al., 2020; van Oppen et al., 2015; Young et al., 2012). The results from this research can be used directly by the Coral Restoration Foundation to influence how they utilize each genotype and may inform decisions that require understanding how thermal physiologies differ amongst genets. For example, the K2 genotype had the highest fitness overall with significantly elevated chlorophyll a concentrations and growth rates (Fig. 2.5D & 2.6C). The elevated growth rates could be attributed to increased carbon translocation in the coral host due to the elevated chlorophyll a levels, which in turn could also play a role in higher thermal optimum and

maximum, wider thermal breadth, and lowered deactivation energy of genotype K2. These results could also be contributed to the symbiont community within the K2 genet, however, current practices generally outplant corals directly from nurseries without altering the symbiont community as strain composition is known to change (O'Donnell et al., 2018). The current thermal performance of genets may be more indicative of success post transplantation, however more research into survival is needed. Conservation managers can target thermally tolerant genotypes for selective breeding programs or integrate a higher number of ramets with others *in situ* to ensure maximum fitness is maintained in the population and genetic pools include the highest performers.

The results from our study indicate that the greatest variation in thermal performance is between genets and we recommend restoration groups consider characterizing thermal tolerances of all available genets to identify those expressing phenotypic plasticity in performance and thermal optimums. Identifying thermally plastic corals can alter the shape and curve of TPCs in different environments, which can then serve as a basis for adaptation in the wild at restoration sites (Baums et al., 2019; Drury et al., 2017; Schulte et al., 2011). These characterizations will be integral in deciding which genets to restore at specific sites based on environmental data and knowledge of local sites used for restoration. By identifying the most resilient coral genets, practitioners can focus on maximizing survival and supplementing genetic diversity by creating sites with both thermally tolerant genets and those which may be locally adapted. We believe integrating coral thermal tolerance assessments and pre-selecting thermally resilient corals (genets) with the complementary use of an irrigated sprinkler technique has the potential to benefit coral persistence on small local scales.

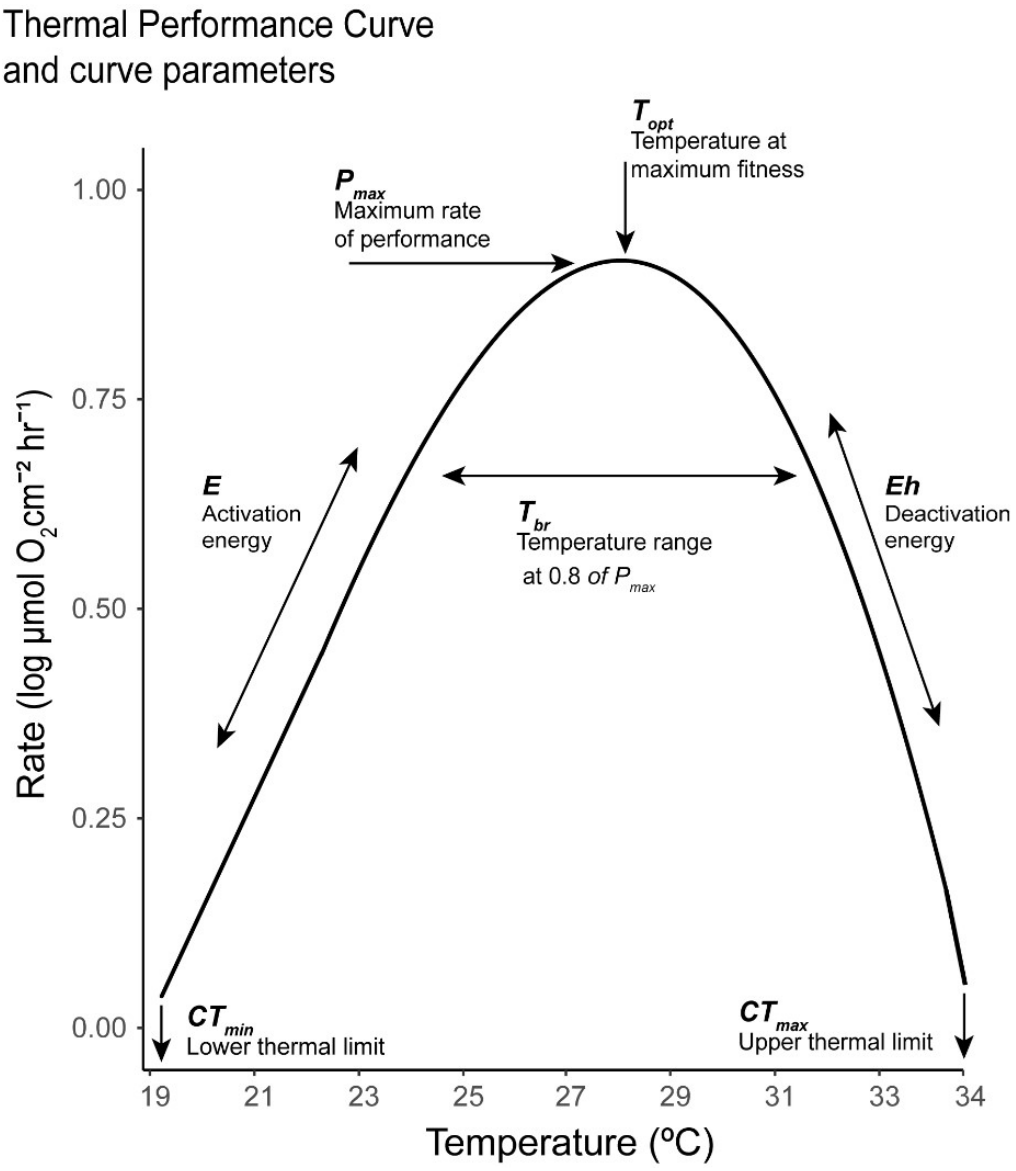


**Figure 2.1 Hypothetical thermal performance curve and parameters**

Thermal performance curve denoting parameter metrics ($CT_{min}$, $E$, $P_{max}$, $T_{opt}$, $Eh$, $CT_{max}$, and $T_{br}$). In this study we estimated and compared thermal sensitivities, $E$, $Eh$, $T_{br}$, peak performance rates $P_{max}$, and thermal parameters $T_{opt}$ and $CT_{max}$ for gross photosynthesis in coral associated *Symbiodinaceae* and gross respiration in the Caribbean coral *Acropora cervicornis*.

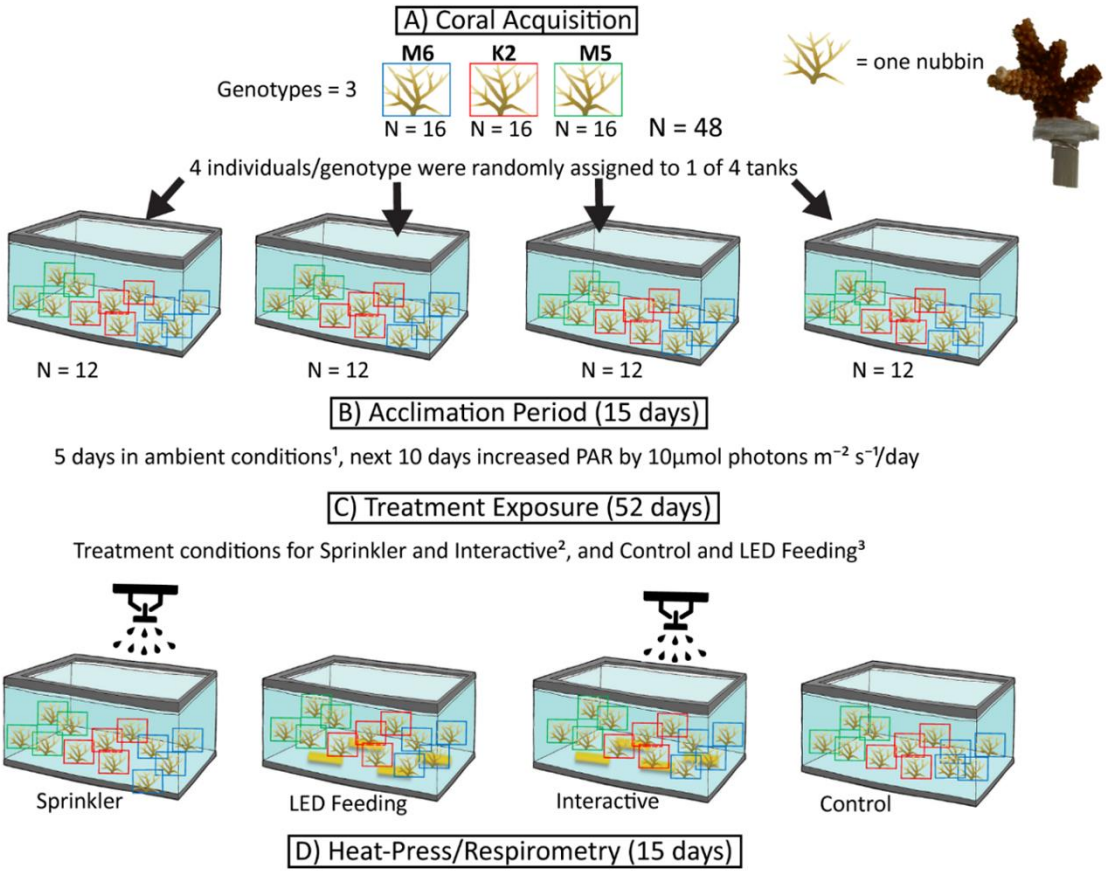


| | Day 0 | Day 1 | Day 2 | Day 3 | Day 4 | Day 5 | Day 6 | Day 7 | Day 8 | Day 9 | Day 10 | Day 11 | Day 12 | Day 13 | Day 14 |
|---|---|---|---|---|---|---|---|---|---|---|---|---|---|---|---|
| Temperature at 7am | 27°C | 27.5°C | 28°C | 28.5°C | 29°C | 29.5°C | 30°C | 30.5°C | 31°C | 31.5°C | 32°C | 32.5°C | 33°C | 33.5°C | 34°C |
| Respirometry | Yes | No | Yes | No | Yes | No | Yes | No | Yes | No | Yes | No | Yes | No | Yes |
| Temperature at 7pm | 27.5°C | 28°C | 28.5°C | 29°C | 29.5°C | 30°C | 30.5°C | 31°C | 31.5°C | 32°C | 32.5°C | 33°C | 33.5°C | 34°C | Corals Frozen |

**Figure 2.2 Experimental set up and heat stress methodology**

Methodological procedure from A) coral acquisition and tank assignments, B) laboratory acclimation period, C) treatment setup and exposure to corals, and D) schedule of respirometry and heat stress temperature increases. In B)[1] ambient condition consisted of a PAR at 450 ± 3µmol photons $m^{-2}$ $s^{-1}$, 35ppt salinity and 27°C. For B)[2] sprinkler and interactive treatment were set to 450 ± 3µmol photons $m^{-2}$ $s^{-1}$, 35ppt salinity and 27°C. In B)[3] the LED feeding and control treatments were set to 650 ± 3µmol photons $m^{-2}$ $s^{-1}$, 35ppt salinity and 27°C. Yellow rectangles represent LED lights set underneath corals nubbins in the LED feeding and Interaction tank.

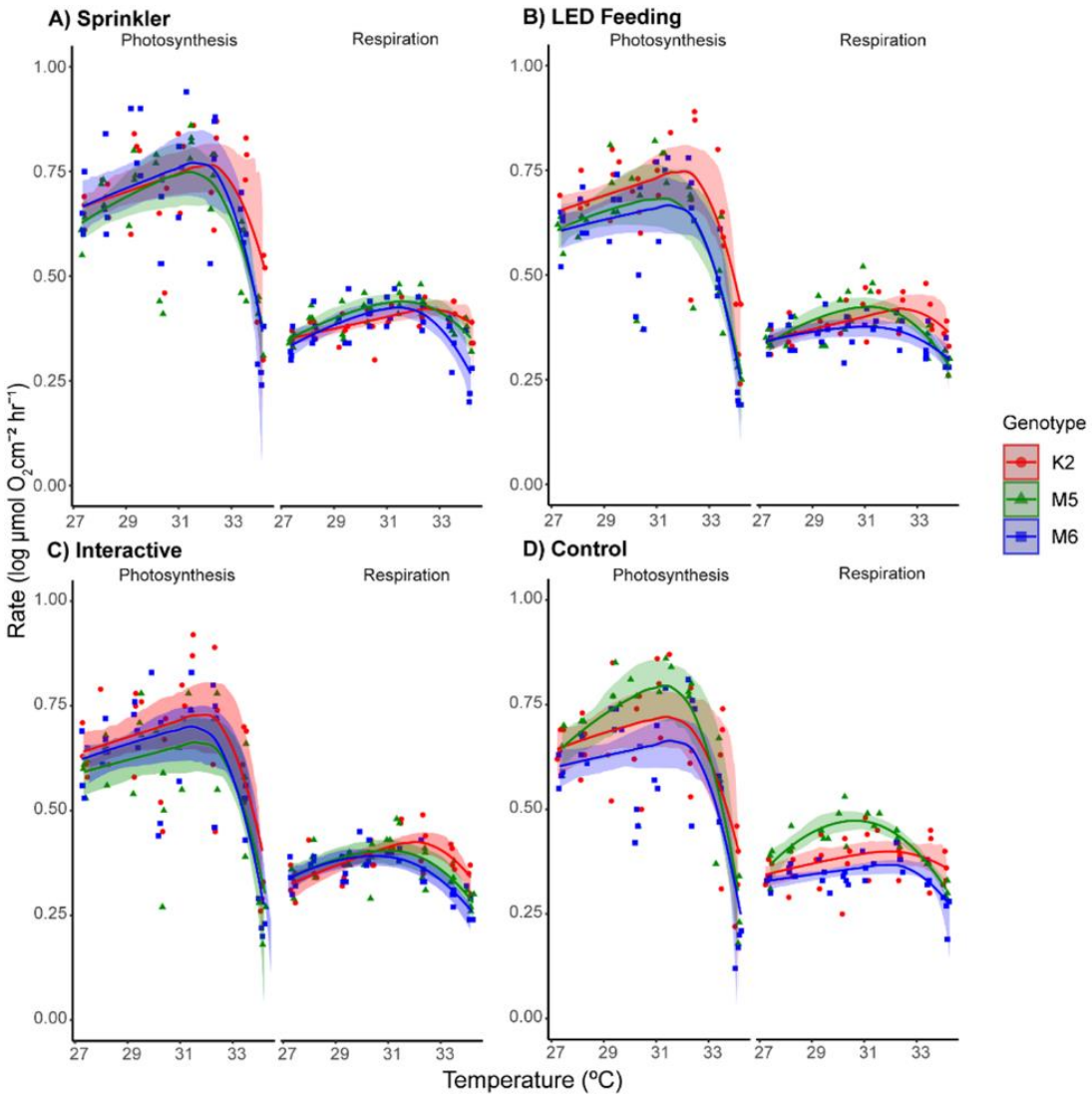


**Figure 2.3 Genotype-specific thermal performance curves**

Gross photosynthesis (Photosynthesis panels) and respiration (Respiration panels) for mass-specific change in oxygen across three genets (n =48) for eight temperatures. Fitted lines (green, red, and blue) represent medians from four ramets in each genotype within each of the four treatments. Transparent green, red, and blue represent ±95% bootstrap confidence bands. Each red circles (K2), green triangles (M5), and blue squares (M6) represent one ramet in each treatment; A) irrigated sprinkler system; B) LED feeding; C) interaction with sprinkler and LED feeding; and D) control. Individual ramets were measured at each of the 8 temperatures resulting n =96 metabolic rate points for each photosynthesis and respiration curve except for in the control (D.) where the fragment M50Cd was removed due to outlier status (n = 88 In the green M5 average genotype curves).

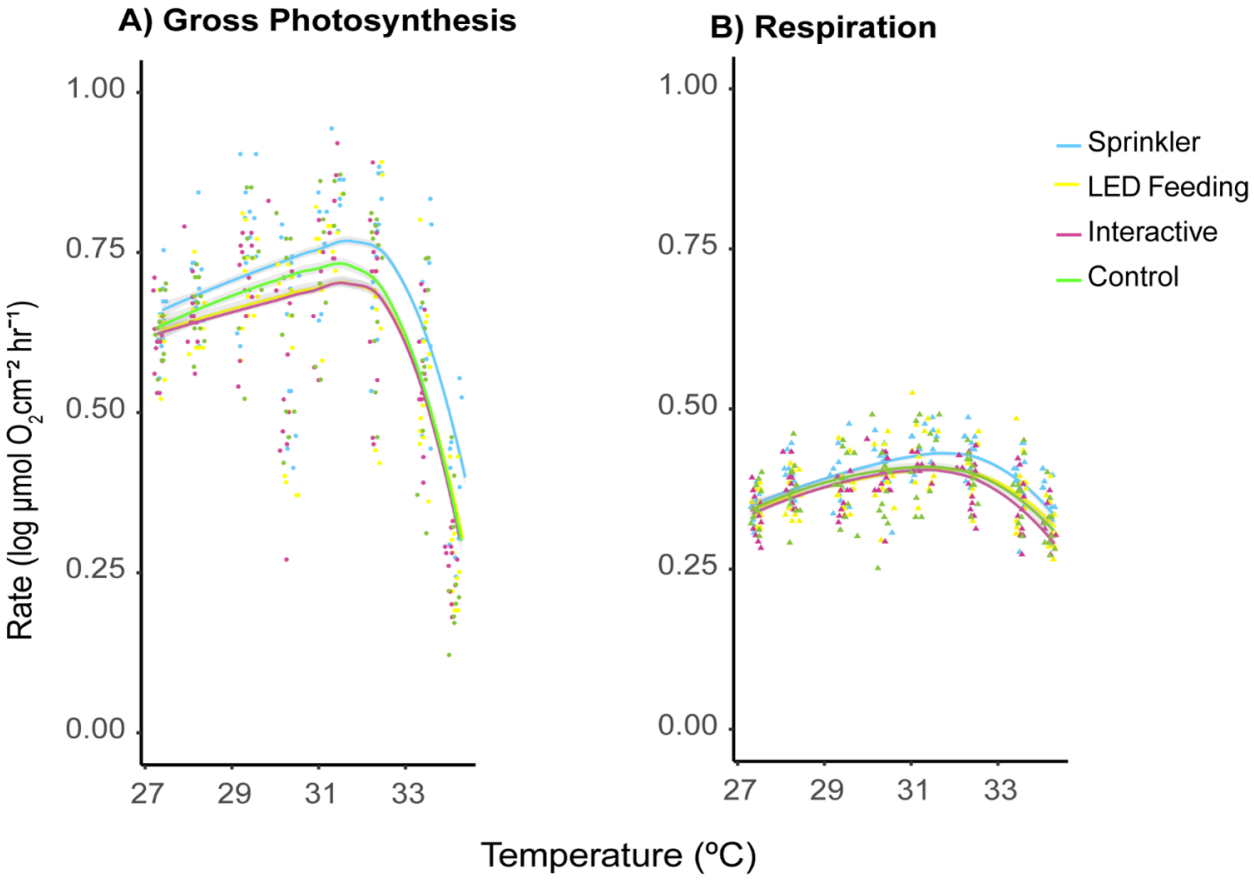


**Figure 2.4 Thermal performance curves by treatment**

Gross photosynthesis (A) and respiration (B) for mass-specific change in oxygen for each treatment. Fitted lines are medians from 12 ramets in each treatment, blue = sprinkler, yellow = LED feeding, pink = interactive, and green = control. ±95% bootstrap confidence bands have been removed for ease of viewing. Ramets (n =12/treatment) are represented by circles (photosynthesis) and triangles (respiration) in colors of each treatment.

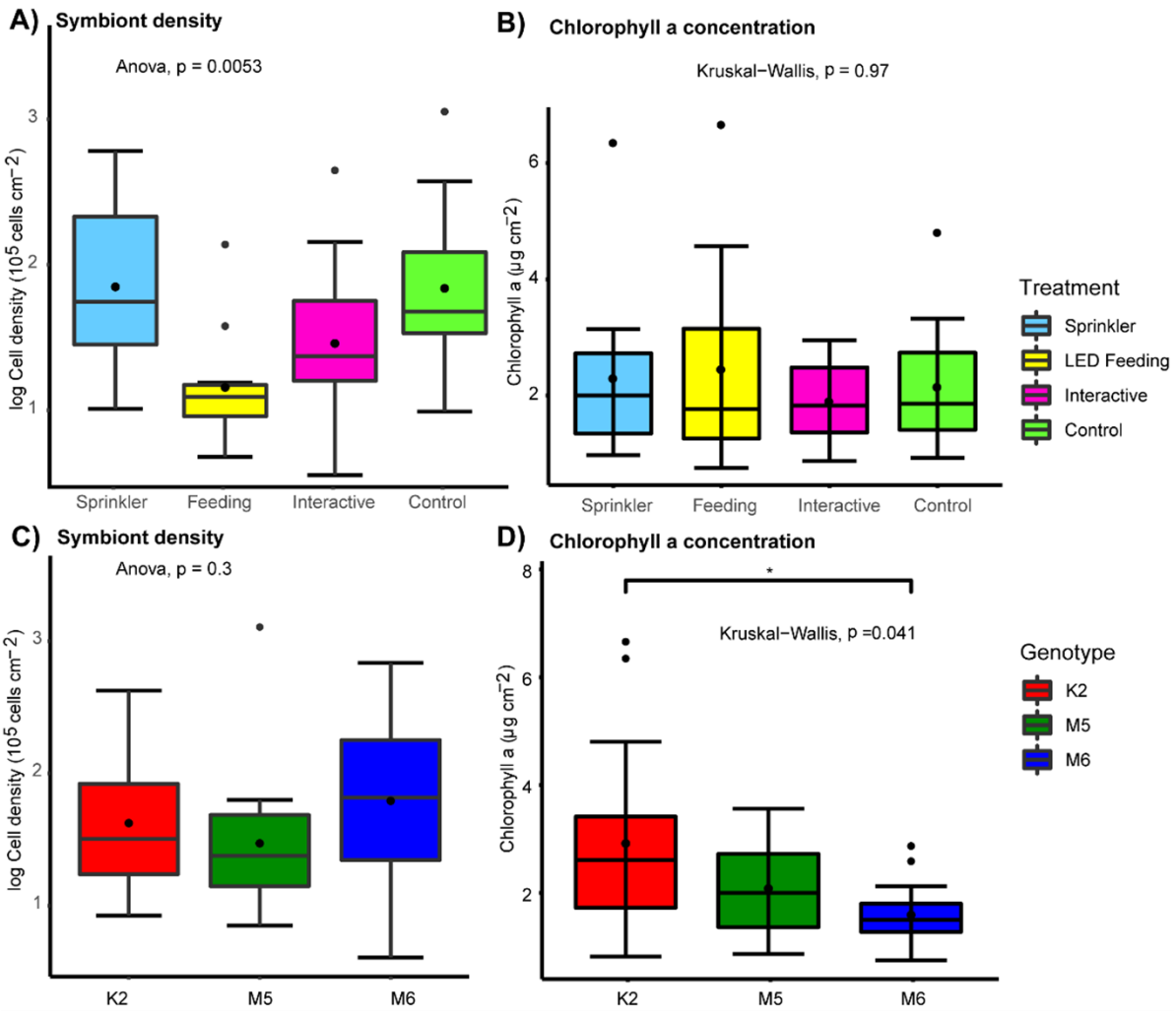


**Figure 2.5 Symbiont physiological comparisons**

Box and whisker plots for symbiont physiology between treatments (A and B) and genets (C and D) for symbiont density (A & C) and chlorophyll a content (B & D). Centerlines show the median values (n = 48), black circles are means, and whiskers are 1.58*IQR (inter-quantile range) upper and lower ranges. Light blue boxes represent the sprinkler treatment, yellow is the feeding treatment, pink is the interactive treatment, and the control is green. Genets are depicted as K2 is red, green as M5, and dark blue boxes are M6.

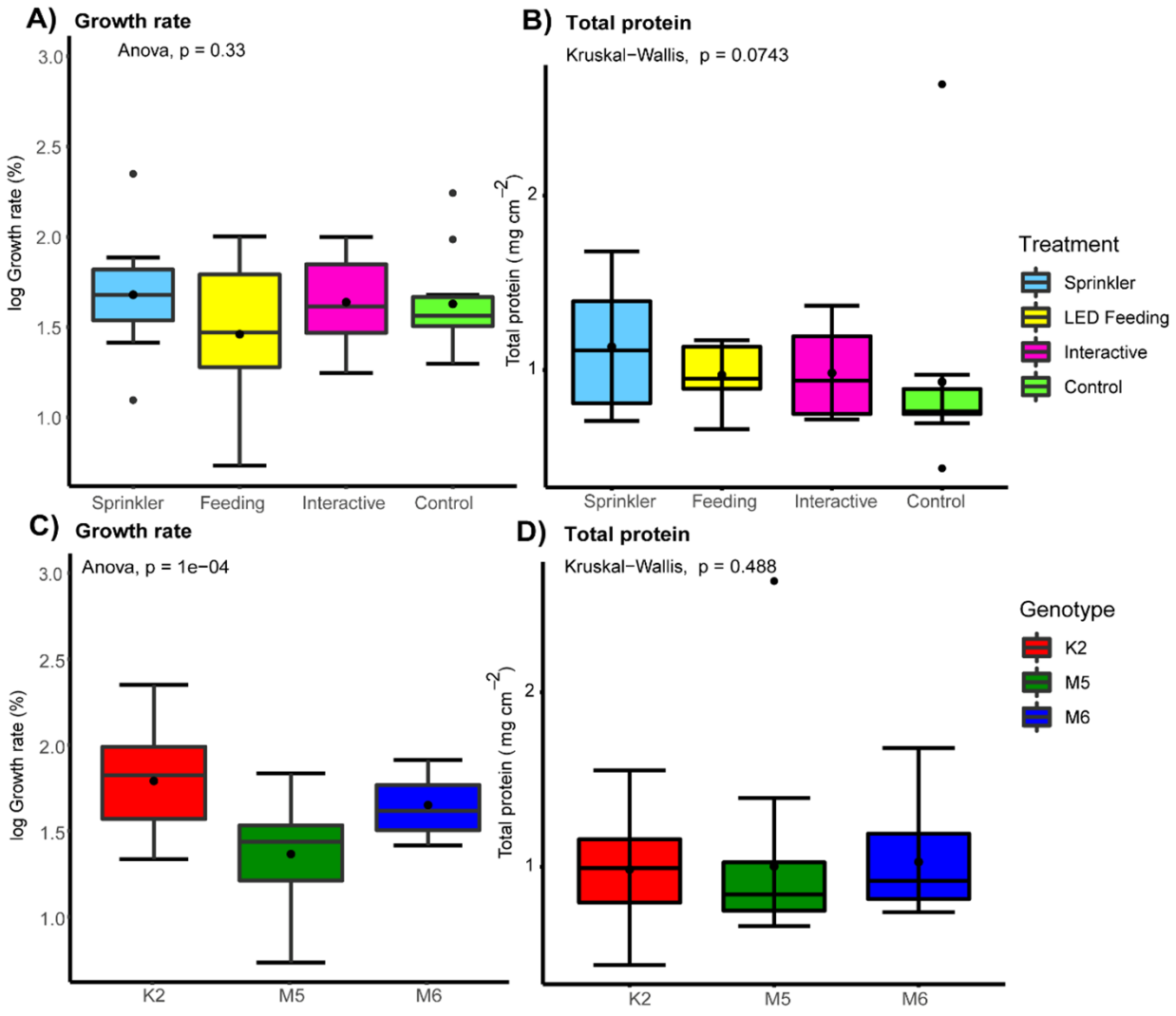


**Figure 2.6 Host physiological comparisons**

Box and whisker plots of coral physiology between treatments (A and B) and genets (C and D) for growth rates density (A & C) and total protein content (B & D). Centerlines show the median values (n = 48), black circles are means, and whiskers are 1.58*IQR (inter-quantile range) upper and lower ranges. Light blue boxes represent the sprinkler treatment, yellow is the feeding treatment, pink is the interactive treatment, and the control is green. Genets are depicted as K2 is red, green as M5, and dark blue boxes are M6.

# CHAPTER 3: CORAL GENOTYPE AND SITE INFLUENCE SURVIVAL, HEALTH, AND METABOLISM OF RESTORED *ORBICELLA ANNULARIS* CORALS ACROSS THE FLORIDA REEF TRACT

## Introduction

The scleractinian framework-building *Orbicella* species complex (*annularis, franksi*, and *faveolata*) once dominated shallow coral reefs of the Greater Caribbean (Budd & Johnson 1999; Jackson 1992; Precht & Miller 2007), However, over the last 25 years this species complex has experienced dramatic declines (Aronson & Precht 2001a; Bruno et al., 2019; Edmunds 2007; Kuffner & Toth 2016; Moulding & Ladd, 2022). In recent decades, species composition in the Florida Reef Tract (FRT) has diverged from previously stable baselines dominated by reef-building corals (90% *Acropora* and *Orbicella* spp.) to assemblages dominated by "weedy" species (*Porites astreoides* and *Siderastrea siderea*) (Toth et al., 2019). Additionally, long-term monitoring in the Florida Keys has revealed no evidence of coral recovery in total coral cover or reduction in macroalgae abundance over decades of study (Porter & Meier 1992; Somerfield et al., 2008; Ruzicka et al., 2013).

The decline in coral due primarily to temperature stress (Hughes et al., 2018; Eakin et al., 2019; McClanahan et al., 2019) has elicited an increase in coral restoration, which is primarily focused on transplanting fast-growing branching corals (e.g., *Acropora* spp.). While these practices often result in post-transplantation survival of ~60–70% (up to 18 months of monitoring), species in the genus *Orbicella* have frequently been overlooked (Boström-

Einarsson et al., 2020). Due to their slow growth rates, these species have only recently been included in active coral restoration projects (<5%) (Boström-Einarsson et al., 2020). However, incorporating *Orbicella* spp. into restoration activities could optimize reef recovery and enhance coral preservation better than *Acropora* spp., which are highly susceptible to mortality from disease and bleaching events (Aronson and Precht, 2001b; Muller et al., 2018). In addition, *Acropora* is subject to post-depositional loss due to its delicate branching morphology (Enos & Perkins, 1977; Shinn et al., 1982, 2003). Therefore, for the best long-term investment and achievement of conservation goals, including a hardier coral species like *Orbicella annularis*, may improve reef persistence and recovery (Toth et al., 2019).

Coral restoration is still in its infancy. Projects around the world are adopting multiple techniques and methodologies that are often inadequately designed, lack clear objectives, and have limited monitoring (Boström-Einarsson et al., 2020). For instance, restoration strategies have yet to embrace approaches that account for genetic by environmental factors (GxE) influencing survival (Baums, 2008), despite preliminary work addressing this topic in the field (Bliss, 2015; Drury et al., 2017). This may be due, in part, to the assumption that corals act as an "open" system, characterized by planktonic larvae connecting coral populations through high levels of gene flow (Hellberg, 2006). While gene flow increases genetic diversity by mixing potentially adaptive genetic variation between populations, restoration projects attempt to enhance gene flow by haphazardly transplanting corals of various genotypes onto vulnerable natural reefs (Carnicer et al., 2017). However, current evidence of local recruitment in corals opposes the "open" system view (Hellberg, 2006; Kenkel et al., 2015; Solè-Cava & Thorpe, 1991) challenging the effectiveness of increasing genetic diversity via transplantation efforts (Baums, 2008). An alternative to this current approach is to identify which genotypes currently

outperform (metabolically and physiologically) others across multiple sites and transplant those successful genets according to the environment in which they perform best. Matching coral genotypes to environments in which they thrive may increase effective gene flow with natural populations and provide the greatest chance of local recruitment and potentially increase reef resilience.

The capacity of corals to acclimatize to environmental stressors are vital to understanding their long-term persistence in changing environments (i.e., global climate change) (Valladares et al., 2014; Van Oppen et al., 2015). Local adaptation and acclimatization are influenced by the environment and genotype of individuals, which determines responses to novel environments. Phenotypic plasticity is the ability of a genotype to express distinct phenotypes in various environments and is critical under rapid environmental changes because it is a short-term response occurring within one generation (Hochachka & Somero, 2002). The extent of plasticity varies among genotypes and can positively influence acclimatization to novel environments (Simpson 1953; West-Eberhard 1989; Kelly 2019), and when high levels of intraspecific plasticity are evident, it has been suggested that plasticity itself is evolving in populations (Scheiner 1993; Pigliucci 2005). In restoration scenarios, transplanting highly plastic individuals may have a selection advantage if plasticity produces phenotypes with higher fitness than locally adapted individuals, or is less energetically costly to maintain (Dewitt et al., 1998; Hendry, 2016).

Adaptation is a genetic response which occurs over generations and is driven by recurring or consistent environmental pressures and genotypic profiles (Nelson et al., 2007). While current coral restoration activities base transplantation methodology on the assumption that local adaptation does not occur in marine organisms (Hellberg, 2007), recent evidence suggests high

levels of population structure diversity even within individual reefs (Drury et al., 2016; Voolstra et al., 2021; Baums, 2008; Thomas et al., 2017; Devlin-Durante & Baums, 2017). Therefore, to understand the extent of local adaptation and plasticity among coral genotypes, transplantation studies assessing coral health and survival along environmental gradients can illuminate intraspecific plastic and adaptive responses, which can serve to improve restoration programs (Todd, 2008).

To date, coral performance metrics in translocation and GxE studies have primarily assessed survival, growth rates, disease prevalence, and physiological data (symbiont density, chlorophyll a content, and protein) to understand coral responses to transplantation, bleaching, and recovery processes (Barott et al., 2021; Bliss, 2015; Drury et al., 2017; Ladd et al., 2017; Pausch et al., 2018; Million et al., 2022). While these responses are important in understanding coral susceptibility and performance across multiple sites, metabolic data links the rate of energy use and uptake to the distribution of resources for coral survival (Brown et al., 2004). Supplementing coral tissue health response data with metabolic data (net photosynthesis rates) provides a more robust understanding of coral resilience across environmental locations, specifically when considering thermal threats.

In this study, we used a transplantation design to analyze fitness across four genotypes of *Orbicella annularis* corals currently used by the Coral Restoration Foundation (CRF) in Key Largo, Florida. The goal of this study was to quantify health responses in four genotypes of *Orbicella annularis* corals transplanted at four reef sites spanning the FRT. The CRF provided the four genotypes used most in their restoration program for this study. Specifically, we tested for differences in tissue health (presence and absence of disease, tumors, boring animals, and blotchiness; percent tissue health, mortality, bleaching, paling, and algae overgrowth) and

metabolic (net photosynthesis rates) responses across genotypes and sites to identify the possible mechanisms (adaptation and/or acclimatization) driving resilience in corals post-transplantation.

The Florida Reef Tract is the third largest barrier reef in the world and was designated as a marine sanctuary in 1990 (Lapointe & Matzie, 1996). The reef tract is partitioned into four regions: Upper Keys, Middle Keys, Lower Keys, and Marquesas based on environmental variations and geographical components (Ginsburg & Shinn, 1995). Since 1996, the Coral Reef Evaluation and Monitoring Project (CREMP) has been monitoring the benthos and logging environmental data at 40 reef sites, including the four reef sites used in this study, which occupy the Upper, Middle, and Lower Keys (Carysfort, Conch Reef, Tennessee Reef, and Looe Key). CREMP has reported a decline in species richness and coral cover with no significant recruitment levels since 1996 (Ruzicka et al., 2013). Overall, there has been severe loss of coral cover and abundance following disease outbreaks (white plague and stony coral tissue loss disease (SCTLD)) and six mass bleaching events from 1987–2014 resulting in nearly 90% loss in corals (Donovan et al., 2020; Gardner et al., 2003; Precht et al., 2016; Walton et al., 2018).

Due to multiple interacting currents (Florida Current, the Gulf of Mexico Loop Current, and the Southwest Florida Shelf currents), flow from the Everglades via the Shark River Slough, tidal exchange between the Florida and Biscayne Bay, and freshwater discharge sites along the Florida Keys, the FRT regions vary in their physical, chemical, and biological composition (Boyer & Jones, 2002). Therefore, water quality differs across the FRT boundaries, and regions do not represent enclosed ecosystems (Gibson et al., 2008). The transplantation sites for this study were within shallow reef assemblages, which have not shown regional trends in community structure based on geographical position. Rather the Upper and Lower Keys have been shown to be more similar to each other than those from Middle Keys in community

structure (Jaap et al., 2008). However, Maliao et al. (2008) using a 5-year data set, found differences in water quality across the FRT regions where the main parameters driving variation were temperature, salinity, dissolved oxygen, chlorophyll a, total phosphorus, and turbidity. Variation was found for total water quality and coral cover across the three regions, placing the Upper and Middle Keys into a group that was significantly different than the Lower Keys region. The Upper and Middle Keys were roughly homogenous with lower water quality, salinity, temperature, dissolved oxygen, chlorophyll a, and turbidity than the Lower Keys. However, previous research contradicts these findings which revealed decadal patterns in water quality in the FRT and found the poorest water quality occurs in the Middle Keys region (Lapointe & Clark, 1992) differing from the Upper Keys and the highest water clarity region in the Lower Keys (Boyer & Jones, 2002; Szmant & Forrester, 1996; Klein & Orlando, 1994).

Based on regional variation in temperature, water quality data, and overall geography along the FRT, we hypothesized that all four genotypes, which were originally collected from one of our transplantation sites (Conch Reef, Upper Keys), would have higher survival, photosynthetic rates, and health outcomes (increased healthy tissue, decreased bleaching, paling, mortality, and algae overgrowth) when compared to the two more southern sites Tennessee Reef (Middle Keys), and Looe Key (Lower Keys), with similar outcomes at Carysfort which also occupies the Upper Keys region. We expected to find evidence of intraspecific variation in coral health responses due to genetic variation across genotypes, resulting in GxE interactions. Specifically, this study answered the following questions: 1) Are *Orbicella annularis* corals locally adapted to their "home" reef (Conch Reef) or region? and 2) Is there a difference in survival outcomes and health responses across sites and genotypes?

## Materials and Methods

Coral Acquisition and Health

On February 4th, 2019, the Coral Restoration Foundation provided 64 individual corals from four genotypes (16/genotype) taken from their Tavernier nursery tree (N 24°58'55.6" W 80°26'9.999" at ~9.5m) using SCUBA. Corals were removed from the tree and tagged as "A" which represents the Coral Restoration Foundations nomenclature for OANN-1, "B" (OANN-17), "C" (OANN-18), and "D" (OANN-23). All four genotypes were collected from wild colonies located on the back reef at Conch reef (see Appendix 3; Figure S3.1). OANN-1: A was collected in 2013 and OANN-17: B, 18: C and 23: D were collected in the summer of 2016. All genotypes were taken to the Tavernier nursery tree located a maximum of 2.9km from original collection sites and ~4km from the transplantation table location at Conch reef. After tagging corals, a subset of individuals (n= 32, 8/genotype) were measured for oxygen evolution (1 sec intervals) for four-min to quantify their photosynthetic rate using the CISME respirometry diving device (Community In situ MEtabolism, Qubit Systems CISME instruments LLC, Fig. 3.1). This portable closed-system respirometer is a non-destructive and non-invasive approach to measuring changes in oxygen. Individual corals were set in a flow cup and securely closed inside the incubation chamber and set to a flow rate of 950mL $min^{-1}$ and light levels to 975µmol $m^{-2}$ $s^{-1}$ throughout the duration of the experiment. These settings were prescribed by the CISME's inventor Dr. Alina Szmant from the University of North Carolina Willington (personal communications).

Subsequently, all corals that were to be transplanted to one of the four sites underwent a health assessment which was repeated in May, August, and December of 2019 including CISME measurements on a subset of individuals (n= 32, 8/genotype). Health was quantified by using a

presence/absence approach for tumors on living coral tissue, organisms such as polychaetes that bore into coral skeletons, signs of diseases, and overall blotchy tissue. Using the AGRRA (Atlantic and Gulf Rapid Reef Assessment) coral indicators guide and protocol we estimated the percent of total tissue condition of each individual coral for the following parameters: healthy, white, mortality, algae overgrowth, and pale (Kramer, 2003), with 100% tissue quantified by healthy, white and mortality, with pale and algae overgrowth making up a percentage of healthy and mortality respectively.

After the first initial CISME and health assessments, four corals from each genotype grown on ceramic frag plugs (Tavernier nursery) were randomly chosen and secured to one of four 30x90cm platforms (made of non-toxic HDPE flexible plastic mesh fencing material) using latex castration bands on the underside of the mesh top and placed tightly over ceramic plug base. The mesh served as the tabletop of the four transplantation tables (Fig. 3.1) and was transferred into a cooler filled with seawater on location and subsequently transported to the Florida Institute of Oceanography Keys Marine Lab on Long Key, Layton Florida. Mesh tabletops with 16 secured corals were placed into a 511-liter outdoor mesocosom raceway supplied with filtered sea water from Florida Bay. From February 6$^{th}$–7$^{th}$ coral tables were deployed at the four target reefs (Fig. 3.2): Conch Reef (N 24°57’22.3” W 80°27’26.8”) Carysfort (N 25°12’24.3” W 80°13’16.1”), Tennessee Reef (N 24°44’43.8” W 80°46’54.8”) and Looe Key (N 24°32’48.058” W 81°24’11.1”) under the Florida Keys National Marine Sanctuary permit #FKNMS-2018-165. Four enamel covered fence t-posts were hammered into sandy substrate <2m from living reef and mesh tabletops were secured to posts with zip ties (Fig. 3.1). Subsequent CISME and health monitoring surveys were done May 27–29$^{th}$, August 2–5$^{th}$, and December 14–17$^{th}$, 2019 and due to travel restrictions during the COVID-19 epidemic coral

tables were removed May 30–June 3rd, 2021. All surviving corals were then permanently transplanted at each reef location.

Colony-level tissue health was determined by estimating percent coverage of health parameters for each individual coral at each site and recorded February, May, August, and December 2019. Healthy tissue meeting a score of 5 or 6 on the CoralWatch coral health chart (see Appendix 3; Figure S3.2) were considered healthy tissue and a percent of total living tissue with this color was approximated. Tissue scoring a 2–4 was considered pale tissue, and a score of 1 was regarded as bleached. Tissue mortality was scored by signs of exposed skeleton without living tissue present. Dead tissue was approximated with and without algae overgrowth and separated into total mortality which included percent algae cover over previously living tissue, and total algae overgrowth did not include recently dead tissue without algae.

Site Selection

The four transplantation sites used in this study were haphazardly chosen from restoration sites currently used for coral transplantation by the CRF. All transplantation sites were located roughly 9.6km seaward of Florida's archipelago coast and are considered bank reefs composed of spur and groove formations (Shinn, 1963). Each reef site has a reef crest at 5–10m depth adjacent to a sloping fore-reef which extends down to 30–35m. Reefs are characterized as having spur and groove formations which break into patch reefs seaward of the reef crests (Leichter et al., 2003). All transplantation tables were deployed at each site in a sandy patch adjacent to living reef structures (<2m). Fence posts were driven into the sandy substrate (7–8m depth) using a fence post driver until 60cm of posts were above the benthos. The tabletop mesh with attached corals were then zip tied to the four posts 30cm above the benthos to ensure water circulation and to avoid sedimentation. Tables were the preferred method of transplantation to ensure easy

access to each coral for CISME measurements which required corals to be placed inside the device's incubation chamber.

Temperature and Environmental Data

Temperature data from January 2019–January 2020 was accessed from the Coral Reef Evaluation and Monitoring Program's (CREMP) *in situ* temperature probes located at each of the four transplantation sites in this study. Probes were located at ~7.5m depth and ~ 0.5–1.60km away from each transplantation table deployed in this study. Temperature data was separated by site, and we compared daily, monthly and yearly means, maxima, and ranges using linear *lm* models in R statistical software at an 0.05 alpha to determine significant effects. Due to variability in water quality parameters over time in the FRT, we retrieved *in situ* environmental data collected from the Southeast Environmental Research Center's (SERC) water quality monitoring network from February 2019–January 2020. We evaluated differences across ten water quality measurements taken at each individual site. All parameters were collected at depth (temperature, total nitrogen (TN), total phosphorus (TP), ratio of nitrogen to phosphorus (TN:TP), salinity, dissolved oxygen (DO), total organic carbon (TOC), and light attenuation coefficient (Kd)), except for chlorophyll a, and % $O_2$ saturation, which were collected on the surface at each reef site. Using Principal Component Analysis (PCA) we determined the percent variance explained by the environmental parameters of the reef sites. The PCA was performed on scaled and centered data using the *prcomp* function in the Vegan package (Oksanen et al., 2007). The clustering analyses showed no significant differences in environmental parameters across sites during 2019 and health outcomes were analyzed with the more in-depth CREMP temperature data (see Appendix 3; Figure S3.3).

Statistical Analyses

The *lm* function in R was used to analyze CREMP temperature data. Using ANOVA and Tukey's HSD post hoc tests for pairwise significance we compared temperatures across sites and time. To identify differences in monthly thermal histories we compared each site to a 0.05 alpha using the same methodology.

A census of living corals was recorded for survival analyses at each survey time points (February, May, August, and December). Survival curve estimates were approximated using two methods: a non-parametric Kaplan-Meier estimation approach and parametric regression models to extrapolate survival outcomes (across sites, genotypes, and genotypes at each site) past the censored timeframe using Gaussian (reef site and genotype) and extreme (interaction of genotype and site) distributions. Survival curves were estimated in R using the *survfit* (Kaplan-Meier) and *survreg* (regression models) functions in the *Survival* package (Therneau & Lumley, 2010). Data was right-censored and missing corals were excluded from the analyses (n= 6). To determine whether health outcomes influenced survival, we ran several Cox proportional hazards (CPH) regression models using the *cox.zph* function in the *Survival* package and extracted hazard ratios (HR). The Cox model makes the assumption that all individuals have equal mortality rate and is modulated by a hazard ratio. The hazard ratio provides the odds of individuals to progress towards death when compared to other groups. A hazard ratio of 1 reflects no effect, < 1 indicated prolonged survival, and >1 suggests an increased risk of death. To select the best Cox model which integrated percent tissue health parameters, we used Akaike's information criterion (AIC) and identified health responses that contributed to the hazard ratio.

Oxygen evolution data was collected on an underwater android tablet with CISME software and surface area normalized, net photosynthesis rates were extracted from linear

regression models in R (v.4.2.1). Surface area estimates were quantified in $cm^2$ from pictures taken at each survey time point in ImageJ v1.53 software (Abràmoff et al., 2004). To determine initial responses to transplantation, net photosynthesis rates were modelled using generalized linear models (GLM) with fixed effects, reef, genotype, time, and their interactions. Predicted values were extracted from the model with all three fixed effects and data was compared between February and May. Coral health was identical in February, therefore, to compare health post-transplantation net photosynthesis rates, presence absence data, and percent tissue health data were compared between May, August and December using a GLM with fixed effects, reef, genotype, and time and their interactions. Presence/absence health data was run through a GLM under a binomial error distribution using the *glm* function in R with the same terms, and net photosynthesis rates and percent tissue condition were run with a Poisson error distribution. Predicted values were extracted from GLM models and used to calculate confidence intervals and plotted with package *ggplots2*.

**Results**

We found no indications of local adaptation to Conch Reef when assessing presence/absence and survival data including hazard ratios. Survival varied between sites with Tennessee Reef having the lowest survival (75%) compared to 100% survival at Carysfort, Conch Reef, and Looe Key, however, genotypes did not differ in their survival across all sites. There was evidence of survival outcomes influenced by GxE, which drove the differences in survival across sites. However, percent tissue health, and photosynthetic responses were most similar between Carysfort and Conch Reef, suggesting corals had better health response to these reefs and may be adapted/acclimated to the water quality and temperature profiles of the Upper

Keys region. Additionally, net photosynthesis and percent health data showed significant differences across genotypes and in GxE, providing evidence of strong intraspecific variation to novel environments. Overall, *Orbicella annularis* coral genotypes responded differently in percent tissue scores and net photosynthesis across transplantation sites (GxE) with fluctuating plasticity in health responses, supported by significant differences in percent tissue health, net photosynthesis rates, survival rates, and hazard ratios.

Temperature

*In situ* temperature data retrieved from the CREMP monitoring program was found to differ across reefs in daily mean temperatures (see Appendix 3; Figure S3.4; linear model: $p = 6.4e^{-03}$), sites, months, and their interaction ($p = 2.2e^{-16}$). Carysfort differed significantly from both Tennessee Reef ($p = 0.015$) and Looe Key ($p = 6.6e^{-03}$), but not Conch ($p = 0.07$). Conch, Tennessee, and Looe Key did not differ from each other and had on average higher daily temperature means than Carysfort, where highest temperatures were found at the most southern Looe Key and decreased moving north. The model that explained variation in temperature between sites the best was average daily temperature range (Fig. 3.3), where Conch Reef had the largest range which differed from Tennessee, Carysfort and Looe Key with the smallest range ($p = 8.6e^{-08}$). Temperature range and exposure to at least 5 days above 31℃ varied among sites in July and August. We found that Carysfort, Looe Key, and Tennessee were exposed to at least 5 days of continuous 31℃ average maximum daily temperature, and Conch Reef experienced four days at 31℃ in July but nonconsecutively. The sequential exposure above the mean monthly maximum triggered bleaching at the three sites, while Conch Reef was unaffected. After the August survey, all reefs experienced at least 9 consecutive days above 31℃, triggering a second bleaching event at all reef sites.

Survival and Death Hazards

Survival varied across sites (log-rank test: $p = 8.0e^{-06}$, $\chi^2 = 26.5$) in Kaplan-Meier estimates, however genotypic differences were above a 0.05 alpha (Fig. 3.3; $p = 0.1$, $\chi^2 = 5.4$). This analysis indicated that Conch Reef, Carysfort, and Looe Key had 100% survival after 314 days, while Tennessee Reef's survival was 75% (54%–100%, confidence intervals) at 179 days. Tennessee Reef censoring and health monitoring was not performed in December 2019 due to inclement weather conditions. After 314 days survivorship was 100% for genotypes A and C, 94% for B, and 90% for D; however, these differences were not statistically significant. Deaths in genotype B and D at Tennessee Reef drove differences in survival when comparing genotype and environmental interactions. All genotypes at Conch, Carysfort, and Looe key had 100% survival including genotypes A and C at Tennessee reef, however B (57%) and D (44%) had significantly less survival. Compared to Kaplan-Meier survival estimates, the parametric survival curves (Fig. 3.3) showed similar trends in extrapolated data with significant differences across sites (log-likelihood: $p = 6.1e^{-07}$, $\chi^2 = 31.69$) and for GxE ($p = 3.1e^{-04}$, $\chi^2 = 41.13$), but not across genotypes ($p = 0.059$, $\chi^2 = 7.43$).

Fitted Cox models followed a similar trend in survival curve analyses but integrated health parameters to determine impacts to risk of death. Algae overgrowth was the only health parameter that influenced the hazard ratio and when included with site, genotype, and their interaction was the best model. Hazard ratios at Conch, Carysfort, and Looe were all less than 1 and differed from Tennessee reef. When compared to Conch reef, Carysfort and Looe both had an HR of 1 and Tennessee had an elevated risk of death (Table 3.1). Genotypic variation was non-significant globally, but when HR were compared between sites, A and C both had prolonged survival and B and D had an increased risk of death. Genotype by environmental

comparisons were globally significant (log-rank: $p = 0.03$), however pairwise comparisons showed no significant differences in hazard ratios. Algae overgrowth also significantly affected the death risk and presence of algae on living tissue increased the risk of death.

Health and Photosynthesis

We found no significant differences in presence/absence data across sites, genotypes, time, or their interactions for organisms boring into live coral tissue, coral tumors, infections from diseases, and overall blotchy coral tissue (see Appendix 3; Figure S3.5). Percent tissue health data (healthy tissue, bleached tissue, pale tissue, mortality, and algae overgrowth) and net photosynthesis rates were compared between all reef sites, genotypes, time, and their interactions. Due to the correlation among the tissue condition parameters (i.e., percent healthy tissue is negatively correlated to the combination of bleached, pale, mortality, and algae overgrowth), percent healthy tissue and mortality are only reported here. Tissue health analyses revealed differences across sites and GxE interactions in categories of overall tissue condition metrics, healthy tissue, bleached tissue, pale tissue, mortality, and algae overgrowth. Genotypic differences occurred in all parameters except for healthy and bleached tissue (Fig. 3.5)

Conch Reef and Carysfort had similar percent tissue health ($p = 0.94$) but were significantly different from both Looe Key ($p < 2e^{-16}$) and Tennessee Reef (Fig. 3.4A, $p = 1.06e^{-07}$). While there were no differences among averaged (across individuals within the same genotype) percent health among genotypes (A= 80.2%, B= 82.6%, C= 85.2%, and D= 84.2%) and time in tissue health, GxE, and the interaction of time, genotype and reef was significantly different ($p < 2e^{-16}$).

Tissue mortality varied across sites, genotypes, time, and their interactions, including GxE ($p < 2e^{-16}$). Tennessee reef had the highest rates of mortality (Fig. 3.5E) with an average

28% tissue loss (SD= 37.8), while Carysfort (1.72%, SD= 4.03), Conch (2.33%, SD= 5.44), and Looe (2.6%, SD=4.29) had significantly lower percent tissue death ($p = 1.19e^{-08}$). Mortality across genotypes was highest in three of the four genotypes, A (6.23%, SD=17.1), B (6.88%, SD= 21.6), and D (9.4%, SD= 26) across all sites, which were all significantly different from genotype C (5%, SD= 8.46) with the least tissue death. In addition, time, GxE, and the interaction of the terms differed significantly for tissue mortality. Algae overgrowth a subset of mortality occurred most frequently in Tennessee with 24% average (SD= 38.1), which differed ($p < 2e^{-16}$) from all other reefs that experienced almost no overgrowth (Conch= 0%, Sd= 0; Carysfort= 0%, SD= 0; and Looe= 0.2%, SD= 0.147). Variation in algae overgrowth was significantly different across genotypes where C (0.89%, SD= 3.95) and A (3.02%, SD= 13.7) had the least amount and B (5.36%, SD= 21.8) and D (7.98%, SD= 26.3) had the most.

Net photosynthesis rates varied by site ($p <2.^{e-16}$) with Carysfort having the highest overall mean rate (1809 µmol $O_2$/kg, SD= 1132) and differing from all other sites. Conch (1092 µmol $O_2$/kg, SD= 608) and Looe Key (771 µmol $O_2$/kg, SD= 356) had similar rates (Fig. 3.5D). Tennessee had the lowest photosynthetic rates (666 µmol $O_2$/kg, SD= 330) which differed significantly from all other sites. Genotype C had the highest rate of photosynthesis (1155 µmol $O_2$/kg, SD= 903), which differed from all other genotypes (D; µmol $O_2$/kg, SD= 536, A; 943 µmol $O_2$/kg, SD= 480, and B; 953 µmol $O_2$/kg, SD= 793). All time points differed in photosynthesis as well as statistically significant interactions between genotype, reef, and their interactions. Initial photosynthetic rates (February) and those taken three months (May) post-transplantation were quantified and compared to identify variation between reefs (see Appendix 3; Figure S3.7). In February rates differed across sites; where corals transplanted to Carysfort had statistically higher rates than those transplanted to Conch reef, which had the lowest. In May

there was a significant increase in net photosynthesis at Conch reef which differed significantly from both Looe Key and Tennessee reef. To assess initial responses in coral photosynthesis after transplantation, rates from May were pooled by reef and genotype and subtracted from February (Fig. 3.6). We found that Conch reef had significantly higher difference in net photosynthesis rates from February to May, which differed from all other reefs.

Overall, corals at Carysfort had the top responses in all six of the health parameters at this reef. Carysfort had the lowest overall occurrence of bleaching, paling, mortality, and algae overgrowth, and the highest percentage of healthy tissue and photosynthetic rates (May-December). Conch Reef did relatively well with four top responses, which were statistically similar with Carysfort (percent healthy, bleached, mortality, and algae overgrowth of tissue). Conch Reef also showed positive increases in net photosynthesis after 3-months post transplantation. Looe key was similar to both Carysfort and Conch reef in two parameters, percent mortality and algae overgrowth, but had the highest percentage of bleaching overall. Tennessee reef had five out of the six health parameters (net photosynthesis, tissue health, mortality, paling, and algae overgrowth) with statistically lower values than all other reefs. Genotypes varied across all reef sites, with genotype C performing the best in all six health parameter metrics, followed by A which had three statistically similar health responses as C (percent healthy, bleached, and algae overgrowth). Genotype D was equal to C and A in healthy tissue, bleached and pale tissue however had the lowest photosynthesis rates, and highest mortality and algae overgrowth. Highest average pale corals were most prevalent in genotype B, and algae overgrowth and overall mortality was statistically different from the highest performing genotype, C.

## Discussion

This study investigated health, survival, and photosynthetic rates in *Orbicella annularis* corals at the genotypic and site level to understand how this species acclimates after transplantation to reefs with different temperature profiles. We hypothesized that all coral genets would exhibit elevated survival, photosynthesis rates, and health performance at Conch Reef with similar response at Carysfort, which also occupies the Upper Keys region, when compared to the two southern sites. We found significant variability in survival and health at reef sites, and intraspecific responses provide evidence that the four genotypes in this species can acclimatize to different environments. However not all sites accommodate all genets, and some genotypes outperform others.

Our results also indicated that there were no differences in survival at Conch, Carysfort, or Looe Key. However, survival at Tennessee Reef (75%) was significantly difference, suggesting there is no evidence of local adaptation in these genotypes. In contrast, we found that for all three reefs with 100% survival with hazard ratios of 1 (Conch, Carysfort, and Looe), not all corals responded similarly in health metrics. For instance, bleaching, mortality, paling, algae overgrowth, and percent healthy tissue all varied among sites, after temperature peaked in July and August (Fig. 3.7). July and August were the two hottest months in 2019, and when we compared daily temperature means, and maxima we found that Conch Reef had significantly lower mean and maximum temperatures throughout July (Fig. 3.7, linear model: means; $p < 2.2e^{-16}$, F= 39.43, maxima; $p < 2.2e^{-16}$, F= 38.66). Health assessments on August 2$^{nd}$–5$^{th}$ revealed extensive bleaching at Carysfort (18.3%, SD= 15.9), Looe Key (25.4%, SD= 28.9), and Tennessee Reef (13.75%, SD= 15.2), where all differed significantly from Conch (1.79%, SD= 2.49; $p = 4.3e^{-04}$). When looking at the August temperature data (Fig. 3.7) we found the average

temperature across sites were similar and ~0.5℃ warmer than July means, with statistically similar means and maxima between all sites. The number of consecutive days at 31℃ mean maxima was much higher than in July where Conch Reef experienced 12 consecutive days, Carysfort 11 days, and Looe Key 9 days. We suspect the prolonged exposure to higher temperatures caused a second bleaching event, which was evident in December with increased bleaching at Conch Reef (15.6%, SD= 19.7), but a reduction at Carysfort (0.8%, SD= 1.74) and Looe Key (5.14%, SD= 5.59).

The recovery from bleaching at Carysfort and Looe Key apparent in December most likely occurred more rapidly than corals at Conch Reef due to bleaching hormesis, where corals were primed with five to seven continuous days of temperatures at 31℃ or higher in July. In August, these thermally primed reefs (Carysfort and Looe Key) most likely displayed a stress memory from pre-exposure in July, where the mild stressor resulted in an initial physiological cost but enabled improved responses when exposed to the more severe temperatures in August (Martell, 2023; Hackerott et al., 2021; Putnam et al., 2017; Hawkins et al., 2017). For example, in a 2008 study, Middlebrook and colleagues (2008) compared non-photochemical quenching, xanthophyll cycling, symbiont densities, and photosynthetic efficiency in corals that were exposed to 31℃ for 48hrs before a replicated bleaching event to those that were not in the pre-stress treatment. Results from this study showed pre-stress treatment corals had more effective photoprotective mechanisms at play that reduced bleaching severity. Similarly, in the Florida Keys, thermal tolerance was found to increase across multiple annual bleaching events where the second year had less bleaching severity, despite exposure to higher temperatures (Gintert et al., 2018; Fisch et al., 2019). We believe thermal priming of corals in July contributed to faster bleaching recovery at Carysfort (0.8%, SD= 1.74) and Looe Key (5.14%, SD= 5.59) after the

August bleaching event, but not Conch Reef (average December bleaching:15.6%, SD= 19.7) which did not bleach in July. Interestingly, Carysfort had significantly less bleached corals than Looe Key ($p = 0.01$) in December, suggesting local adaptation/acclimatization to the Upper Keys region due to rapid recovery at Carysfort that experienced July and August bleaching.

Surprisingly, Tennessee Reef and Conch reef had similar temperature profiles throughout 2019 but Tennessee Reef differed significantly in survival, CPH, and five of the six health metrics, where hazard ratios were driven by algae overgrowth which only occurred at Tennessee Reef (Fig. 3.5F.). Based on the environmental similarities found within the two regions these sites occupy (Upper and Middle), we did not expect Tennessee Reef to have such drastic differences in coral responses, especially considering the elevated health metrics seen at Looe Key. The environmental data we analyzed showed no difference across reef sites for 2019 water quality metrics (see Appendix 3; Figure S3.3), and while it has been shown that coral transplantation survival is influenced by environmental conditions (Toth et al., 2018; van Woesik et al., 2021) variability among reefs within subregions of the FRT is also common. In fact, the greatest variation along the FRT was found among reefs on a 10–20km scale (Murdoch & Aronson, 1999). Florida coral cover at any given reef did not affect coral cover on neighboring or nearby reefs due to differences in exposure to outflow from the Florida Bay, which varies in temperature, salinity, nutrients, and sediment loads (Murdoch & Aronson, 1999, Ginsburg & Shinn, 1995). In a long-term assessment on survival in restored *Acropora cervicornis* corals, Banister & van Woesik, 2021 found significant differences in survival across reefs within subregions. Moreover, two of the sites used in this study (Carysfort and Conch) were ranked highest (#4 and #7 out of 67 sites) for outplant survival. Although Banister & van Woesik's

(2021) study was performed with *Acropora spp.*, survival and health in our study showed these two sites were the most successful for short-term *Orbicella annularis* restoration as well.

Our results suggest that Tennessee Reef is not an ideal restoration site for these corals. The poor health outcomes at Looe Key and Tennessee are concordant with our hypothesis that southern sites would have lower survival (Tennessee) and health outcomes. Even though Looe Key had high survival, their overall health was significantly lower than corals at Carysfort and Conch, suggesting corals at this site may survive short-term restoration, but the acclimatization process at this reef reduces health metrics. Warm temperatures at Looe Key drove health responses, specifically bleaching responses which were highest overall at this reef (Fig. 3.5B). To determine long-term success and persistence of corals at this reef, longer monitoring periods of health and temperature could reveal if and when corals at this reef are successful at acclimatizing to the thermal profile. It is important to note that the high survival rates in this study were achieved after only 11-months and may inflate the actual survival rates of corals in restoration (Boström-Einarsson et al., 2020). This study showed that *Orbicella annularis* corals perform best in the Upper Keys region at Carysfort and Conch and show evidence of localized adaptation and/or acclimatization to the similar thermal histories at these reefs based on their survival and health responses. Our results indicate that survival and health outcomes differed between sites with two clear successes (Carysfort and Conch), one failure (Tennessee), and a potential restoration site for one of the four genotypes at Looe Key.

Assessing the responses of corals across transplantation sites can reveal generalist genotypes (Warner, 1997; Smith et al., 2007; Drury et al., 2017) capable of acclimatizing across multiple sites, specialist genotypes (D'Croz & Mate, 2004; Kassen, 2002) that thrive in specific environments, and genotypes that are both generalists and site-specialists (Vermeij et al., 2007).

This information can then be used to make decisions on where to transplant certain genotypes, thereby reducing death due to haphazard restoration methodology. Adaptation of coral genotypes to novel environments is in part due to changes in algal symbiont inhabiting coral cells (Baums, 2008; Little et al., 2004; Berkelmans & van oppen, 2006). However, the corals in this study did not have their symbiont identity verified. Yet, *Orbicella annularis* corals across Florida, particularly those living within the same reef area, have been shown to harbor identical associations of *Symbiodinaceae*, which remained stable over time and through sustained bleaching events (Thornhill et al., 2006; Thornhill et al., 2009). Because the corals in this study all originated from the same backreef area at Conch Reef and were subsequently transferred to the same nursery tree for ~2 years, we believe they probably conformed to this trend housing similar algal communities and their responses to transplantation was primarily a result of genetic variation. In addition, corals sharing a nursery tree in a shared environment over time minimizes the impacts of long-term acclimatization from the origin site, which isolates genetic effects and can heighten our understanding of local adaptive responses (Kawecki & Ebert, 2004).

Assuming that these genotypes have similar symbiont communities and because they originated at Conch reef, the variation in survival and health are attributed to the plastic and adaptive traits possessed by the different genotypes (Seebacher et al., 2012; Seebacher et al., 2015). Our results indicated that there was no significant variation in genotypic survival across all reefs, however when compared using CPH models there were differences in hazard ratios driven by algal growth primarily on genotypes B and D (Table 3.1). These reduced hazard ratios matched the health data for genotypes B and D where both had the lowest performance in three of the six health metrics (Fig. 3.5). Genotype A had three of the highest health metrics, but also was equal in percent tissue mortality with genotypes B and D. Clearly the highest performer of

all genotypes was C, which topped all six of the health parameters, suggesting this genotype may express phenotypically plastic traits suitable for a wide range of habitats (Spitze & Sadler, 1996; Kawecki & Ebert, 2004). Likewise, genotype C had consistent fitness over all reef sites (Fig. 3.5), suggesting they are a generalist genotype (Drury et al., 2017).

The majority of the variation in coral responses occurred on the genotype by environmental interaction level. Overall, these interactions suggest that genotypes are locally adapted to the Upper Keys regions, where all genotypes had elevated health and survival at Carysfort and Conch reef, supporting the conclusion that native Upper Keys corals are in general more responsive to their region of origin. Genotypic by environmental interactions were significant for every parameter, including survival, hazard ratios, photosynthetic rates, and health metrics. From the results of this study, we have found that the four genotypes do not acclimatize comparably across sites but vary in their survival and overall health. Our results will inform the CRF as to which reef sites are best suited for restoration of *Orbicella annularis* corals, the highest performing genotype, and which genotypes will persist at each site. Carysfort had overall the best coral responses and genotype A was the highest performer, however genotype B, C, and D each had elevated health responses similar to the top performer in two of the six parameters. Conch Reef also had high coral performance throughout this study, specifically with genotype B, which had the most positive responses at Carysfort reef and at Conch Reef. Genotype D, however, performed best at Conch Reef and had four out of six top performance values and genotype A had three. Based on genotype A, B, and D's success at the two reefs in the Upper Keys region these genotypes may be considered specialists for this region. While Looe Key had lower performance and health compared to the Upper Key sites overall, genotype C had the best

responses at this site compared to all other sites and has potential for this genotype to perform well long-term.

Sustained survival depends on a coral's ability to reproduce offspring with successful recruitment. *Orbicella annularis* corals are broadcast spawners and release large amounts of sperm and eggs into the water column where fertilization occurs. Compared to brooding corals, broadcast spawning species generally have lower recruitment rates because they depend on the availability of gametes from other individuals (Richmond & hunter 1990; Edwards 2010). Therefore, to ensure potential gene flow and promote the spread of beneficial genes, the CRF can use this information to ensure the generalist genotype C is represented across the majority of their planned restoration sites, and genotypes A, B and D are primarily placed in the Upper Keys region. Determining restoration success will depend on if these corals are placed in environments where they can grow into health fecund colonies, which may then increase sexual reproduction and adaptation by contributing to assisted gene flow via restoration (Aitken & Whitlock, 2013).

Based on this study coral success is determined by site and genotype, and evidence of local adaptation indicates three of the four genotypes are disadvantaged in sites outside the Upper Keys region. This information is critical for coral restoration practitioners to use, considering future persistence at reefs. With this knowledge, efforts to ensure the physical and evolutionary distance from the source population of these corals (Upper Keys) will need to be in place to reduce the risk of fitness loss in the restored population (Baums, 2008). The identification of these specialist (A, B and D) and a generalist genotype (C) provides support for investigating GxE in coral restoration efforts, which should focus on maximizing genotypic diversity and identifying GxE combinations that enhance reproductive success. Planning restoration initiatives based on GxE interactions also need to consider the effect locally adapted

genotypes may have at transplantation sites outside their region of adaptation. For instance, recombination with transplanted corals can dilute locally adapted genes, which can reduce fitness in the next generation (Baums, 2008). Our results demonstrate that understanding genotypic success across reefs will contribute to our understanding of phenotypic plasticity and adaptive responses that can help maintain coral populations, contributing to long term persistence.

**Table 3.1 Hazard ratios from survival analyses**

Cox proportional hazard ratios and 95% confidence intervals with likelihood ratio test p-values comparing sites, genotypes, and the influence of algae overgrowth on projected survival hazards. Asterix denotes significance.

| Characteristic | Hazard Ratio | 95% CI | *p-value* |
|---|---|---|---|
| **Site** | | | $6.833e^{-06}$* |
| Conch | — | — | |
| Carysfort | 1.00 | 0.49 – 2.03 | 0.9 |
| Looe | 1.00 | 0.49 – 2.03 | 0.9 |
| Tennessee | 1,888 | 842 – 5,750 | <0.001* |
| **Genotype** | | | $6.6e^{-02}$ |
| A | — | — | |
| B | 346 | 7.68 – 15,554 | 0.003* |
| C | 15.3 | 0.44 – 527 | 0.13 |
| D | 346 | 7.68 – 15,554 | 0.003* |
| **Algae** | 1.35 | 1.25 – 1.46 | <0.001* |

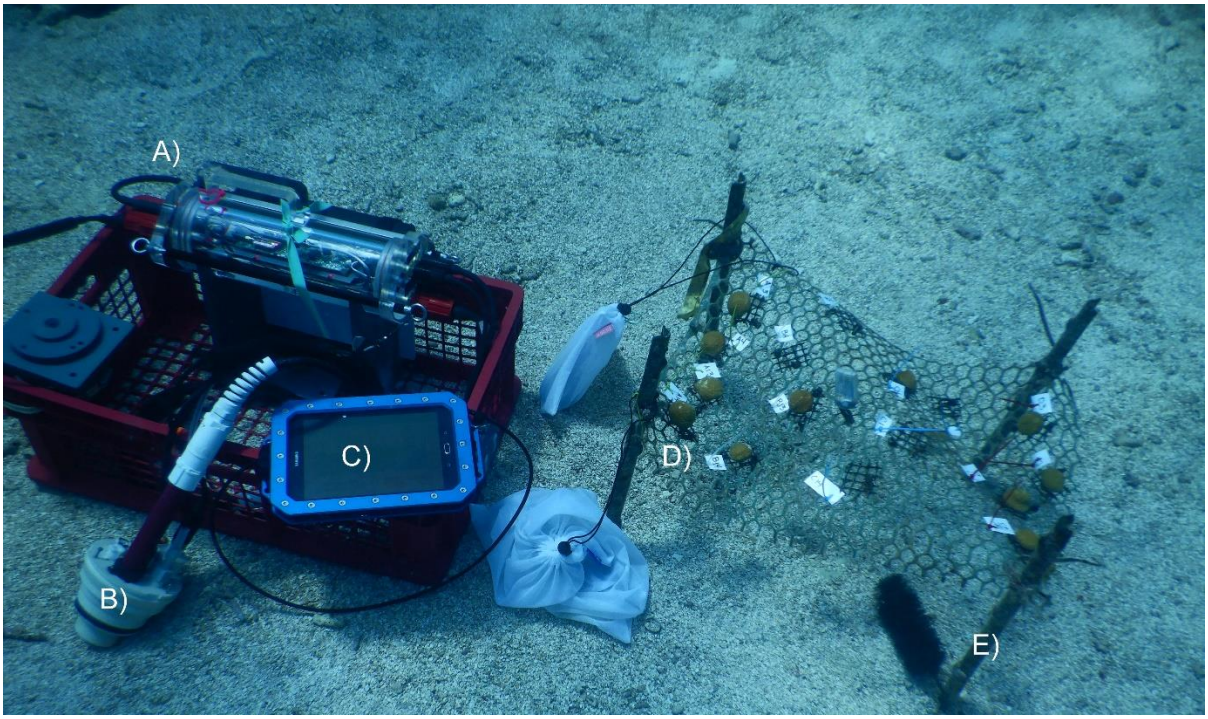


**Figure 3.1 CISME device and transplantation table**

A) CISME diving device with B) flow cup incubation chamber C) underwater tablet. Transplantation table with D) mesh top ziptied to four E) t-post fence table legs, driven 30cm into sandy bottom at ~7–8m depths. Author K.J.G is the photographer.

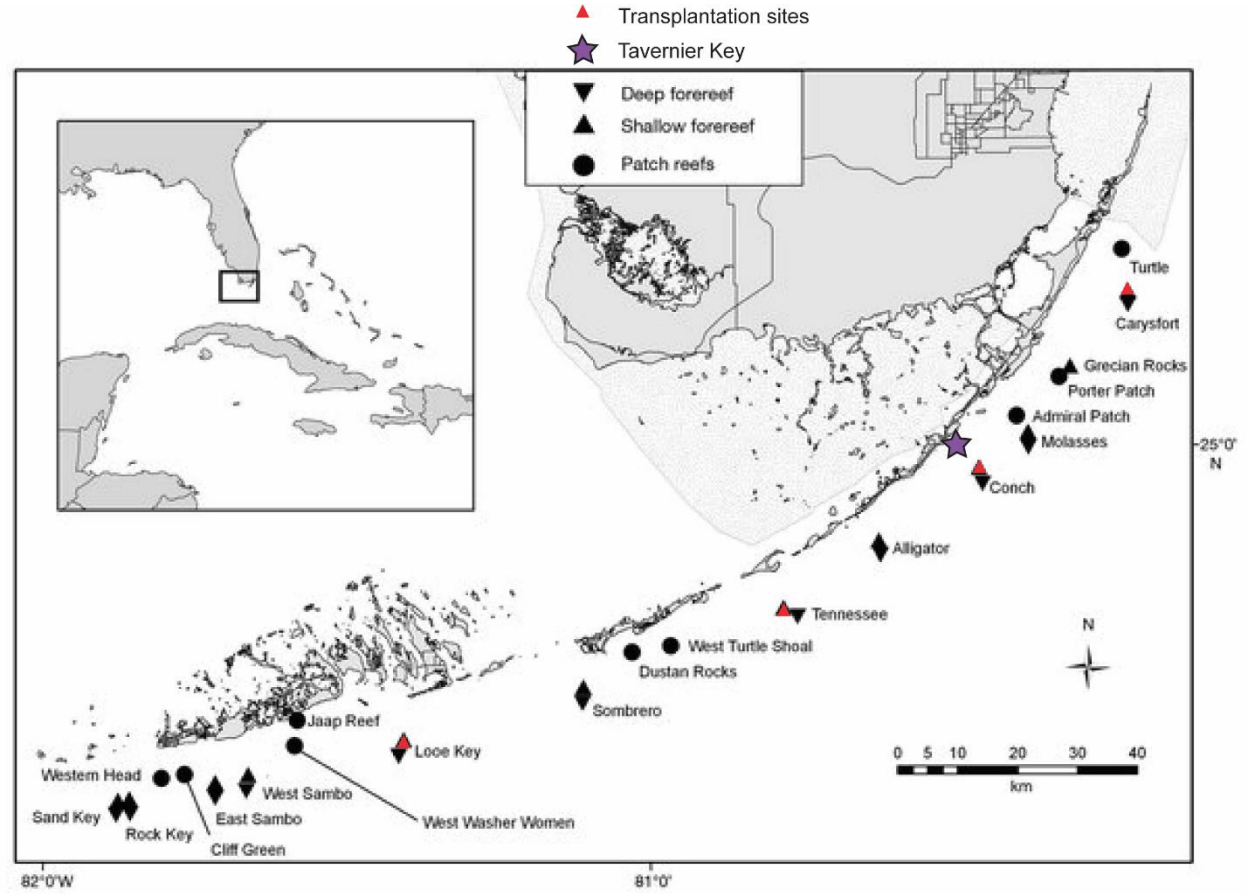


**Figure 3.2 Nursery tree and transplantation sites**

Florida Keys reef tract (FRT) with the four shallow forereef sites (red triangles) used in this study: from North to South is Carysfort, Conch Reef, Tennessee Reef, and Looe Key. All sites are special use areas within the Florida Keys National Marine Sanctuary, except for Carysfort which is a Sanctuary preservation area. The CRF's nursery trees are located at Tavernier Key (purple star) where corals were collected. Redesigned from Ruzicka et al., (2013).

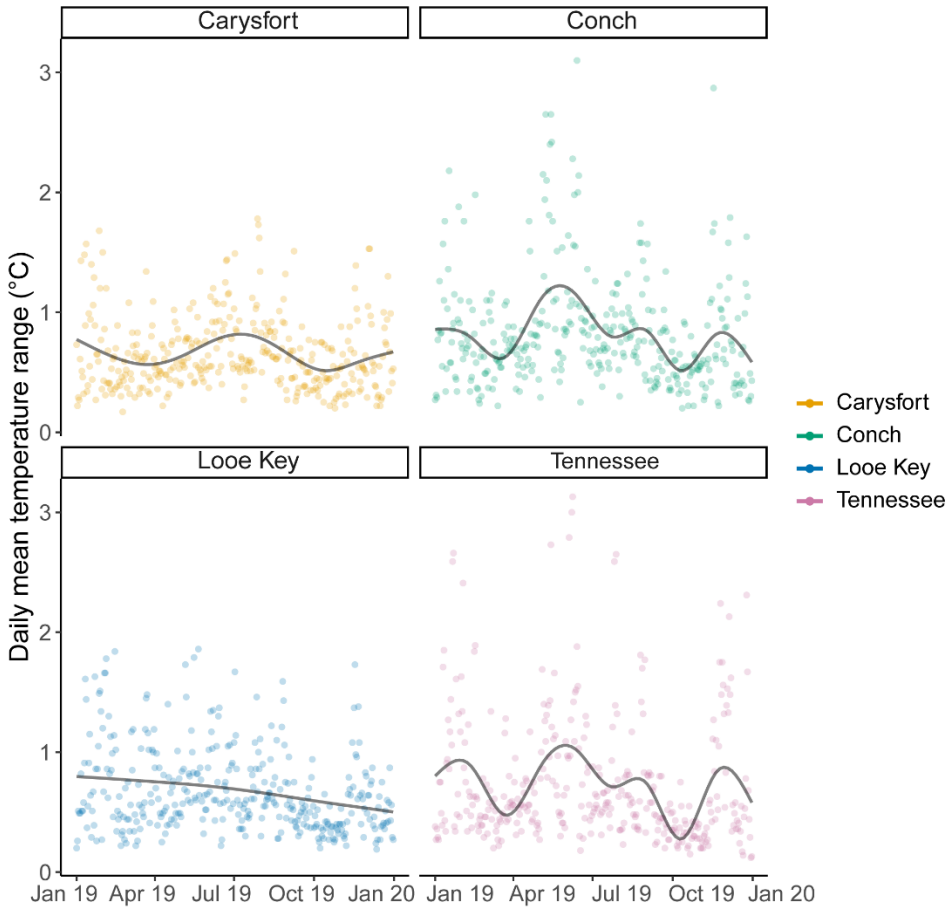


**Figure 3.3 Temperature range at restoration sites**

Average daily temperature range data retrieved from *in situ* CREMP monitoring probes from January 2019 to January 2020. Sites are separated and average daily means plotted with a smooth gam function. Conch Reef (green) had the largest temperature range followed by Tennessee Reef (pink), Carysfort (orange) and Looe Key (blue).

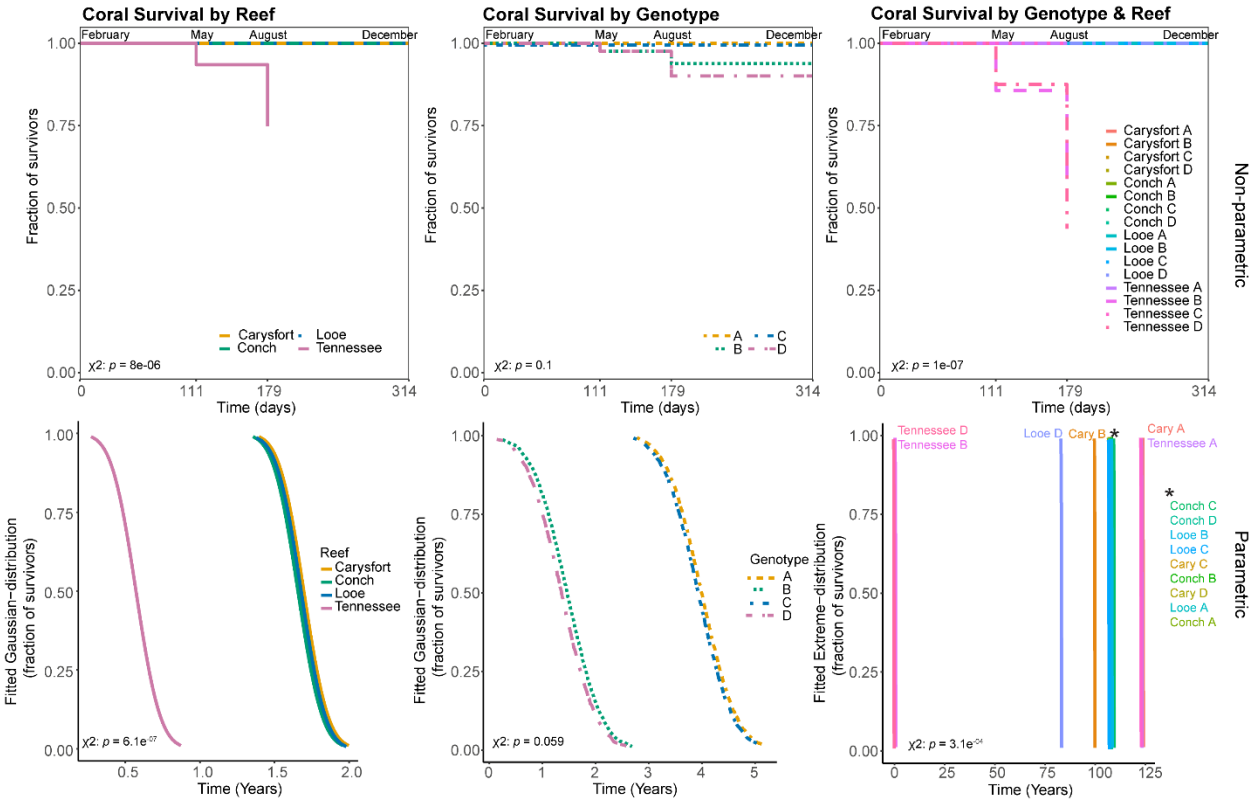


**Figure 3.4 Survival estimates for *Orbicella annularis* corals post-transplantation**

Kaplan-Meier non-parametric and parametric estimated survival probabilities for corals pooled by reef, genotype, and genotypes at each site. Curve differences were assessed using the log-rank test and *p*-values are represented for each. Non-parametric curves show the raw fraction of survivors from February to December, and parametric curves are extrapolated over years.

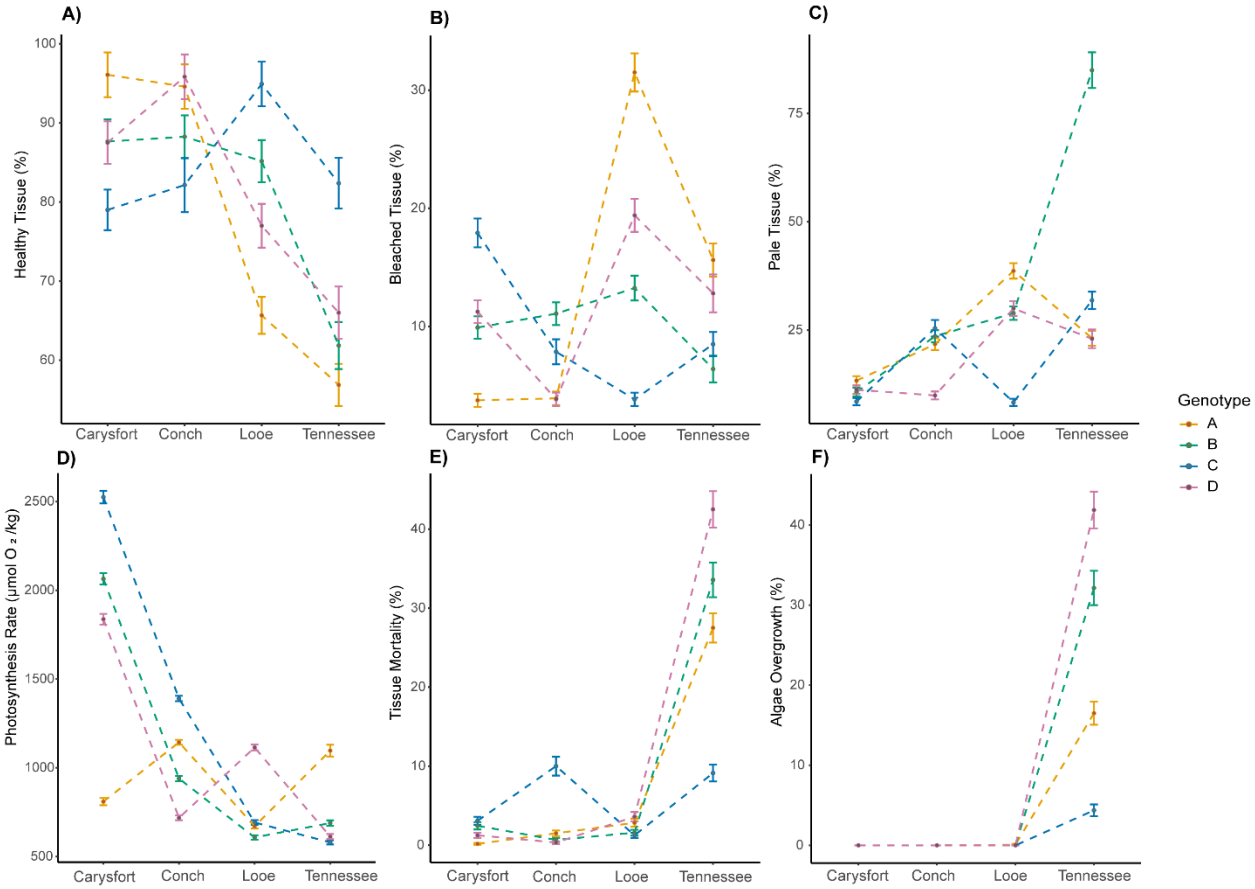


**Figure 3.5 Genotype by environmental interactions in health metrics**

Genotype by environmental interactions across all percent tissue health parameters, healthy A), bleached B), pale (C), net photosynthesis rates (D), mortality (E), and algae overgrowth on previously living tissue (F). Reef sites are on the x-axis and genotypes are depicted by lines, A= orange, B= green, C= blue, and D= pink.

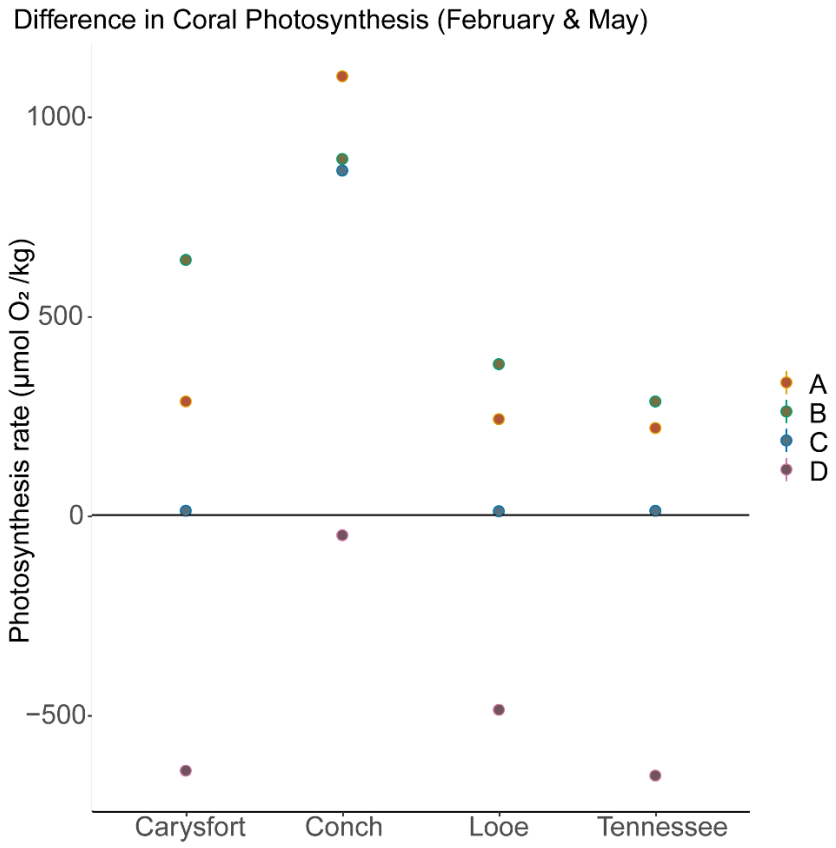


**Figure 3.6 Difference in photosynthetic rate from February to May**

Change in net photosynthesis rates pooled by genotype at each reef site from February to May (n= 16). Points above the horizontal line (no change in net photosynthesis) indicate an increase in rate, and below is a reduction in photosynthesis rates after 3-months post-transplantation. Reefs are indicated on the x-axis and genotypes by points; A= orange, B= green, C= blue, and D= pink.

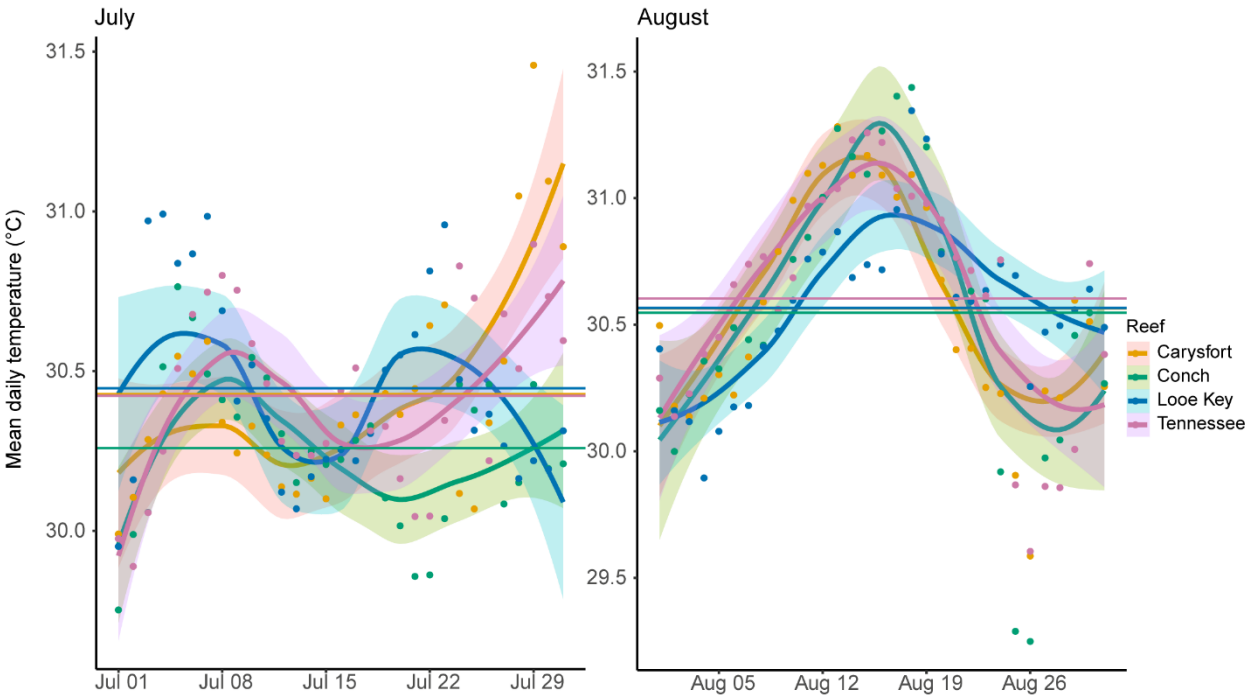


**Figure 3.7 Summer bleaching event temperature profiles**

Mean daily temperature through July and August 2019 at each reef site, Carysfort= orange, Conch= green, Looe= blue, and Tennessee = pink. Horizontal lines indicate average monthly temperature at each site and ribbons are 95% confidence intervals.

# CONCLUSIONS

In the last decade, interest in coral restoration has grown exponentially, with rises in patents, journal articles, and projects (Roch et al., 2023). Despite the increase, there remains a disparity in organizational project designs which lack achievable objectives and have poor standardized monitoring and reporting procedures (Boström-Einarsson et al., 2020). A major oversight to restoration efforts includes investigating genotypic responses of corals intended for restoration and their ability to acclimate to transplantation sites (Baums, 2008). In addition, genotypic responses to thermal stress can allow practitioners to identify heat-resistance corals for use in restoration and can help identify thermally tolerant reef sites and potential refugia (Smith et al., 2016). The goal of this dissertation is to test the hypothesis and determine whether characterizing thermal performance of coral species and genotypes, and investigating genotypic responses to restoration activities can provide practitioners with a strong foundation to build restoration objectives around. Understanding bleaching thresholds and severity in corals can provide a baseline for restoration strategies, including protecting reefs that are thermally resistant, potential refuge, and focusing transplantation initiatives at thermally vulnerable reefs with genotypes harboring elevated thermal optima. Genotypic responses to environments can also serve an important role in extending survival post transplantation and ensuring appropriate gene flow with wild populations.

This research provided evidence of a potential upper-mesophotic thermal refuge in Bermuda (Chapter 1), which should be considered in restoration activities. For instance, corals

with thermal tolerances similar to shallow conspecifics should be protected under MPA's or governmental stewardship areas to promote reef connectivity in the face of global climate change. This protection is even more critical as shallow reefs rapidly degrade, thereby increasing pressure to exploit deep reefs (Bridge et al., 2013). By characterizing thermal performances of both shallow and mesophotic species, practitioners can identify brood stock suitable for preserving connectivity between depth. A prerequisite to this is to ensure populations have adequate vertical connectivity, which is known to vary on spatial scales (Bongaerts et al., 2010, van Oppen et al., 2011; Slattery et al., 2011). The use of this approach can improve our understanding of current thermal tolerances in corals to identify resilient species, genotypes and reefs that may serve as refuge, foster protection of resilient reefs, and be used to predict bleaching severity.

Thermal performance characterizations can also help identify resilient genotypes that outperform others (Chapter 2) and indicate the effectiveness of potential stress-mediation techniques. Current restoration practices lacking standardization can use thermal performance curves as a starting point in conservation efforts. Understanding the thermal limitations of genotypes used in restoration will enable more efficient planning for transplantation initiatives. Additionally, potential restoration sites should be thoroughly vetted in terms of temperature exposure. For instance, reefs vary in their thermal histories and extent of variability which plays an integral role in susceptibility to bleaching (McClanaham et al., 2007; Thompson et al., 2009; Williams et al., 2010), including localized adaptation to temperature regimes, which would be detrimental to corals that originated elsewhere. Transplanting corals of unknown thermal tolerances to reefs without prior knowledge of their thermal limits will reduce the effectiveness of restoration projects.

Similarly, long-term monitoring of coral genotypes across multiple reef sites (Chapter 3) can provide an alternative to characterizing thermal tolerances through identification of local adaptation and acclimatization potential *in situ*. This approach is useful in pinpointing genotypes that are generalists and specialists in their reactions across multiple sites, providing evidence of GxE or lack thereof. However, appropriate controls are essential to these studies, but current restoration designs rarely use them in practice, which further supports the need for standardized methodologies (Lake, 2001; Boström-Einarsson et al., 2020). Understanding which genotypes not only survive but maintain elevated health parameters, including resistance and recovery from bleaching can improve restoration. Although Chapter 3 concluded after 11-months, lengthier monitoring periods (>12-months) should be considered, because short-term monitoring can artificially inflate survival rates (Boström-Einarsson et al., 2020). Including health parameters early and often in restoration surveys can enhance our understanding of coral responses to transplantation, and without these parameters in Chapter 3, our conclusions on local adaptation would be distorted. Integrating health parameters and photosynthesis rates revealed dynamic GxE interactions that would not have been realized if survival was the main metric.

Additionally, using this approach across multiple species will reveal species-specific responses that can alter the success of restoration efforts. For instance, the majority of restoration actions use fast-growing branching corals (59%) with average survival between 60–70% (Boström-Einarsson et al., 2020). Performing restoration with multiple species will require knowledge on their specific responses to transplantation and current methods are based mainly on *Acropora* species. A thorough understanding of intraspecific variation across species used in restoration will improve future efforts, and using GxE analyses on a subset of coral species,

genotypes or functional groups selected for restoration will reduce subsequent failures in the field.

Lastly, coral restoration efforts that use an interdisciplinary approach including transplantation, MPA protection, advanced monitoring technologies (i.e., photomosaics), and stress-mediating interventions (i.e., cool-water injection, shading) can enhance coral conservation (Boström-Einarsson et al., 2020; Westoby et al., 2020). While the stress-mediating intervention (sprinkler treatment) in Chapter 2 was not significantly different from the control, we did see elevated responses in thermal performance and physiological responses. Investigating alternative methods to restoration like stress-mediation may prolong coral persistence while global action against climate change takes effect (Anthony et al., 2017). Integrating multiple approaches that focus on genotypic responses and testing novel interventions with scientific input will enrich current restoration efforts.

This dissertation investigated the role temperature plays on coral responses to provide context for enhancing restoration and conservation using a science-based approach. Together, these results show the importance of understanding thermal tolerances of corals across species and between genotypes within species to reveal potential refuge in Bermuda, heat resistant genotypes in *Acropora cervicornis* corals used in restoration, and the importance of GxE in *Orbicella annularis* genotypes in restoration planning and execution. While this dissertation focused on practical approaches to improve current approaches in Bermuda and the Florida Reef Tract, coral restoration and conservation cannot replace exploited or damaged reefs, and significant action on climate change is needed to ensure the future of these extraordinary ecosystems.

## APPENDIX 1: SUPPLEMENTARY MATERIALS FOR CHAPTER 1

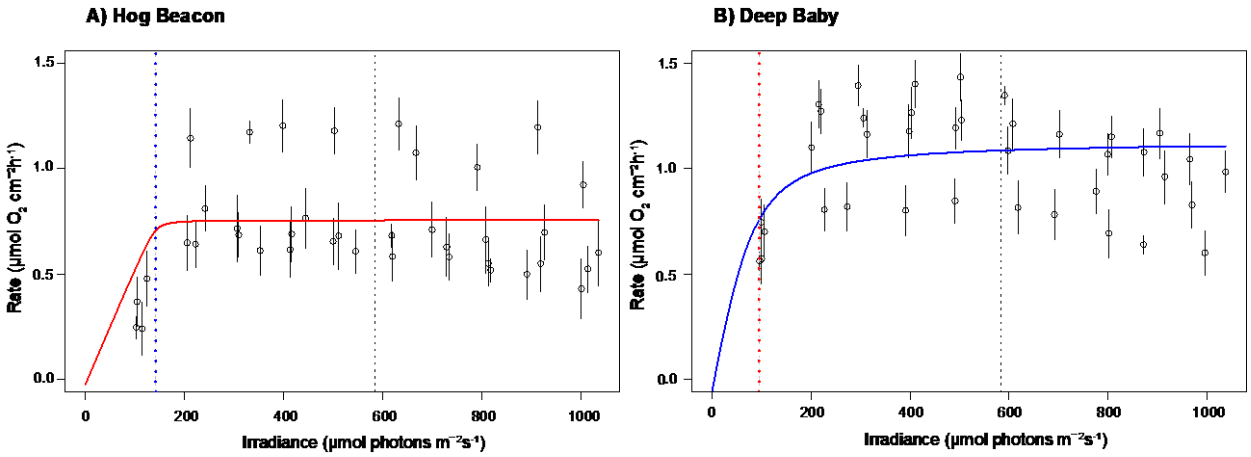


**Figure S1.1** Photosynthetic irradiance curves across 11 light levels, fit to mean photosynthetic rates (mean ± se) of irradiance of two coral fragments from each species (n= 8) at each site. The first dotted line on each graph represents $I_k$ (saturating irradiance; 141.5 µmol photon $m^{-2}$ $s^{-1}$ for shallow Hog Beacon corals and 94.6 µmol photon $m^{-2}$ $s^{-1}$ in upper-mesophotic corals on Deep Baby), the second dashed lines is the mean light level used during thermal performance experiments. Divergence between points represents each of the four species.

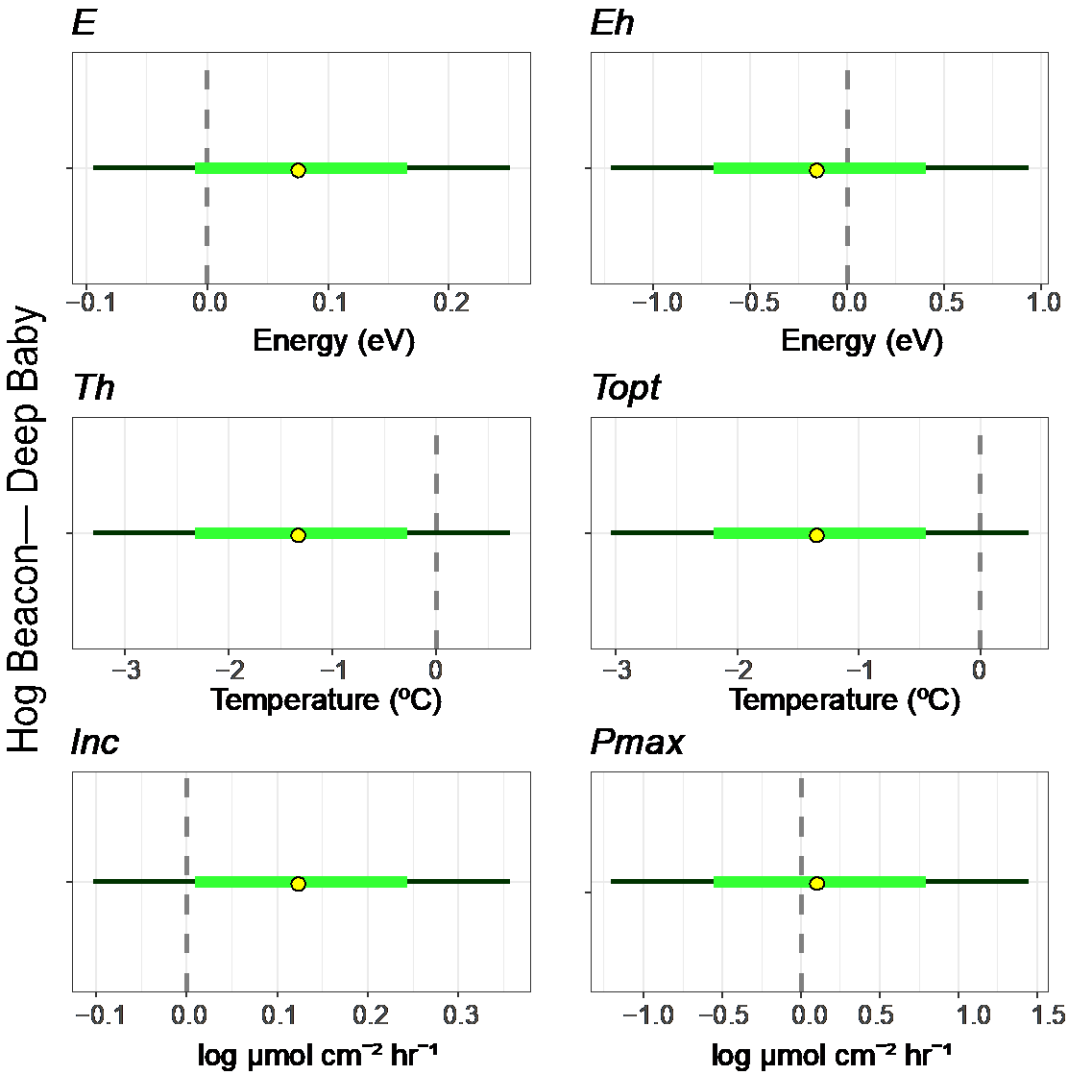


**Figure S1.2** Pairwise comparison between sites for thermal performance parameters for gross photosynthesis (n= 187, 5 unique outliers). Dot and whisker plot represent the mean parameter coefficient estimated from linear regression models (yellow dot) with 50% (light green whiskers) and 95% (dark green whiskers) confidence intervals for each parameter. If whiskers cross the vertical line at 0.0 the populations are not considered statistically different from one another (alpha= 0.05). *E*= activation energy, *Eh*= deactivation energy, *Th*= temperature enzymatic inactivity, $T_{opt}$= thermal optimum, *Inc*= mean performance rate, $P_{max}$= maximum rate of performance.

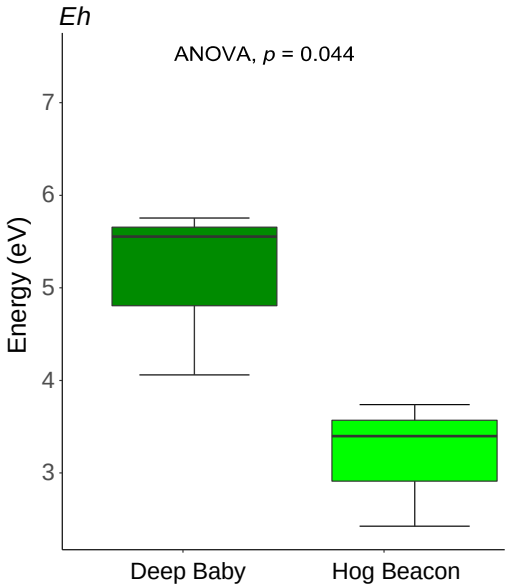


**Figure S1.3** Mean deactivation energy (*Eh*) values with 95% confidence intervals between depth for gross photosynthesis in *D. labyrinthiformis* (n= 48).

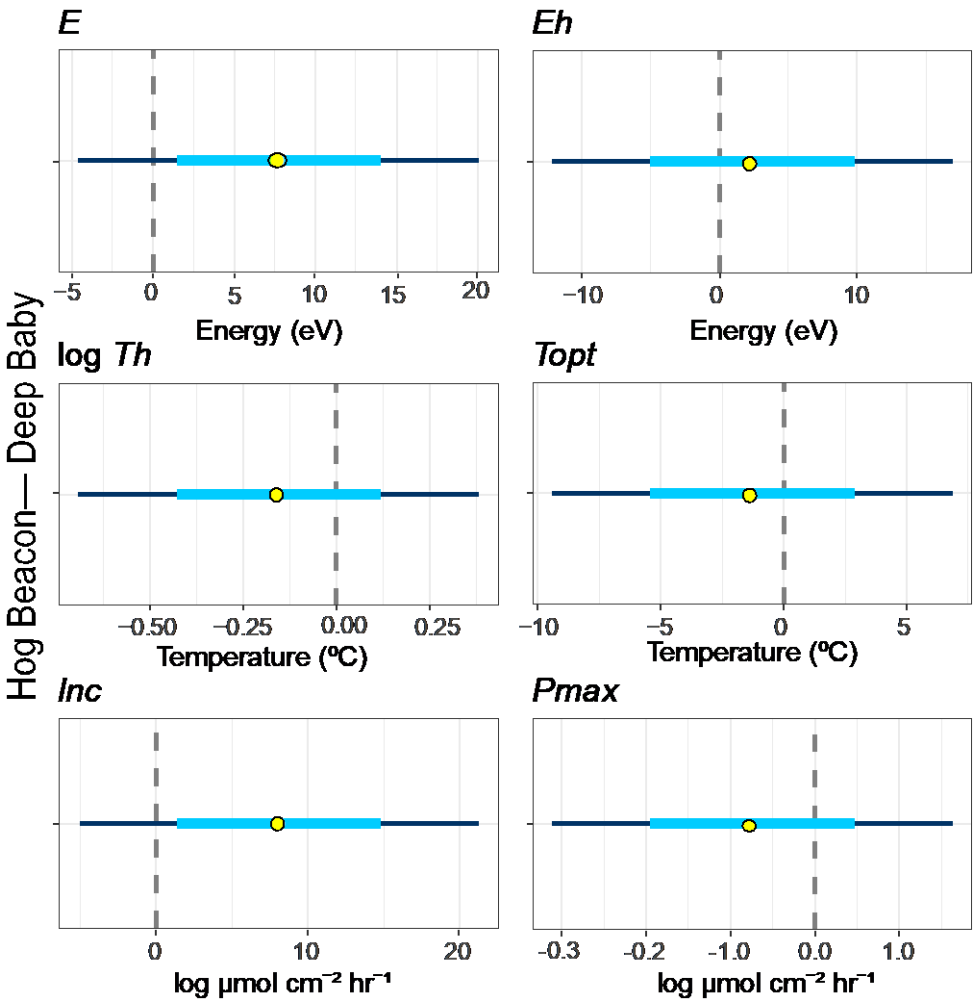


**Figure S1.4** Pairwise comparison between sites for thermal performance parameters for gross respiration (n= 188, 4 unique outliers). Dot and whisker plot represent the mean parameter coefficient estimated from linear regression models (yellow dot) with 50% (light blue whiskers) and 95% (dark blue whiskers) confidence intervals for each parameter. If whiskers cross the vertical line at 0.0 the populations are not considered statistically different from one another (alpha= 0.05). *E*= activation energy, *Eh*= deactivation energy, *Th*= temperature enzymatic inactivity, $T_{opt}$= thermal optimum, *lnc*= mean performance rate, $P_{max}$= maximum rate of performance.

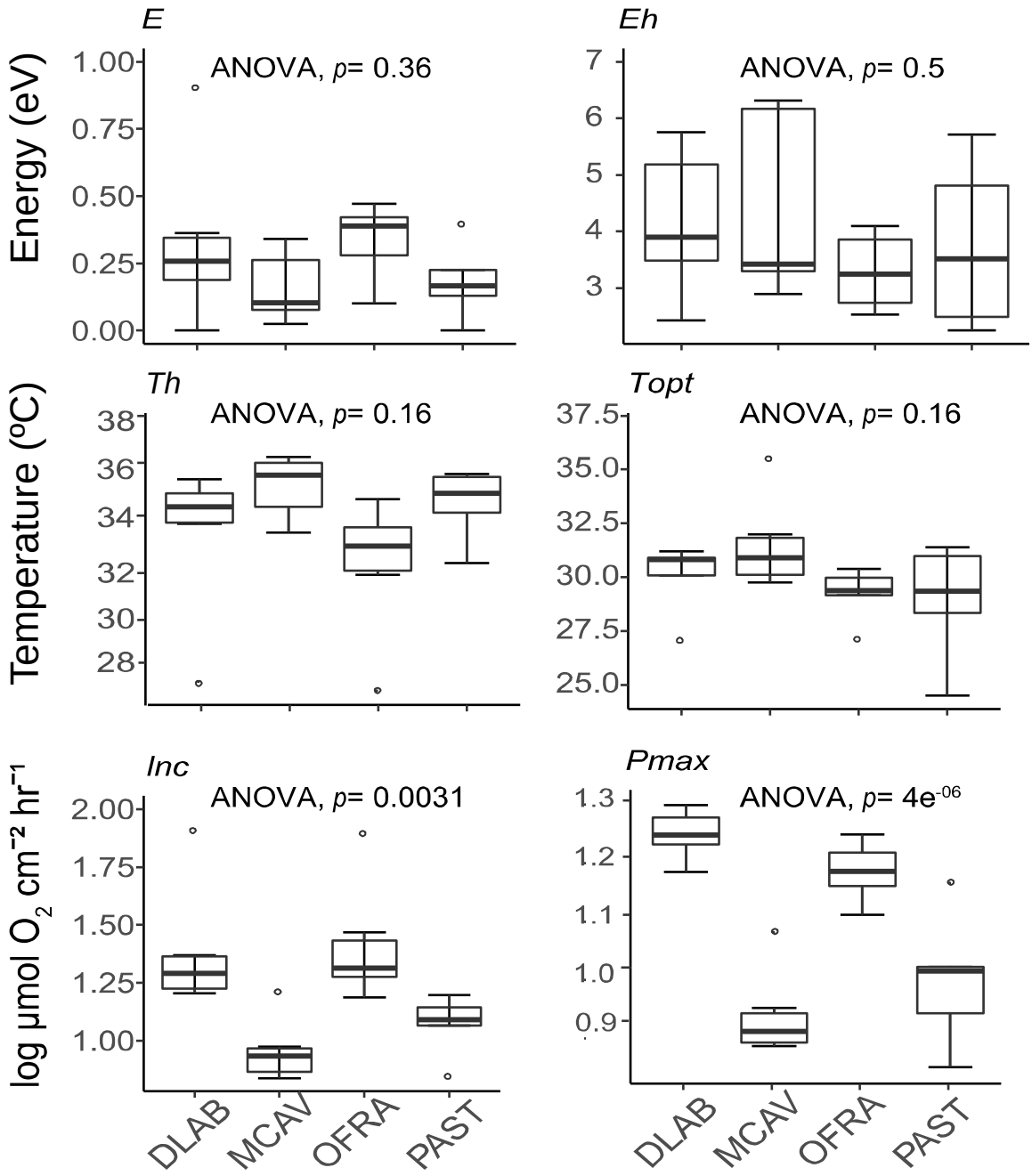


**Figure S1.5** Box and whisker plots comparing gross photosynthesis thermal performance parameters between species (n= 192, outliers are depicted as circles). The centerlines of boxes are median values and whiskers represent upper and lower 1.58*IQR (inter-quantile range). Individual open circles are outliers. ANOVA values of 0.05 and below represent significant differences between species ($P_{max}$, and lnc). DLAB= *Diploria labyrinthiformis*; MCAV= *Montastrea cavernosa*; OFRA= *Orbicella franksi*; and PAST= *Porites astreoides*. *E*= activation energy, *Eh*= deactivation energy, *Th*= temperature enzymatic inactivity, $T_{opt}$= thermal optimum, *lnc*= mean performance rate, $P_{max}$= maximum rate of performance.

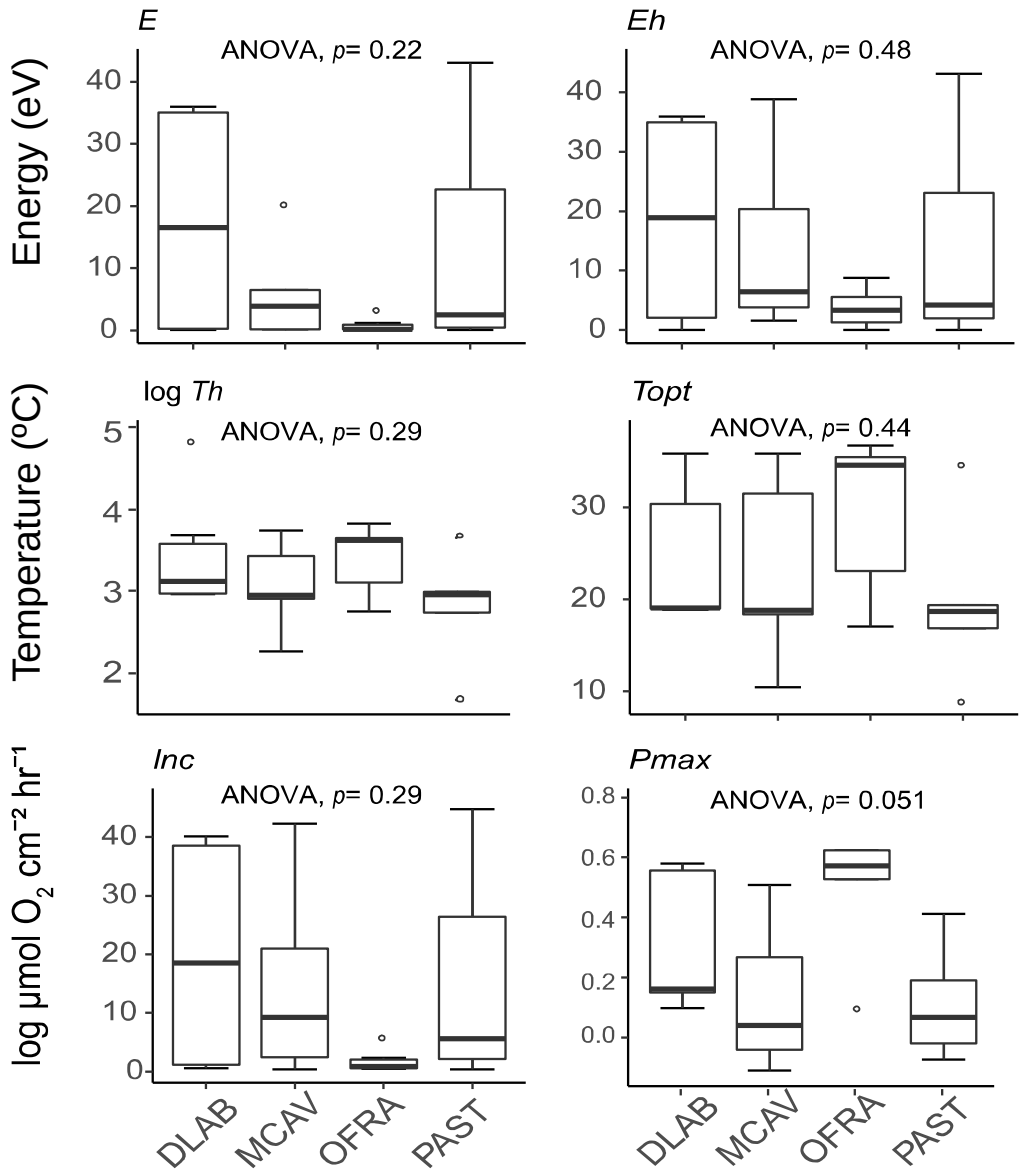


**Figure S1.6** Box and whisker plot comparing gross respiration thermal performance parameters between species (n= 192, outliers are depicted as circles). Centerlines of boxes are median values while whiskers represent upper and lower 1.58*IQR (inter-quantile range). Individual open circles are outliers. ANOVA values of 0.05 and below represent significant differences between species. DLAB= *Diploria labyrinthiformis*; MCAV= *Montastrea cavernosa*; OFRA= *Orbicella franksi*; and PAST= *Porites astreoides*. *E*= activation energy, *Eh*= deactivation energy, *Th*= temperature enzymatic inactivity, $T_{opt}$= thermal optimum, *Inc*= mean performance rate, $P_{max}$= maximum rate of performance.

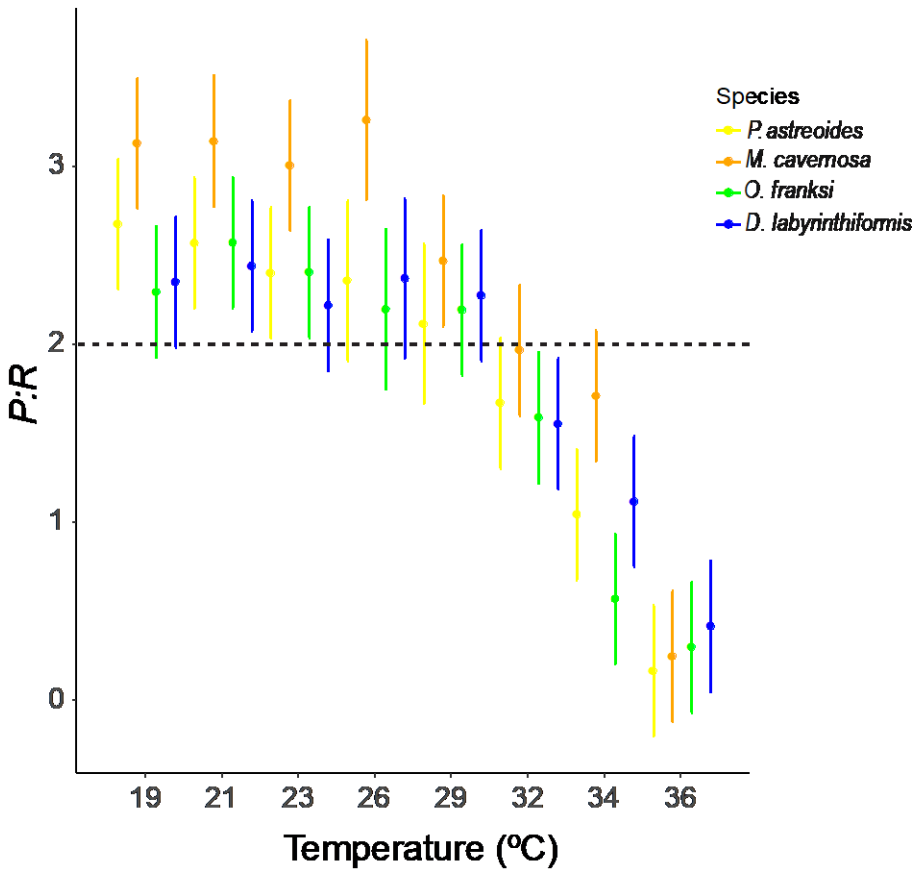


**Figure S1.7** Mean (circles) *P:R* values across depth for each species with 95% confidence intervals (bars) between for all species (n= 192). Black dashed horizontal line depicts the upper threshold of long-term survival.

## APPENDIX 2: SUPPLEMENTARY MATERIALS FOR CHAPTER 2

**Supplementary Table S2.1** Summary statistics for ANOVA tests using linear regression models and Kruskal-Wallis tests for all gross photosynthesis thermal performance parameters. Test statistics are P-statistics for ANOVA's and F-statistics for Kruskal-Wallis. $P_{max}$ = maximum rate of performance, $T_{opt}$ = thermal optimum, $T_{Br}$ = thermal breadth, $CT_{max}$ = upper thermal limit, $E$ = activation energy, and $Eh$ = deactivation energy. The * indicates significance with an alpha < 0.05.

| Performance parameter | Statistical test | Model terms | df | Statistic | *p*-value |
|---|---|---|---|---|---|
| $P_{max}$ | ANOVA | | | | |
| | | Treatment | 3 | 4.485 | 0.0082* |
| | | Genotype | 2 | 2.773 | 0.07395 |
| | | Treatment*genotype | 11 | 4.208 | 0.00064* |
| $T_{opt}$ | ANOVA | | | | |
| | | Treatment | 3 | 0.2413 | 0.867 |
| | | Genotype | 2 | 0.3812 | 0.6855 |
| | | Treatment*genotype | 11 | 0.331 | 0.9721 |
| $T_{Br}$ | Kruskal-Wallis | | | | |
| | | Treatment | 3 | 1.4 | 0.706 |
| | | Genotype | 2 | 4.96 | 0.0836 |
| | | Treatment*genotype | 11 | 8.49 | 0.669 |
| $CT_{max}$ | Kruskal-Wallis | | | | |
| | | Treatment | 3 | 4.24 | 0.236 |
| | | Genotype | 2 | 7.73 | 0.021* |
| | | Treatment*genotype | 11 | 18.7 | 0.0659 |
| $E$ | ANOVA | | | | |
| | | Treatment | 3 | 1.297 | 0.178 |
| | | Genotype | 2 | 1.298 | 0.285 |
| | | Treatment*genotype | 11 | 1.724 | 0.275 |
| $Eh$ | ANOVA | | | | |
| | | Treatment | 3 | 1.35 | 0.274 |
| | | Genotype | 2 | 2.696 | 0.079 |
| | | Treatment*genotype | 11 | 1.344 | 0.245 |

**Supplementary Table S2.2** Summary statistics for ANOVA tests using linear regression models and Kruskal-Wallis tests for all gross respiration thermal performance parameters. Test statistics are P-statistics for ANOVA's and F-statistics for Kruskal-Wallis. $R_{max}$ = maximum rate of performance, $T_{opt}$ = thermal optimum, $T_{Br}$ = thermal breadth, $CT_{max}$ = upper thermal limit, $E$ = activation energy, and $Eh$ = deactivation energy. The * indicates significance with an alpha < 0.05.

| Performance parameter | Statistical test | Model terms | df | Statistic | *p*-value |
|---|---|---|---|---|---|
| $R_{max}$ | Kruskal-Wallis | | | | |
| | | Treatment | 3 | 2.75 | 0.432 |
| | | Genotype | 2 | 10.1 | 0.0064* |
| | | Treatment*genotype | 11 | 21.8 | 0.0261* |
| $T_{opt}$ | ANOVA | | | | |
| | | Treatment | 3 | 2.934 | 0.0453* |
| | | Genotype | 2 | 6.615 | 0.0033* |
| | | Treatment*genotype | 11 | 3.186 | 0.0054* |
| $T_{Br}$ | Kruskal-Wallis | | | | |
| | | Treatment | 3 | 4.21 | 0.24 |
| | | Genotype | 2 | 7.12 | 0.0285* |
| | | Treatment*genotype | 11 | 29.3 | 0.00205* |
| $CT_{max}$ | Kruskal-Wallis | | | | |
| | | Treatment | 3 | 0.182 | 0.98 |
| | | Genotype | 2 | 3.19 | 0.203 |
| | | Treatment*genotype | 11 | 14.2 | 0.224 |
| $E$ | ANOVA | | | | |
| | | Treatment | 3 | 0.748 | 0.53 |
| | | Genotype | 2 | 3.166 | 0.0529 |
| | | Treatment*genotype | 11 | 2.091 | 0.05253 |
| $Eh$ | ANOVA | | | | |
| | | Treatment | 3 | 0.333 | 0.8012 |
| | | Genotype | 2 | 3.961 | 0.0306* |
| | | Treatment*genotype | 11 | 1.844 | 0.1264 |

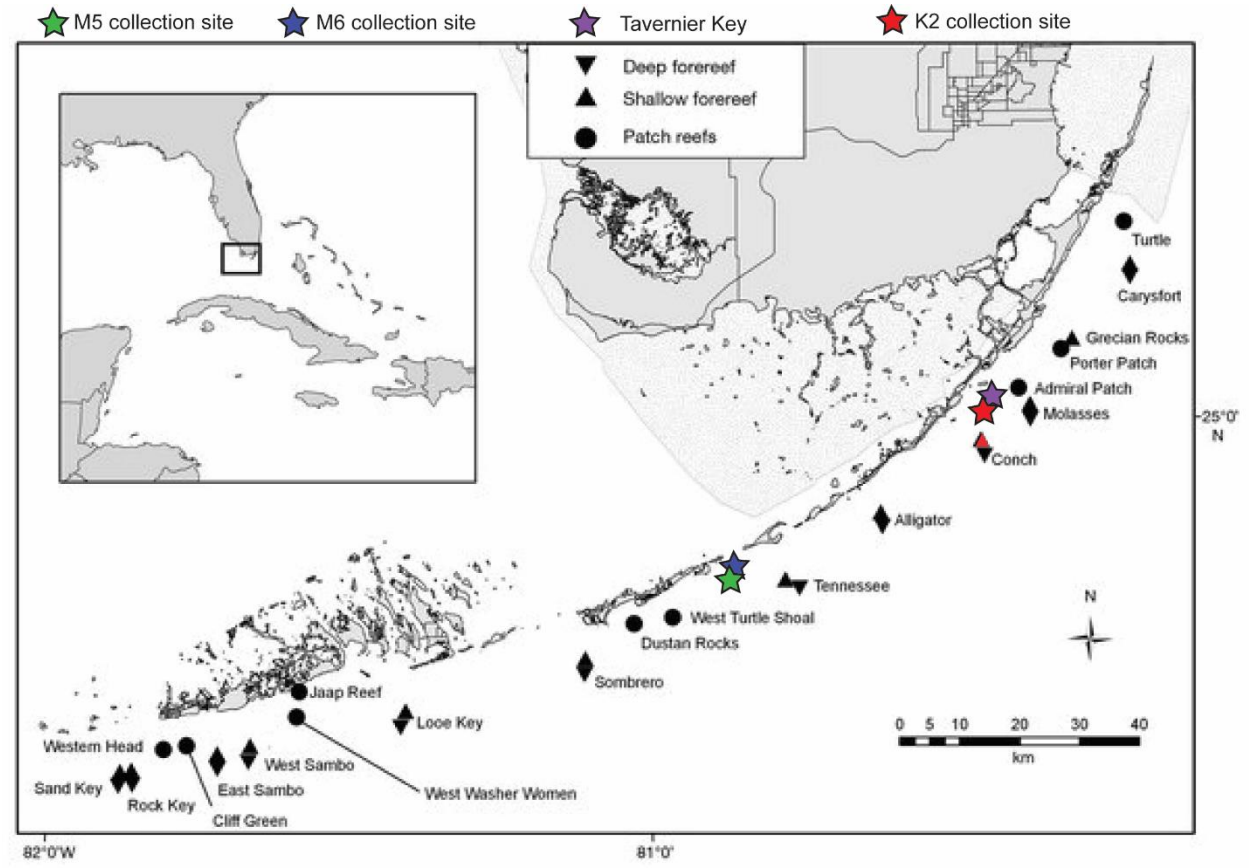


**Figure S2.1** Site locations of Tavernier Key reef (purple star), the collection site of all corals from the CRF nursery. Coral collection occurred on March 1st, 2018, and the daily temperature was 27℃. Original coral collection for each genotype is noted on map, K2 at Ken's live rock farm (Tavernier Key), and M5 and M6 at East Turtle Shoal. Red triangle represents Conch reef, the location of our four-year temperature data. Redesigned from Ruzicka et al., (2013).

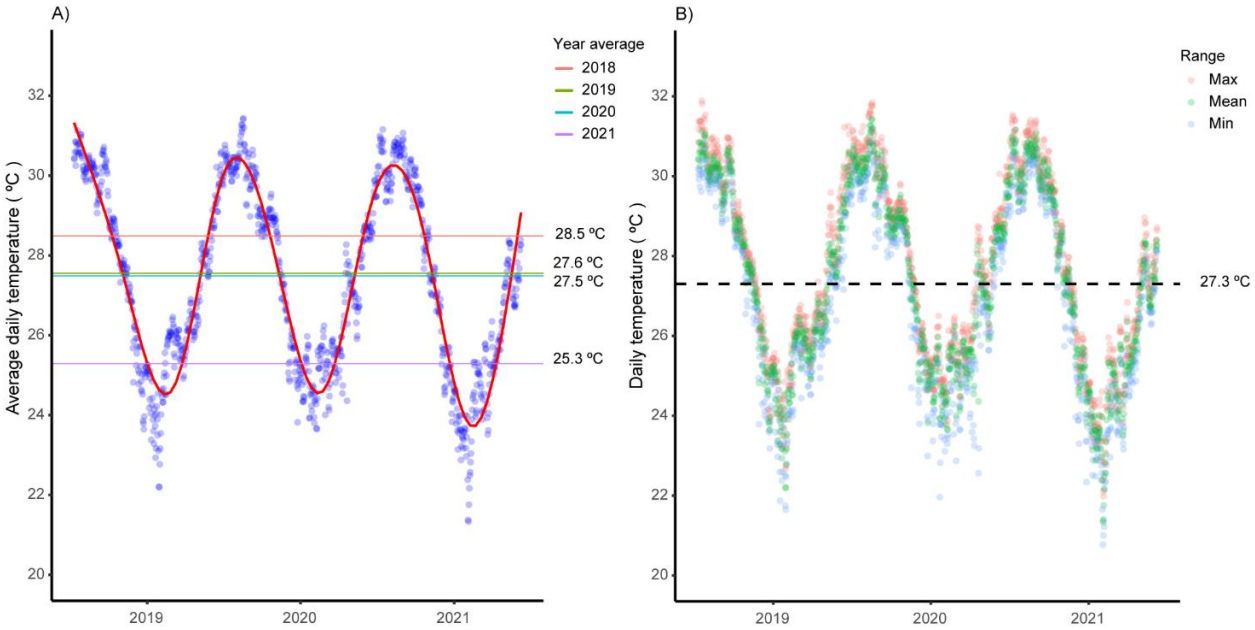


**Figure S2.2** Average daily temperature data from *in situ* CREMP data at Conch reef from 2018-2021. In A) red lines are smooth gam functions, and horizontal lines depict the overall average for each year, 2018 and 2021 have temperature data for 6 months. B) represents daily temperatures separated by maximum, minimum, and mean values for each day. The average temperature across all years is the dashed black horizontal line.

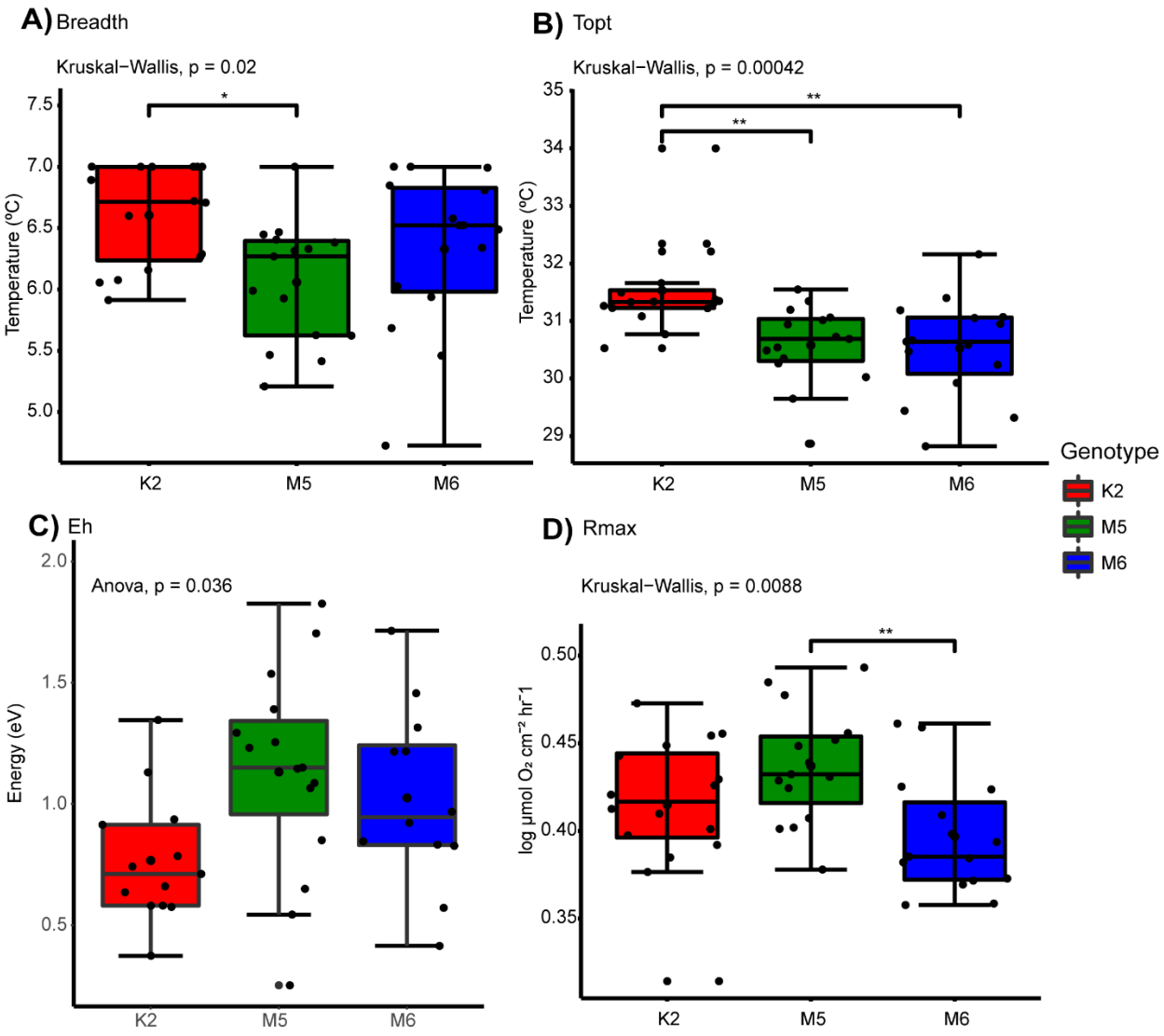


**Figure S2.3** Box and whisker plots for significant gross respiration thermal performance metrics compared between genets. Centerlines show the median values (n = 48) with 1.58*IQR (inter-quantile range) upper and lower ranges (whiskers). Thermal breadth is Breadth ($T_{br}$), thermal optimum is $T_{opt}$, deactivation energy is *Eh*, and $R_{max}$ is performance maximum. Genets are depicted as K2 is red, green as M5, and dark blue boxes are M6.

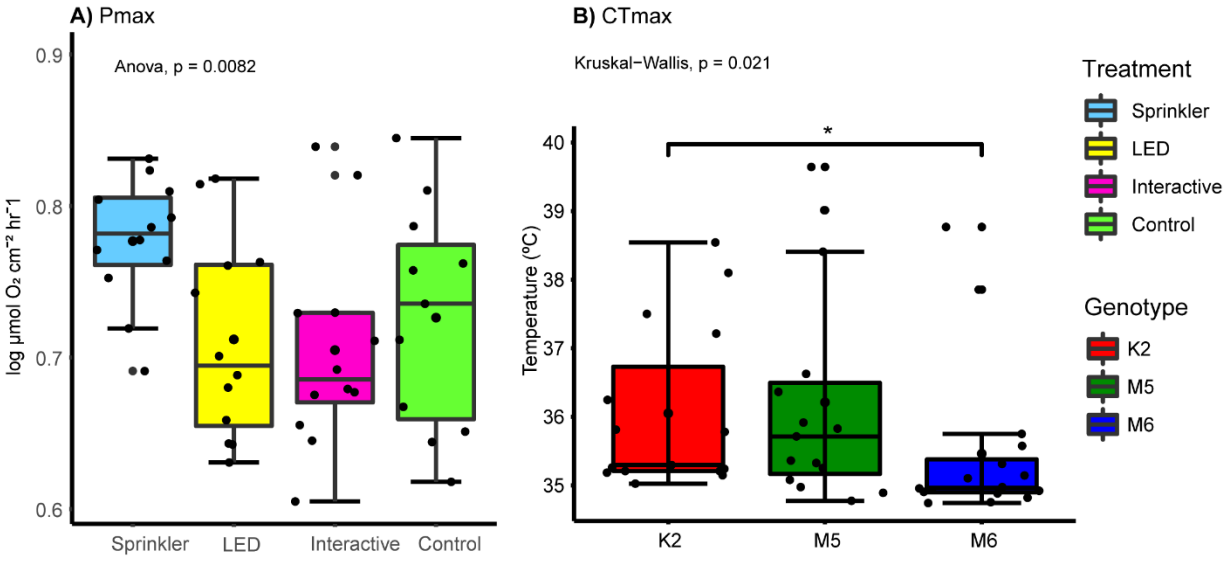


**Figure S2.4** Box and whisker plots for significant gross photosynthesis parametric metrics, performance maximum, $P_{max}$ (A) and upper thermal maximum, $CT_{max}$ (B). Centerlines are median values and whiskers represent upper and lower 1.58*IQR (inter-quantile range).

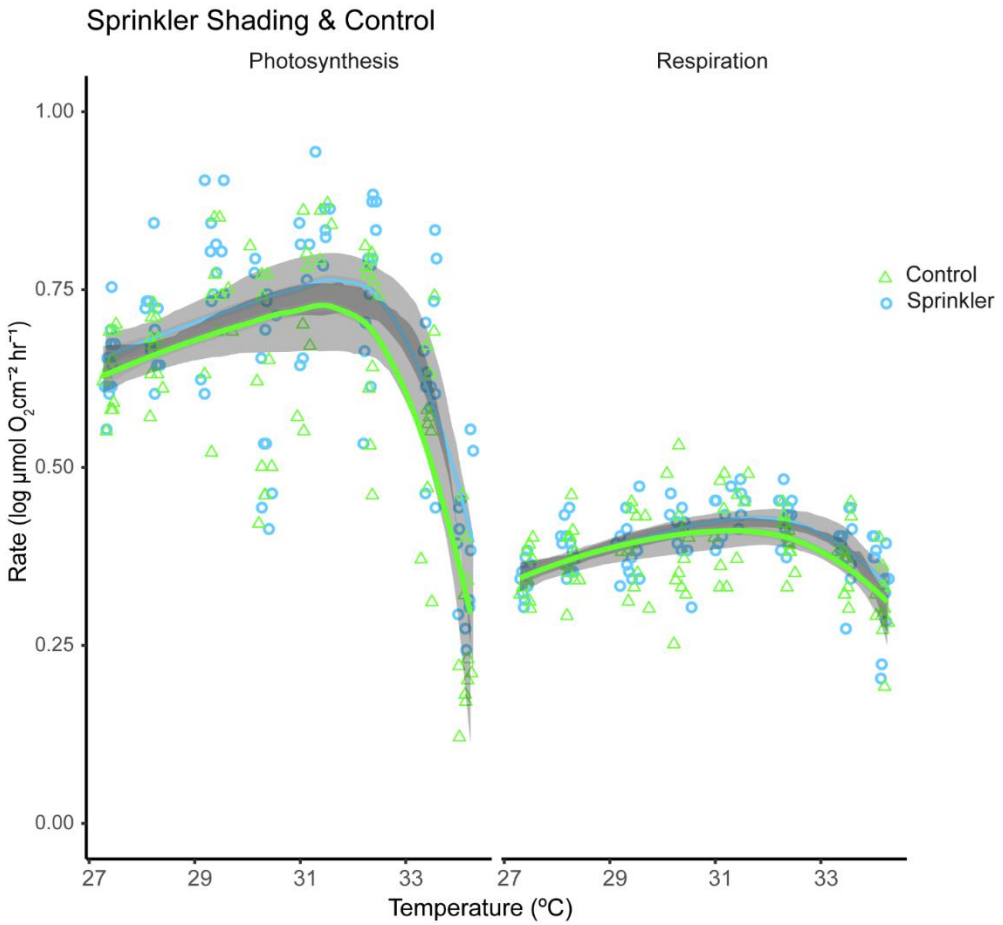


**Figure S2.5** Thermal performance curve comparison between the irrigated sprinkler (blue circles) and control (green triangles) treatments for gross photosynthesis (Photosynthesis panel) and respiration (Respiration panel). Fitted lines represent medians from 12 ramets (n = 4/genotype) in each treatment with gray 95% bootstrap confidence bands. Blue circles (sprinkler individuals) and green triangles (control individuals) represent the rate of oxygen evolution at each temperature (n = 96 metabolic points/curve/treatment), expect in the control where the M50Cd fragment was removed due to outlier status (n = 88 in the green M5 average genotype curves).

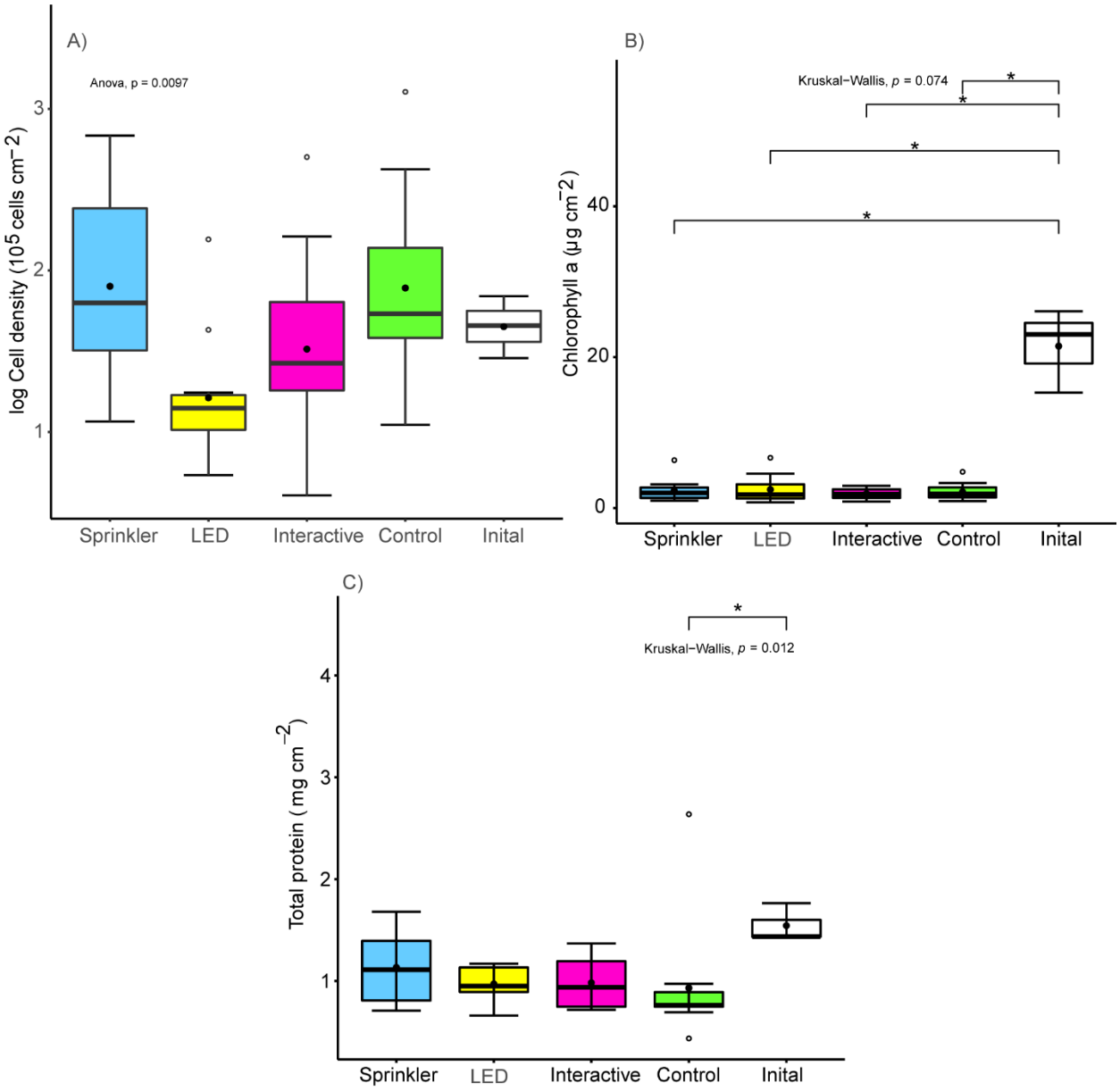


**Figure S2.6** Comparative physiology between treatments after heat stress and initial corals before heat stress (n = 3, one individual per genet). Graph A) represents symbiont densities across all treatments post heat stress and initial values from a subset of corals pre heat stress. Chlorophyll a content is shown in graph B) and total protein content is visualized in graph C).

## APPENDIX 3: SUPPLEMENTARY MATERIALS FOR CHAPTER 3

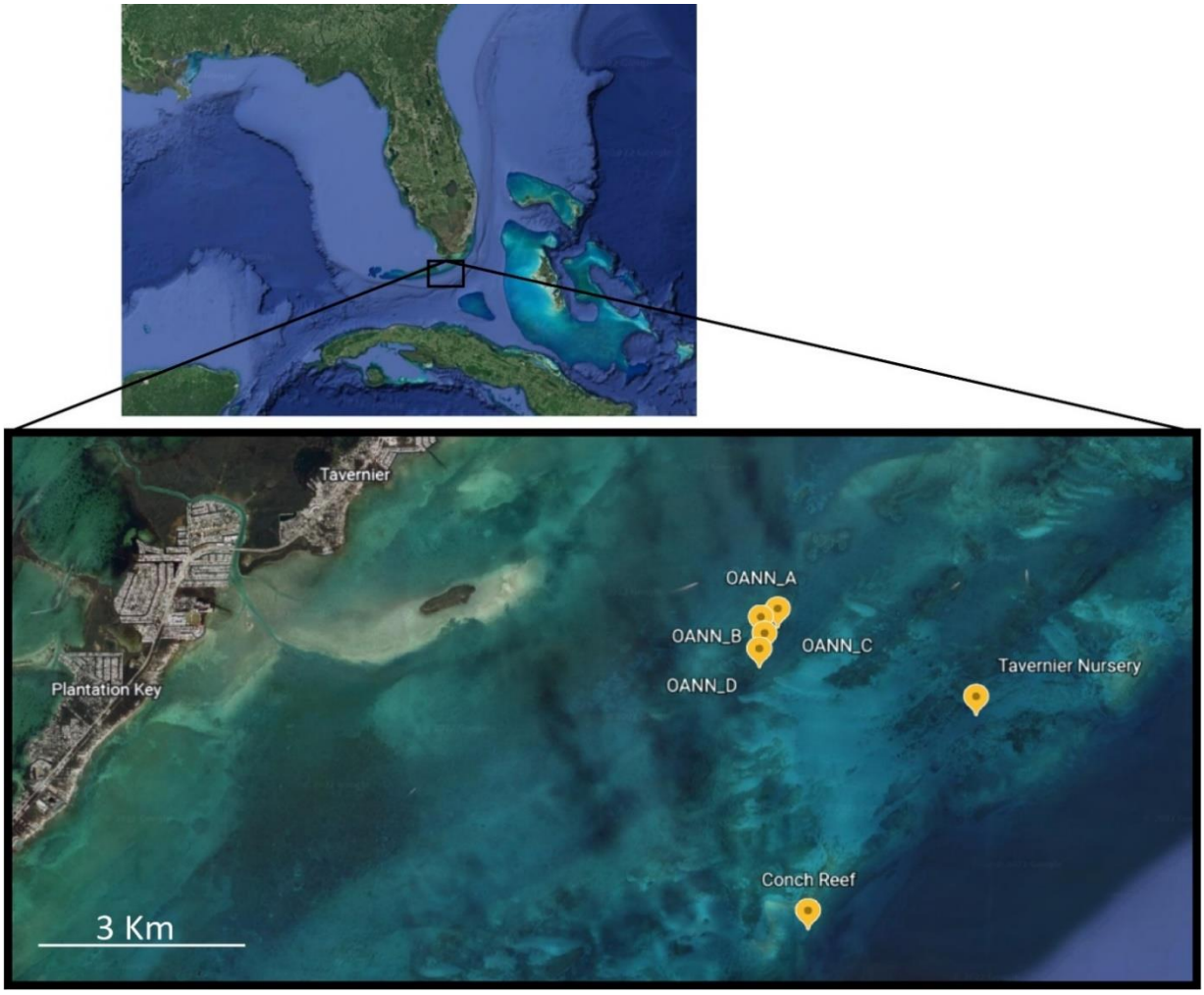


**Figure S3.1** Original collection sites for each genotype of *Orbicella annularis* genotypes used in this study. Genotype A (N 24°59'30.2" W 80°27'48.399"), B (N 24°59'23.2" W80°27'46.699"), C (N 24°59'33.8" W 80°27'40.7"), and D (N 24°59'16.4" W 80°27'49.1"). Corals were moved to the Tavernier Nursery tree (N 24°58'55.6" W 80°26'9.99") where they remained until February 4th, 2019. The "home" reef Conch Reef (N 24°57'22.3" W 80°27'26.8") is also noted.

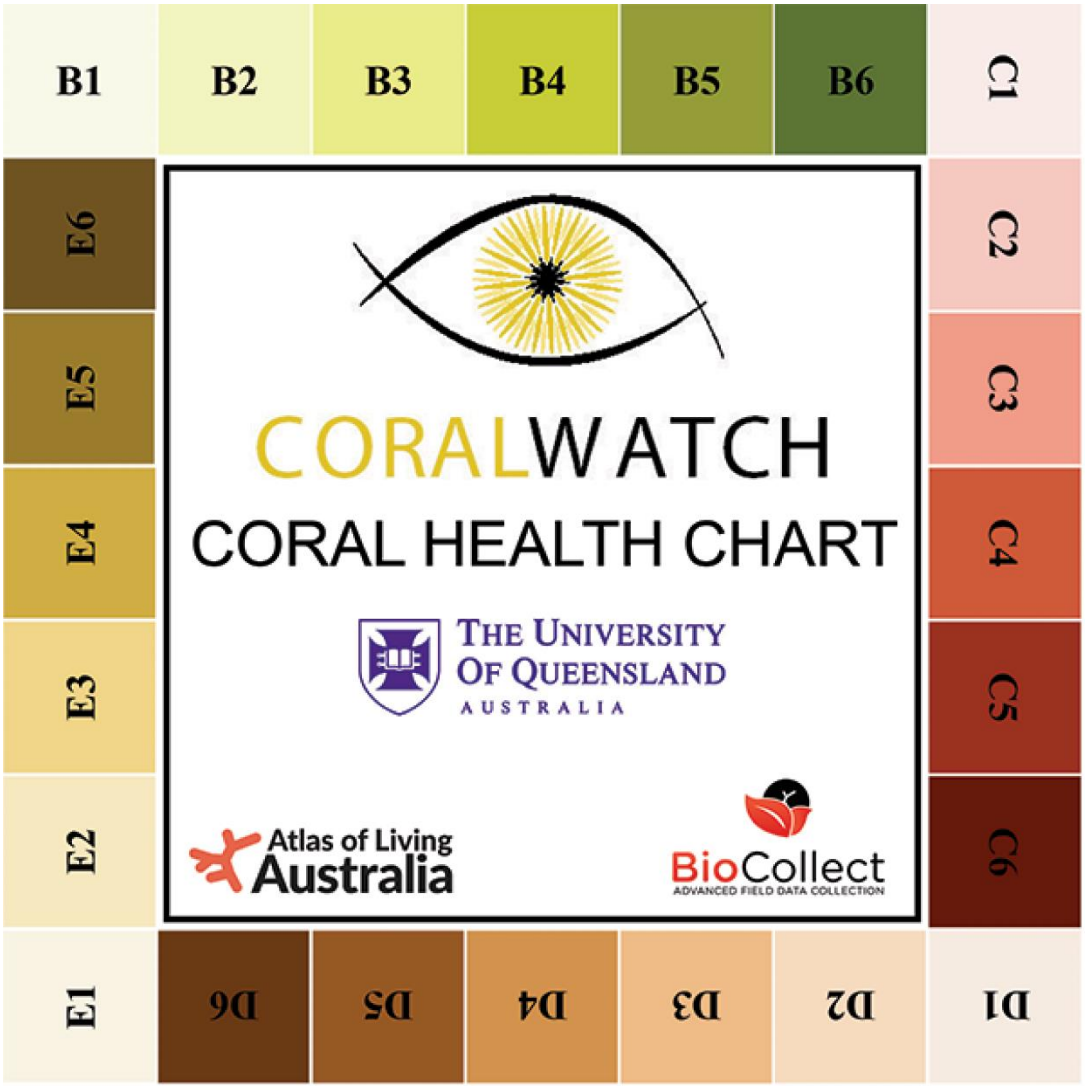


**Figure S3.2** The University of Queensland Australia's CoralWatch coral health chart. This chart was used to estimate coral tissue health, bleaching, and paling responses.

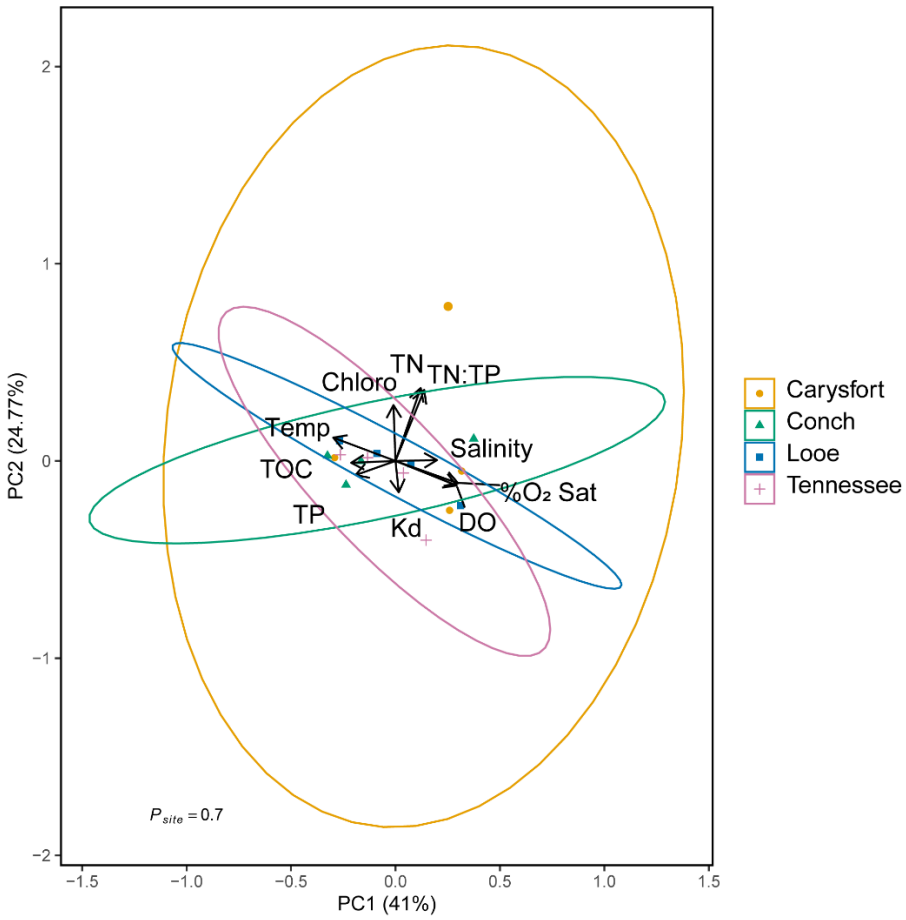


**Figure S3.3** Principal Component Analysis of water quality data clustered by significant effect of reef site. Ellipses represent each site and their clustering patterns. Arrows depict the direction of each variable and their associated PC (TN= total nitrogen (mg/L), TN:TP= molar ratio of total nitrogen and total phosphorus, Salinity (psu), $O_2$ saturation (%), DO= dissolved oxygen (mg/L), Kd= light attenuation coefficient ($m^{-1}$), TP= total phosporus (mg/L), TOC= total organic carbon (mg/L), Temp= temperature (°C), and Chloro is surface chlorophyll a concentration (mg/L). C1 explained 41% of the total variance and the PC was driven by Temp (21%) and TOC (10%). PC2 (y-axis) explains ~25% of total variation driven by TN (32.5%) and Chloro (19%).

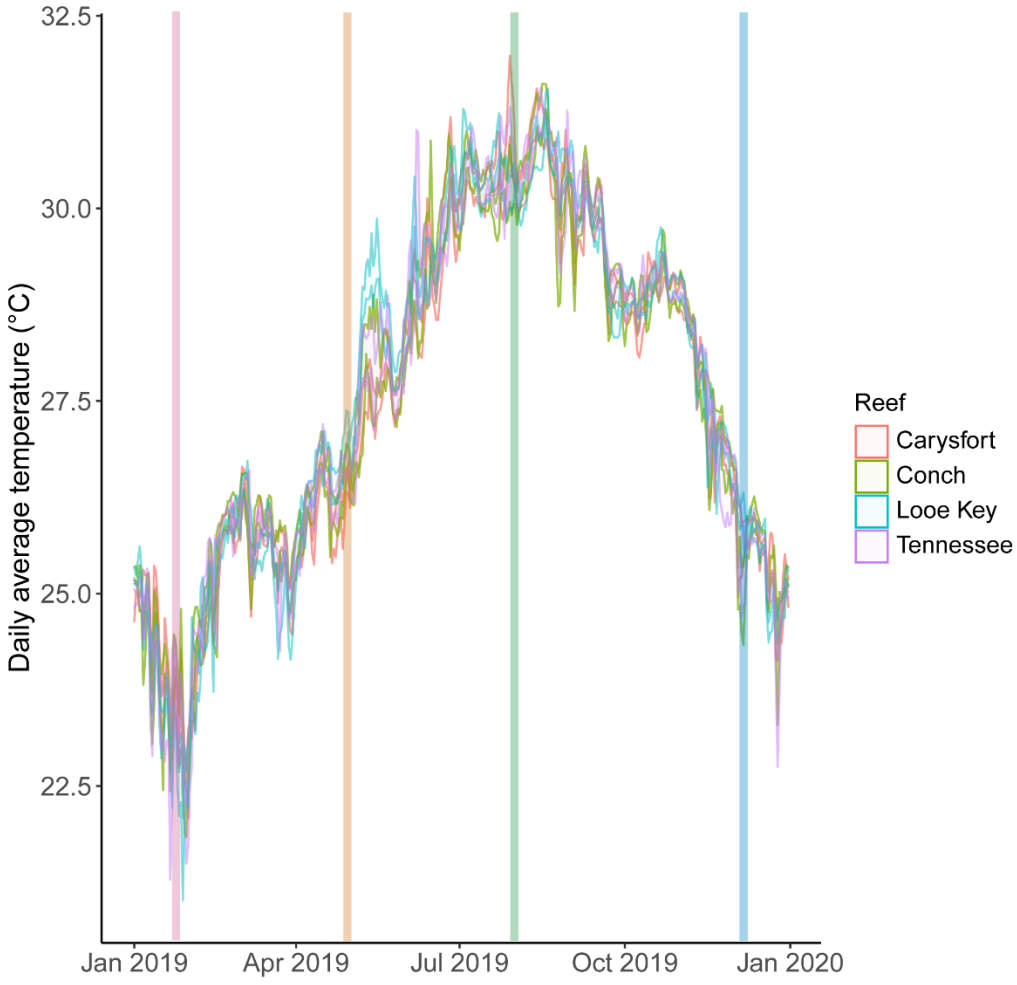


**Figure S3.4** Daily CREMP temperature means for each reef site over 2019. Vertical bars depict monitoring dates throughout the study, pink= February, orange= May, green= August, and blue= December.

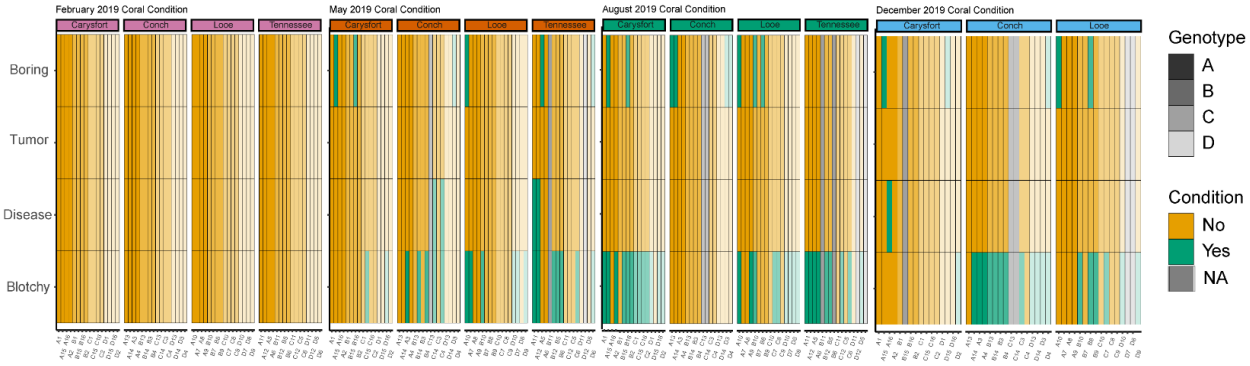


**Figure S3.5** Summary plot showing presence of condition (green) or absence (orange). Data is separated by survey month (February, May. August, and December), reef (note Tennessee was not surveyed in December), and genotypes (darker shades of condition are genotype A and get lighter approaching genotype D). Individual corals are on the x-axis and gray bars depict corals that went missing or died.

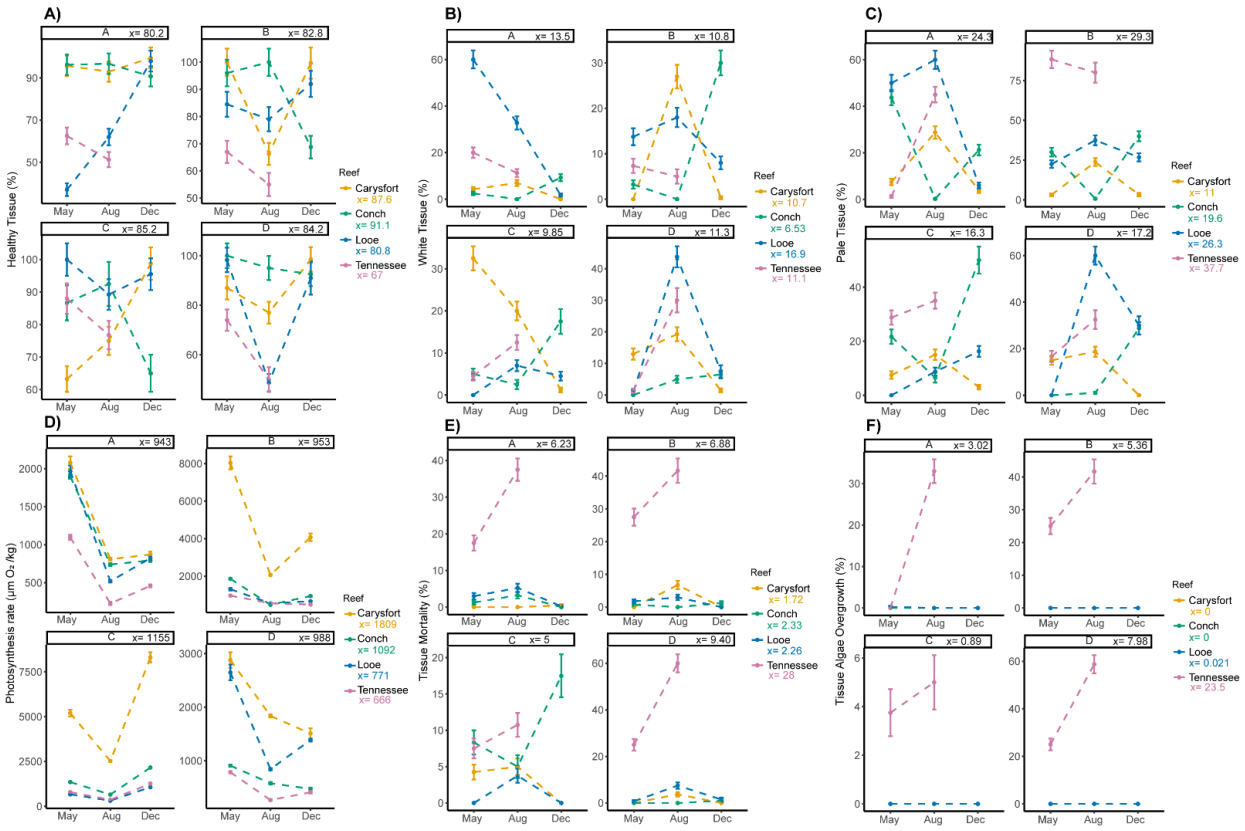


**Figure S3.6** Health parameters with 95% confidence intervals predicted from glm models across survey times (May, August, and December 2019) for mean percent healthy (A), bleached (white, B), pale (C), photosynthesis rates (D), mortality (E) and algae overgrowth on previously living tissue (F) across sites (Carysfort, Conch, Looe, and Tennessee) and grouped by genotypes (A, B, C, and D). Genotypic means are depicted on each graph next to genotype name, and site averages are labeled under each site name for each parameter**.**

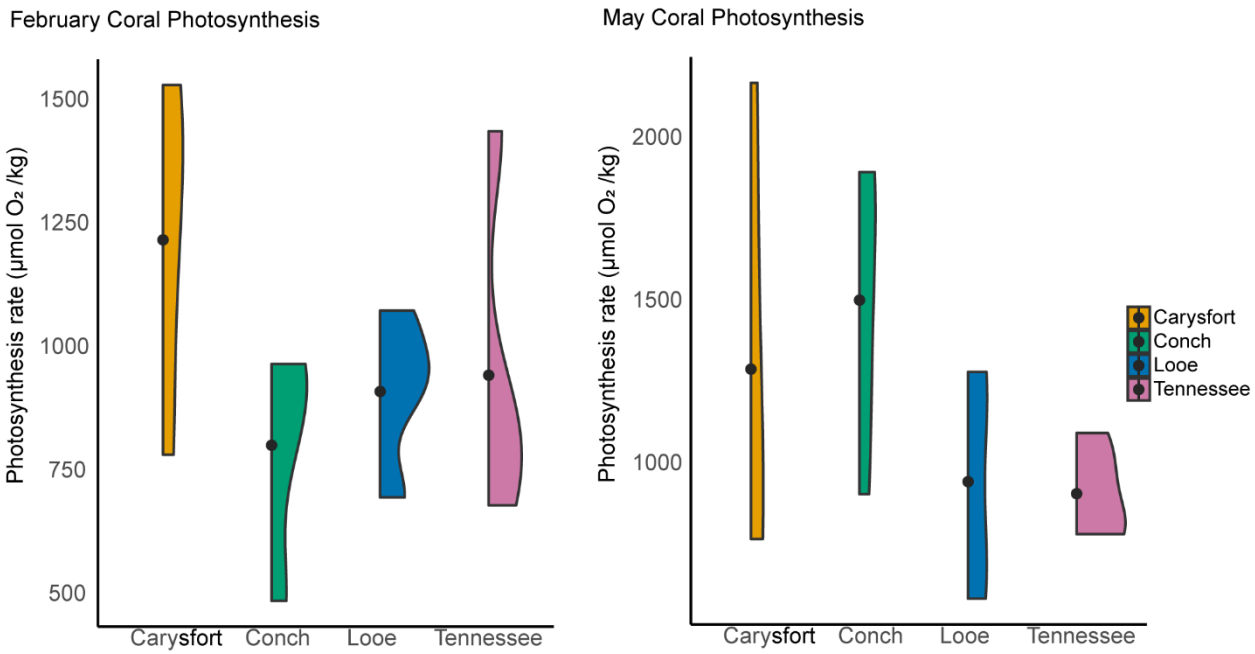


**Figure S3.7** Photosynthesis rates by reef site in February and May. Coral (n= 32) net photosynthesis rates are pooled by reef sites before transplantation (February) and three months post transplantation (May). Carysfort had significantly higher rates than Conch reef in February ($p$ = 0.005, t-test= -7.018), and Conch reef had significantly higher rates than both Looe Key ($p$ = 0.0065, t-test= 6.788) and Tennessee Reef ($p$ = 0.040, t-test= 3.45).

## REFERENCES


Abràmoff, M. D., Magalhães, P. J., & Ram, S. J. (2004). Image processing with ImageJ. Biophotonics international, **11**:7, 36–42.

Agardy, M. T. (1994). Advances in marine conservation: the role of marine protected areas. Trends in ecology & evolution, **9**:7, 267–270

Aichelman, H. E., Zimmerman, R. C., & Barshis, D. J. (2019). Adaptive signatures in thermal performance of the temperate coral Astrangia poculata. Journal of Experimental Biology, **222**:5.

Aitken, S. N., & Whitlock, M. C. (2013). Assisted gene flow to facilitate local adaptation to climate change. Annual review of ecology, evolution, and systematics, **44**, 367–388.

Al-Moghrabi, S., Allemand, D., Couret, J. M., & Jaubert, J. (1995). Fatty acids of the scleractinian coral Galaxea fascicularis: effect of light and feeding. Journal of Comparative Physiology B, **165**:3, 183–192.

Alves, C., Valdivia, A., Aronson, R. B., Bood, N., Castillo, K. D., Cox, C., ... & Bruno, J. F. (2022). Twenty years of change in benthic communities across the Belizean Barrier Reef. PloS one, **17**:1.

Angilletta Jr., M. J., & Angilletta, M. J. (2009). Evolutionary Thermal Biology. In Thermal Adaptation (pp. 1–18). Oxford University Press.

Angilletta M. J. (2009). Looking for answers to question about heat stress: Researchers are getting warmer. Funct Ecol, **23**:231–232.

Angilletta M. J., Bennett A. F., Guderley H., Navas C. A., Seebacher F., Wilson R. S., (2006). Coadaptation: a unifying principle in evolutionary thermal biology. Physiol Biochem Zool, **79**:282–94.

Angilletta M. J., Niewiarowski P. H., Navas C. A. (2002). The evolution of thermal physiology in ectotherms. J Therm Biol, **27**: 249–268.

Anthony, K., Bay, L. K., Costanza, R., Firn, J., Gunn, J., Harrison, P., ... & Walshe, T. (2017). New interventions are needed to save coral reefs. Nature ecology & evolution, **1**:10, 1420–1422.

Anton, A., Randle, J. L., Garcia, F. C., Rossbach, S., Ellis, J. I., Weinzierl, M., & Duarte, C. M. (2020). Differential thermal tolerance between algae and corals may trigger the proliferation of algae in coral reefs. Global change biology, **26**:8, 4316–4327.

Aronson, R. B., & Precht, W. F. (2001a). 9. Evolutionary Paleoecology of Caribbean Coral Reefs. In Evolutionary paleoecology (pp. 171–234). Columbia University Press.

Aronson, R. B., & Precht, W. F. (2001b). White-band disease and the changing face of Caribbean coral reefs. The ecology and etiology of newly emerging marine diseases, 25–38.

Aronson, R. B., W. F. Precht, and I. G. Macintyre. (2006). Global change and biotic homogenization of coral reefs. Geological Society American Abstracts, **38**:535.

Atwoli, L., Baqui, A. H., Benfield, T., Bosurgi, R., Godlee, F., Hancocks, S., Horton, R., Laybourn-Langton, L., Monteiro, C. A., Norman, I., Patrick, K., Praities, N., Rikkert, M. G. M. O., Rubin, E. J., Sahni, P., Smith, R., Talley, N. J., Turale, S., & Vázquez, D. (2021). Call for emergency action to limit global temperature increases, restore biodiversity, and protect health. Journal of Health, Population and Nutrition 2021, **40**:1, 1–4.

Axworthy, J. B., & Padilla-Gamiño, J. L. (2019). Microplastics ingestion and heterotrophy in thermally stressed corals. Scientific Reports 2019, **9**:1, 1–8.

Ayalon, I., de Barros Marangoni, L. F., Benichou, J. I. C., Avisar, D., & Levy, O. (2019). Red Sea corals under Artificial Light Pollution at Night (ALAN) undergo oxidative stress and photosynthetic impairment. Global Change Biology, **25**:12, 4194–4207.

Baer, J., Woodley, C. M., & Pennington, P. L. (2017). Effect of anthropogenic pollutants on sea coral health.

Baird A. H., Guest J. R. (2009). Spawning synchrony in scleractinian corals: Comment on Mangubhai and Harrison (2008). Mar Ecol Prog Ser, **374**:301–304.

Baird, M. E., Green, R., Lowe, R., Mongin, M., & Bougeot, E. (2020). Optimising cool-water injections to reduce thermal stress on coral reefs of the Great Barrier Reef. *Plos one*, **15**:10.

Bairos-Novak, K. R., Hoogenboom, M. O., van Oppen, M. J. H., & Connolly, S. R. (2021). Coral adaptation to climate change: Meta-analysis reveals high heritability across multiple traits. Global Change Biology, **27**:22, 5694–5710.

Bak R. P. M., Nieuwland G., Meesters E. H. (2005) Coral reef crisis in deep and shallow reefs: 30 years of constancy and change in reefs of Curac¸ao and Bonaire. Coral Reefs, **24**:475–479.

Baker, A. C., Glynn, P. W., & Riegl, B. (2008). Climate change and coral reef bleaching: An ecological assessment of long-term impacts, recovery trends and future outlook. Estuarine, Coastal and Shelf Science, **80**:4, 435–471.

Banister, R. B., & van Woesik, R. (2021). Ranking 67 Florida reefs for survival of Acropora cervicornis outplants. Frontiers in Marine Science, **8**, 672574.

Barott, K. L., Huffmyer, A. S., Davidson, J. M., Lenz, E. A., Matsuda, S. B., Hancock, J. R., ... & Gates, R. D. (2021). Coral bleaching response is unaltered following acclimatization to reefs with distinct environmental conditions. Proceedings of the National Academy of Sciences, **118**:22.

Bates, A. E., Cooke, R. S., Duncan, M. I., Edgar, G. J., Bruno, J. F., Benedetti-Cecchi, L., ... & Stuart-Smith, R. D. (2019). Climate resilience in marine protected areas and the 'Protection Paradox'. Biological Conservation, **236**:305–314.

Baumann, J., Grottoli, A. G., Hughes, A. D., & Matsui, Y. (2014). Photoautotrophic and heterotrophic carbon in bleached and non-bleached coral lipid acquisition and storage. Journal of Experimental Marine Biology and Ecology, **461**, 469–478.

Baums, I. B. (2008). A restoration genetics guide for coral reef conservation. Molecular Ecology, **17**:12, 2796–2811.

Baums, I. B., Baker, A. C., Davies, S. W., Ea, A., Grottoli, G., Kenkel, C. D., Kitchen, S. A., Kuffner, I. B., Lajeunesse, T. C., Matz, M. v, Miller, M. W., Parkinson, J. E., Shantz, A. A., Baums, C. :, Baker, A. C., Davies, S. W., Grottoli, A. G., Kenkel, C. D., Kitchen, S. A., … Shantz, A. A. (2019). Considerations for maximizing the adaptive potential of restored coral populations in the western Atlantic. Ecological applicationsm, **29**:8.

Baums, I. B., Johnson, M. E., Devlin-Durante, M. K., & Miller, M. W. (2010). Host population genetic structure and zooxanthellae diversity of two reef-building coral species along the Florida Reef Tract and wider Caribbean. Coral Reefs, **29:**4, 835–842.

Bay, R. A., Rose, N. H., Logan, C. A., & Palumbi, S. R. (2017). Genomic models predict successful coral adaptation if future ocean warming rates are reduced. Science Advances, **3**:11.

Bay, R. A., Rose, N. H., Logan, C. A., & Palumbi, S. R. (2017). Genomic models predict successful coral adaptation if future ocean warming rates are reduced. Science Advances, **3**:11, 1–10.

Becker, D. M., & Silbiger, N. J. (2020). Nutrient and sediment loading affect multiple facets of functionality in a tropical branching coral. Journal of Experimental Biology, **223**:21.

Becker, D. M., Putnam, H. M., Burkepile, D. E., Adam, T. C., Vega Thurber, R., & Silbiger, N. J. (2021). Chronic low-level nutrient enrichment benefits coral thermal performance in a fore reef habitat. Coral Reefs, **40**:5, 1637–1655.

Ben-Zvi, O., Lindemann, Y., Eyal, G., & Loya, Y. (2022). Coral fluorescence: a prey-lure in deep habitats. Communications Biology 2022, **5**:1, 1–8.

Berkelmans, R., & van Oppen, M. J. H. (2006). The role of zooxanthellae in the thermal tolerance of corals: a nugget of hope for coral reefs in an era of climate change. Proceedings of the Royal Society B: Biological Sciences, **273**:599, 2305–2312.

Bessell-Browne, P., Stat, M., Thomson, D., & Clode, P. L. (2014). Coscinaraea marshae corals that have survived prolonged bleaching exhibit signs of increased heterotrophic feeding. Coral Reefs, **33**:3.

Birekland, C. (1997). Life and Death Of Coral Reefs - Charles Birkeland - Google Books. Springer Science & Business Media.

Bliss, B. C. (2015). Translocation of Acropora cervicornis across geographic regions: investigating species recovery and restoration.

Board. O. S., & National Academies of Sciences, E. and M. (2019). A Research Review of Interventions to Increase the Persistence and ... - National Academies of Sciences, Engineering, and Medicine, Division on Earth and Life Studies, Board on Life Sciences,

Ocean Studies Board, Committee on Interventions to Increase the Resilience of Coral Reefs.

Bongaerts P., Frade P. R., Hay K. B., Englebert N., Latijnhouwers K. R. W., Bak R. P. M., Vermeij M. J. A., Hoegh-Guldberg O. (2015). Deep down on a Caribbean reef: Lower mesophotic depths harbor a specialized coral-endosymbiont community. Sci Rep, **5**:1–9.

Bongaerts P., Ridgway T., Sampayo E. M., Hoegh-Guldberg O. (2010). Assessing the 'deep reef refugia' hypothesis: focus on Caribbean reefs. Coral Reefs, **29**:309–327.

Bongaerts P., Riginos C., Brunner R., Englebert N., Smith S. R., Hoegh-Guldberg O. (2017). Deep reefs are not universal refuges: Reseeding potential varies among coral species. Sci Adv, **3**:2.

Boström-Einarsson, L., Babcock, R. C., Bayraktarov, E., Ceccarelli, D., Cook, N., Ferseid, S. C. A., Hancock, B., Harrison, P., Hein, M., Shaver, E., Smith, A., Suggett, D., Stewart-Sinclair, P. J., Vardi, T., & Mcleod, I. M. (2020). Coral restoration – A systematic review of current methods, successes, failures and future directions. Plos One.

Boyer, J. N., & Jones, R. D. (2002). A view from the bridge: external and internal forces affecting the ambient water quality of the Florida Keys National Marine Sanctuary (FKNMS). The Everglades, Florida Bay, and Coral Reefs of the Florida Keys: An Ecosystem Sourcebook. CRC Press, Boca Raton, FL, 609–628.

Brandt M. E., Smith T. B., Correa A. M. S., Vega-Thurber R. (2013). Disturbance Driven Colony Fragmentation as a Driver of a Coral Disease Outbreak. PLoS One, **8**:

Brazeau D. A., Lesser M. P., Slattery M. (2013). Genetic Structure in the Coral, Montastraea cavernosa: Assessing Genetic Differentiation among and within Mesophotic Reefs. PLoS One **8**.

Bridge T. C. L., Hoey A. S., Campbell S. J., Muttaqin E., Rudi E., Fadli N., Baird A. H. (2014). Depth-dependent mortality of reef corals following a severe bleaching event: Implications for thermal refuges and population recovery. Research, **2**:187, 187.

Brown B. E., Dunne R. P., Goodson M. S., Douglas A. E. (2002). Experience shapes the susceptibility of a reef coral to bleaching. Coral Reefs, **21**:119–126.

Brown, B. E. 1997. Coral bleaching: causes and consequences. Coral Reefs, **16**:S129-S138.

Brown, B. E., & Dunne, R. P. (2015). Coral Bleaching: The Roles of Sea Temperature and Solar Radiation. Diseases of Coral, 266–283.

Brown, J. H., Gillooly, J. F., Allen, A. P., Savage, V. M., & West, G. B. (2004). Toward a metabolic theory of ecology. Ecology, **85**:7, 1771–1789.

Bruno J. F., Selig E. R. (2007). Regional Decline of Coral Cover in the Indo-Pacific: Timing, Extent, and Subregional Comparisons. PLoS One, **2**:

Bruno J. F., Sweatman H., Precht W. F., Selig E. R., Schutte V. G. W. (2009). Assessing evidence of phase shifts from coral to macroalgal dominance on coral reefs. Ecology, **90**:1478–1484.

Bruno, J. F., Côté, I. M., & Toth, L. T. (2019). Climate change, coral loss, and the curious case of the parrotfish paradigm: Why don't marine protected areas improve reef resilience?. Annual review of marine science, **11**, 307–334.

Buckley L. B., & Huey R. B. (2016). How extreme temperatures impact organisms and the evolution of their thermal tolerance. Integrative and comparative biology, **56**:1, 98–109.

Budd, A. F., & Johnson, K. G. (1999). Origination preceding extinction during late Cenozoic turnover of Caribbean reefs. Paleobiology, **25**:2, 188–200.

Cacciapaglia, C., & van Woesik, R. (2016). Climate-change refugia: Shading reef corals by turbidity. Global Change Biology, **22**:3, 1145–1154.

Carnicer, J., Wheat, C., Vives, M., Ubach, A., Domingo, C., Nylin, S., ... & Peñuelas, J. (2017). Evolutionary responses of invertebrates to global climate change: The role of life-history trade-offs and multidecadal climate shifts. Global climate change and terrestrial invertebrates, 317–348.

Carpenter K. E., Abrar M., Aeby G., Aronson R. B., Banks S., Bruckner A., Chiriboga A., Cortéz J., Delbeek C., DeVantier L., Edgar G. J., Edwards A., Fenner D., Guzmán H. M., Hoeksema B., Lovell E. R., Moore J. A., Obura D. O., Ochavillo D., Polidoro B. A., Precht W. F., Quilbilan M. C., Reboton C., Richard Z. T., Rogers A., Sanciangco J., Sheppard A., Sheppard C., Smith J., Stuart S., Turak E., Veron J. E. N., Wallace C., Weil E., Wood E. (2008). One-third of reef-building corals face elevated extinction risk from climate change and local impacts. Science, **321**, 560–563.

Carte, B. K. (1996). Biomedical potential of marine natural products. Bioscience, **46**:4, 271–286.

Castillo K. D., & Helmuth, B. S. T. (2005). Influence of thermal history on the response of Montastraea annularis to short-term temperature exposure. Marine Biology, **148**:2, 261–270.

Castillo, K. D., Ries, J. B., Bruno, J. F., & Westfield, I. T. (2014). The reef-building coral Siderastrea siderea exhibits parabolic responses to ocean acidification and warming. Proceedings of the Royal Society B: Biological Sciences, **281**:1797.

Cesar, H. (1996). Work in progress toward environmentally and socially sustainable developments: Economic Analysis of Indonesian Coral Reefs.

Cheal, A. J., M. A. MacNeil, M. J. Emslie, and H. Sweatman. (2017). The threat to coral reefs from more intense cyclones under climate change. Global Change Biology, **23**:1511–1524.

Clayton, W. S., & Lasker, H. R. (1982). Effects of light and dark treatments on feeding by the reef coral Pocillopora damicornis (Linnaeus). Journal of Experimental Marine Biology and Ecology, **63**:3, 269–279.

Coates K. A., Fourqurean J. W., Kenworthy W. J., Logan A., Manuel S. A., Smith S. R. (2013). Introduction to Bermuda: Geology, Oceanography and Climate. pp 115–133.

Coelho, V. R., Fenner, D., Caruso, C., Bayles, B. R., Huang, Y., & Birkeland, C. (2017). Shading as a mitigation tool for coral bleaching in three common Indo-Pacific species. Journal of Experimental Marine Biology and Ecology, **497**, 152–163.

Coles S. L., & Jokiel, P. L. (1977). Effects of temperature on photosynthesis and respiration in hermatypic corals. Marine Biology, **43**:3, 209–216.

Coles, S. L., Bahr, K. D., Rodgers, K. S., May, S. L., McGowan, A. E., Tsang, A., Bumgarner, J., & Han, J. H. (2018). Evidence of acclimatization or adaptation in Hawaiian corals to higher ocean temperatures. PeerJ, **6**:

Conlan, J. A., Bay, L. K., Severati, A., Humphrey, C., & Francis, D. S. (2018). Comparing the capacity of five different dietary treatments to optimise growth and nutritional composition in two scleractinian corals. PLOS ONE, **13**:11.

Cook C. B., Logan A., Ward J., Luckhurst B., Berg C. J. (1990). Elevated temperatures and bleaching on a high latitude coral reef: the 1988 Bermuda event. Coral Reefs, **9**:45–49.

Courtney T. A., Kindeberg T., Andersson A. J. (2020). Coral calcification responses to the North Atlantic Oscillation and coral bleaching in Bermuda. PLoS One, **15**:11.

Courtney T. A., Lebrato M., Bates N. R., Collins A., De Putron S. J., Garley R., Johnson R., Molinero J. C., Noyes T. J., Sabine C. L., Andersson A. J. (2017). Environmental controls on modern scleractinian coral and reef-scale calcification. Sci Adv, **3**.

Cox, C., Valdivia, A., McField, M., Castillo, K., & Bruno, J. F. (2017). Establishment of marine protected areas alone does not restore coral reef communities in Belize. Marine ecology progress series, **563**:65–79.

Craik, W., Kenchington, R., & Kelleher, G. (1990). Coral-reef management. Ecosystems of the World, 25.

Csaszar, N. B., Ralph, P. J., Frankham, R., Berkelmans, R., & van Oppen, M. J. (2010). Estimating the potential for adaptation of corals to climate warming. PloS one, **5**:3.

Cunning, R., Silverstein, R. N., & Baker, A. C. (2015). Investigating the causes and consequences of symbiont shuffling in a multi-partner reef coral symbiosis under environmental change. Proceedings of the Royal Society B: Biological Sciences, **282**:1809.

Cziesielski M. J., Schmidt-Roach S., Aranda M. (2019) The past, present, and future of coral heat stress studies. Ecology and Evolution, **9**:17, 10055–10066.

D'Croz, L., & Maté, J. L. (2004). Experimental responses to elevated water temperature in genotypes of the reef coral Pocillopora damicornis from upwelling and non-upwelling environments in Panama. Coral Reefs, **23**, 473–483.

Darling E. S., Alvarez-Filip L., Oliver T. A., Mcclanahan T. R., Côté I. M. (2012). Evaluating life-history strategies of reef corals from species traits. Ecol Lett, **15**:1378–1386.

De'ath G., Fabricius K. E., Sweatman H., Puotinen M. (2012). The 27-year decline of coral cover on the Great Barrier Reef and its causes. Proc Natl Acad Sci, **109**:17995–17999.

DeCarlo, T. M., Cohen, A. L., Wong, G. T. F., Davis, K. A., Lohmann, P., & Soong, K. (2017). Mass coral mortality under local amplification of 2 °C ocean warming. Scientific Reports 2017, **7**:1, 1–9.

Devlin-Durante, M. K., & Baums, I. B. (2017). Genome-wide survey of single-nucleotide polymorphisms reveals fine-scale population structure and signs of selection in the threatened Caribbean elkhorn coral, Acropora palmata. PeerJ, **5**.

DeWitt, T. J., Sih, A., & Wilson, D. S. (1998). Costs and limits of phenotypic plasticity. Trends in ecology & evolution, **13**:2, 77–81.

DiPerna, S., Hoogenboom, M., Noonan, S., & Fabricius, K. (2018). Effects of variability in daily light integrals on the photophysiology of the corals Pachyseris speciosa and Acropora millepora. PLoS ONE, **13**:9.

Dixon G. B., Davies S. W., Aglyamova G. A., Meyer E., Bay L. K., Matz M. V. (2015). Genomic determinants of coral heat tolerance across latitudes. Science, **348**:1460–1462.

Dixon, J. A., Fallon Scura, L., & van't Hof, T. (1993). Meeting ecological and economic goals: marine parks in the Caribbean. Ambio (Sweden).

Donner, S. D., Skirving, W. J., Little, C. M., Oppenheimer, M., & Hoegh-Guldberg, O. V. E. (2005). Global assessment of coral bleaching and required rates of adaptation under climate change. Global Change Biology, **11**:12, 2251–2265.

Donovan, C., Towle, E. K., Kelsey, H., Allen, M., Barkley, H., Besemer, N., ... & Viehman, S. (2020). Coral reef condition: A status report for US coral reefs.

Driml, Sally., & Great Barrier Reef Marine Park Authority. (1994). Protection for profit: economic and financial values of the Great Barrier Reef World Heritage Area and other protected areas: a report to the Great Barrier Reef Marine Park Authority. **83**:

Drury, C., Dale, K. E., Panlilio, J. M., Miller, S. V., Lirman, D., Larson, E. A., ... & Oleksiak, M. F. (2016). Genomic variation among populations of threatened coral: Acropora cervicornis. BMC genomics, **17**:(1), 1–14.

Drury, C., Manzello, D., & Lirman, D. (2017). Genotype and local environment dynamically influence growth, disturbance response and survivorship in the threatened coral, Acropora cervicornis. PLoS One, **12**:3.

Eakin, C. M., Sweatman, H. P., & Brainard, R. E. (2019). The 2014–2017 global-scale coral bleaching event: insights and impacts. Coral Reefs, **38**:4, 539–545.

Eddy, T. D., Lam, V. W. Y., Reygondeau, G., Cisneros-Montemayor, A. M., Greer, K., Palomares, M. L. D., Bruno, J. F., Ota, Y., & Cheung, W. W. L. (2021). Global decline in capacity of coral reefs to provide ecosystem services. One Earth, **4**:9, 1278–1285.

Edmunds, P. J., & Elahi, R. (2007). The demographics of a 15-year decline in cover of the Caribbean reef coral Montastraea annularis. Ecological Monographs, **77**:1, 3–18.

Edwards, A. J. (2010). Reef rehabilitation manual.

Emanuel, K. (2005). Increasing destructiveness of tropical cyclones over the past 30 years. Nature, **436**:7051, 686–688.

Enos, P., & Perkins, R. D. (1977). Quaternary sedimentation in south Florida. Geological Society of America, **174**.

Espinosa, E. P., & Allam, B. (2006). Comparative growth and survival of juvenile hard clams, Mercenaria mercenaria, fed commercially available diets. Zoo Biology, **25**:6, 513–525.

Ferrier-Pagès, C., Rottier, C., Beraud, E., & Levy, O. (2010). Experimental assessment of the feeding effort of three scleractinian coral species during a thermal stress: Effect on the rates of photosynthesis. Journal of Experimental Marine Biology and Ecology, **390**:2, 118–124.

Fisch, J., Drury, C., Towle, E. K., Winter, R. N., & Miller, M. W. (2019). Physiological and reproductive repercussions of consecutive summer bleaching events of the threatened Caribbean coral Orbicella faveolata. Coral Reefs, **38**, 863–876.

Fitt, W. K., Mcfarland, F. K., Warner, M. E., & Chilcoat, G. C. (2000). Seasonal patterns of tissue biomass and densities of symbiotic dinoflagellates in reef corals and relation to coral bleaching. In Limnol. Oceanogr, **45**:3.

Fong, J., Poquita-Du, R. C., & Todd, P. A. (2021). Plastic responses in the coral Pocillopora acuta to extreme low-light conditions with and without food provision. Marine Biology, **168**:7.

Forsman, Z. H., Kimokeo, B. K., Bird, C. E., Hunter, C. L., & Toonen, R. J. (2012). Coral farming: Effects of light, water motion and artificial foods. Journal of the Marine Biological Association of the United Kingdom, **92**:4, 721–729.

Frade P. R., Bongaerts P., Englebert N., Rogers A., Gonzalez-Rivero M., Hoegh-Guldberg O. (2018). Deep reefs of the Great Barrier Reef offer limited thermal refuge during mass coral bleaching. Nat Commun, **9**:1, 3447.

Frankowiak, K., Wang, X. T., Sigman, D. M., Gothmann, A. M., Kitahara, M. v., Mazur, M., Meibom, A., & Stolarski, J. (2016). Photosymbiosis and the expansion of shallow-water corals. Science Advances, **2**:11.

Fraundorfer, M. (2022). Global Governance in the Age of the Anthropocene. Palgrave Macmillan.

Freeman, R. K., Vallières, E., Verrier, E. D., Karmy-Jones, R., & Wood, D. E. (2001). Coral bleaching: Interpretation of thermal tolerance limits and thermal thresholds in tropical corals. Coral Reefs, **20**:1, 51–65.

Gardner, T. a, I. M. Côté, J. a Gill, A. Grant, and A. R. Watkinson. (2003). Long-term region-wide declines in Caribbean corals. Science, **301**:958–60.

Gardner, T. A., Côté, I. M., Gill, J. A., Grant, A., & Watkinson, A. R. (2003). Long-term region-wide declines in Caribbean corals. science, **301**:5635, 958–960.

Gibson, P. J., Boyer, J. N., & Smith, N. P. (2008). Nutrient mass flux between florida bay and the florida keys national marine sanctuary. Estuaries and coasts, **31**, 21–32.

Gil, M. A., Baskett, M. L., Munch, S. B., & Hein, A. M. (2020). Fast behavioral feedbacks make ecosystems sensitive to pace and not just magnitude of anthropogenic environmental change. Proceedings of the National Academy of Sciences, **117**:41, 25580–25589.

Ginsburg, R. N., & Shinn, E. A. (1995). Preferential distribution of reefs in the Florida reef tract: the past is the key to the present. Oceanographic Literature Review, **8**:42, 674.

Gintert, B. E., Manzello, D. P., Enochs, I. C., Kolodziej, G., Carlton, R., Gleason, A. C. R., & Gracias, N. (2018). Marked annual coral bleaching resilience of an inshore patch reef in the Florida Keys: A nugget of hope, aberrance, or last man standing? Coral Reefs 2018, **37**:2, 533–547.

Glynn, P. W. (1984). Widespread coral mortality and the 1982–83 El Niño warming event. Environmental Conservation, **11**:2, 133–146.

Glynn, P. W. 1991. Coral-reef bleaching in the 1980s and possible connections with global warming. Trends in Ecology & Evolution **6**:175–179.

Gonzalez-Espinosa, P. C., & Donner, S. D. (2021). Cloudiness reduces the bleaching response of coral reefs exposed to heat stress. Global Change Biology, **27**:15, 3474–3486.

Goodbody-Gringley G., Marchini C., Chequer A. D., Goffredo S. (2015). Population structure of Montastraea cavernosa on shallow versus mesophotic reefs in Bermuda. PLoS One, **10**:1–17.

Goodbody-Gringley G., Wong K. H., Becker D.M., Glennon K., de Putron S. J. (2018). Reproductive ecology and early life history traits of the brooding coral, Porites astreoides, from shallow to mesophotic zones. Coral Reefs, **37**:483–494.

Gouezo, M., Golbuu, Y., Fabricius, K., Olsudong, D., Mereb, G., Nestor, V., ... & Doropoulos, C. (2019). Drivers of recovery and reassembly of coral reef communities. Proceedings of the Royal Society B, **286**:1897.

Gould, K., Bruno, J. F., Ju, R., & Goodbody-Gringley, G. (2021). Upper-mesophotic and shallow reef corals exhibit similar thermal tolerance, sensitivity and optima. Coral Reefs.

Grottoli, A. G., Rodrigues, L. J., & Palardy, J. E. (2006). Heterotrophic plasticity and resilience in bleached corals. Nature 2006, **440**:7088, 1186–1189.

Guest J. R., Baird A. H., Maynard J. A., Muttaqin E., Edwards A. J., Campbell S. J., Yewdall K., Affendi Y. A., Chou L. M. (2012). Contrasting patterns of coral bleaching susceptibility in 2010 suggest an adaptive response to thermal stress. PLoS One, **7**:3.

Hackerott, S., Martell, H. A., & Eirin-Lopez, J. M. (2021). Coral environmental memory: causes, mechanisms, and consequences for future reefs. Trends in Ecology & Evolution, **36**:11, 1011–1023.

Haslun J. A., Strychar K. B., Buck G., Sammarco P. W. (2011). Coral Bleaching Susceptibility Is Decreased following Short-Term (1–3 Year) Prior Temperature Exposure and Evolutionary History. J Mar Biol, **2011**:1–13.

Hawkins, T. D., & Warner, M. E. (2017). Warm preconditioning protects against acute heat-induced respiratory dysfunction and delays bleaching in a symbiotic sea anemone. Journal of Experimental Biology, **220**:6, 969–983.

Hellberg, M. E. (2006). No variation and low synonymous substitution rates in coral mtDNA despite high nuclear variation. BMC evolutionary biology, **6**:1, 1–8.

Hellberg, M. E. (2007). Footprints on water: the genetic wake of dispersal among reefs. Coral Reefs, **26**:3, 463–473.

Hendry, A. P. (2016). Key questions on the role of phenotypic plasticity in eco-evolutionary dynamics. Journal of Heredity, **107**:1, 25–41.

Henson, S. A., Beaulieu, C., Ilyina, T., John, J. G., Long, M., Séférian, R., Tjiputra, J., & Sarmiento, J. L. (2017). Rapid emergence of climate change in environmental drivers of marine ecosystems. Nature Communications 2017, **8**:1, 1–9.

Hii, Y. S., Soo, C. L., & Liew, H. C. (2009). Feeding of scleractinian coral, Galaxea fascicularis, on Artemia salina nauplii in captivity. Aquaculture International, **17**:4, 363–376.

Hill R., Szabó M, Rehman A. U., Vass I., Ralph P. J., Larkum A. W. D. (2014). Inhibition of photosynthetic CO2 fixation in the coral Pocillopora damicornis and its relationship to thermal bleaching. J Exp Biol, **217**:2150–2162.

Hill, R., Brown, C. M., DeZeeuw, K., Campbell, D. A., & Ralph, P. J. (2011). Increased rate of D1 repair in coral symbionts during bleaching is insufficient to counter accelerated photo-inactivation. Limnology and Oceanography, **56**:1, 139–146.

Hill, R., Larkum, A. W. D., Prášil, O., Kramer, D. M., Szabó, M., Kumar, V., & Ralph, P. J. (2012). Light-induced dissociation of antenna complexes in the symbionts of scleractinian corals correlates with sensitivity to coral bleaching. Coral Reefs, **31**:4, 963–975.

Hinderstein L. M., Marr J. C. A., Martinez F. A., Dowgiallo M. J., Puglise K. A., Pyle R. L., Zawada D. G., Appeldoorn R. (2010). Theme section on "Mesophotic Coral Ecosystems: Characterization, Ecology, and Management." Coral Reefs, **29**:247–251.

Hochachka, P. W., & Somero, G. N. (2002). Biochemical adaptation: mechanism and process in physiological evolution. Oxford university press.

Hoegh-Guldberg O. (1999). Climate Change, coral bleaching and the future of the world' s coral reefs. Ove Hoegh-Guldberg. Mar Freshw Res, **50**:839–866.

Holbrook, N. J., Oliver, E. C. J., Hobday, A. J., & Benthuysen, J. (2020). Keeping pace with marine heatwaves CSIRO project View project Examining the ecological consequences of climatedriven shifts in the structure of NE Atlantic kelp forests View project.

Holbrook, N. J., Scannell, H. A., sen Gupta, A., Benthuysen, J. A., Feng, M., Oliver, E. C. J., Alexander, L. v., Burrows, M. T., Donat, M. G., Hobday, A. J., Moore, P. J., Perkins-Kirkpatrick, S. E., Smale, D. A., Straub, S. C., & Wernberg, T. (2019). A global assessment of marine heatwaves and their drivers. Nature Communications, **10**:1.

Hoogenboom, M. O., Anthony, K. R. N., & Connolly, S. R. (2006). Energetic cost of photoinhibition in corals. Marine Ecology Progress Series, **313**, 1–12.

Houlbrèque, F., & Ferrier-Pagès, C. (2009). Heterotrophy in Tropical Scleractinian Corals. Biological Reviews, **84**:1, 1–17.

Houlbrèque, F., Tambutté, E., Allemand, D., & Ferrier-Pagès, C. (2004). Interactions between zooplankton feeding, photosynthesis and skeletal growth in the scleractinian coral Stylophora pistillata. Journal of Experimental Biology, **207**:9, 1461–1469.

Howells, E. J., Beltran, V. H., Larsen, N. W., Bay, L. K., Willis, B. L., & van Oppen, M. J. H. (2011). Coral thermal tolerance shaped by local adaptation of photosymbionts. Nature Climate Change 2012, **2**:2, 116–120.

Huey R. B., Kingsolver J. G. (1989). Evolution of thermal sensitivity of ectotherm performance. Trends Ecol Evol, **4**:131–5.

Huey R. B., Kingsolver J. G. (1993). Evolution of resistance to high temperature in ectotherms. Am Nat, **142**: 21–46.

Huey, R. B., & Kingsolver, J. G. (2019). Climate warming, resource availability, and the metabolic meltdown of ectotherms. The American Naturalist, **194**:6, 140–150.

Hughes, A. D., & Grottoli, A. G. (2013). Heterotrophic Compensation: A Possible Mechanism for Resilience of Coral Reefs to Global Warming or a Sign of Prolonged Stress? PLOS ONE, **8**:11.

Hughes, T. P., Anderson, K. D., Connolly, S. R., Heron, S. F., Kerry, J. T., Lough, J. M., ... & Wilson, S. K. (2018). Spatial and temporal patterns of mass bleaching of corals in the Anthropocene. Science, **359**:6371, 80–83.

Hughes, T. P., Kerry, J. T., Álvarez-Noriega, M., Álvarez-Romero, J. G., Anderson, K. D., Baird, A. H., Babcock, R. C., Beger, M., Bellwood, D. R., Berkelmans, R., Bridge, T. C., Butler, I. R., Byrne, M., Cantin, N. E., Comeau, S., Connolly, S. R., Cumming, G. S., Dalton, S. J., Diaz-Pulido, G., … Wilson, S. K. (2017). Global warming and recurrent mass bleaching of corals. Nature 2017, **543**:7645, 373–377.

Hughes, T. P., Kerry, J. T., Baird, A. H., Connolly, S. R., Dietzel, A., Eakin, C. M., Heron, S. F., Hoey, A. S., Hoogenboom, M. O., Liu, G., McWilliam, M. J., Pears, R. J., Pratchett, M. S., Skirving, W. J., Stella, J. S., & Torda, G. (2018). Global warming transforms coral reef assemblages. Nature 2018, **556**:7702, 492–496.

Jaap, W. C., Szmant, A., Jaap, K., Dupont, J., Clarke, R., Somerfield, P., ... & Kellison, G. T. (2008). A perspective on the biology of Florida Keys coral reefs. In Coral Reefs of the USA (pp. 75–125). Springer, Dordrecht.

Jackson J. B. C., Donovan M. K., Cramer K. L. L. V. (2014). Status and Trends of Caribbean Coral Reefs- 1970–2012–2014 Caribbean Coral Reefs - Status Report 1970–2012 (1). Glob Coral Reef Monit Network, IUCN, Gland Switz.

Jackson, J. B. (1992). Pleistocene perspectives on coral reef community structure. American Zoologist, **32**:6, 719–731.

Jeffrey, S. W., & Humphrey, G. F. (1975). New spectrophotometric equations for determining chlorophylls a, b, c1 and c2 in higher plants, algae and natural phytoplankton. Biochemie Und Physiologie Der Pflanzen, **167**:2, 191–194.

Jiang, L., Sun, Y. F., Zhang, Y. Y., Tian, Y., Lei, X. M., Zhou, G. W., ... & Huang, H. (2021). Ocean acidification alters the thermal performance curves of brooded larvae from the reef coral Pocillopora damicornis. Coral Reefs, **40**:1437–1449.

Jokiel, P. L., & Maragos, J. E. (1978). Coral Buoyant Weighing. Coral Reefs: Research Methods.

Jokiel, P. L., and S.L. Coles. (1977). Effects of temperature on mortality and growth of Hawaiian reef corals. Marine Biology, **43**:201–208.

Jones, A. M., Berkelmans, R., van Oppen, M. J. H., Mieog, J. C., & Sinclair, W. (2008). A community change in the algal endosymbionts of a scleractinian coral following a natural bleaching event: field evidence of acclimatization. Proceedings of the Royal Society B: Biological Sciences, **275**:1641, 1359–1365.

Jurriaans, S., & Hoogenboom, M. O. (2019). Thermal performance of scleractinian corals along a latitudinal gradient on the Great Barrier Reef. Philosophical Transactions of the Royal Society B, **374**:1778.

Jurriaans, S., & Hoogenboom, M. O. (2020). Seasonal acclimation of thermal performance in two species of reef-building corals. Marine Ecology Progress Series, **635**:55–70.

Jurriaans, S., Hoogenboom, M. O., & Ferrier-Pages, C. (2021). Similar thermal breadth of two temperate coral species from the Mediterranean Sea and two tropical coral species from the Great Barrier Reef. Coral Reefs, **40**:4, 1281–1295.

Kahng S. E., Akkaynak D., Shlesinger T., Hochberg E. J., Wiedenmann J., Tamir R., Tchernov D. (2019). Light, Temperature, Photosynthesis, Heterotrophy, and the Lower Depth Limits of Mesophotic Coral Ecosystems. pp 801–828.

Kahng S. E., Copus J. M., Wagner D. (2014). Recent advances in the ecology of mesophotic coral ecosystems (MCEs). Curr Opin Environ Sustain, **7**:72–81.

Kahng S. E., Wagner D., Lantz C., Vetter O., Gove J., Merrifield M. (2012). Temperature related depth limits of warm-water corals. Ecol mesophotic coral reefs.

Kahng S., Copus J. M., Wagner D. (2016). Mesophotic Coral Ecosystems. Mar Anim For, **10**:

Kassen, R. (2002). The experimental evolution of specialists, generalists, and the maintenance of diversity. Journal of evolutionary biology, **15**:2, 173–190.

Kawecki, T. J., & Ebert, D. (2004). Conceptual issues in local adaptation. Ecology letters, **7**:12, 1225–1241.

Kelleher, G. (1999). Guidelines for marine protected areas. IUCN, Gland, Switzerland and Cambridge, UK.

Kelly, M. (2019). Adaptation to climate change through genetic accommodation and assimilation of plastic phenotypes. Philosophical Transactions of the Royal Society B, **374**:1768.

Kenkel, C. D., Aglyamova, G., Alamaru, A., Bhagooli, R., Capper, R., Cunning, R., deVillers, A., Haslun, J. A., Hédouin, L., Keshavmurthy, S., Kuehl, K. A., Mahmoud, H., McGinty, E. S., Montoya-Maya, P. H., Palmer, C. v., Pantile, R., Sánchez, J. A., Schils, T., Silverstein, R. N., … Matz, M. v. (2011). Development of gene expression markers of acute heat-light stress in reef-building Corals of the genus porites. PLoS ONE, **6**:10.

Kenkel, C. D., Almanza, A. T., & Matz, M. V. (2015). Fine-scale environmental specialization of reef-building corals might be limiting reef recovery in the Florida Keys. Ecology, **96**:12, 3197–3212.

Kennedy, E. V., Perry, C. T., Halloran, P. R., Iglesias-Prieto, R., Schönberg, C. H., Wisshak, M., ... & Mumby, P. J. (2013). Avoiding coral reef functional collapse requires local and global action. Current Biology, **23**:10, 912–918.

Kingsolver, J. G., & Woods, H. A. (2016). Beyond Thermal Performance Curves: Modeling Time-Dependent Effects of Thermal Stress on Ectotherm Growth Rates. The American Naturalist, **187**:3, 283–294.

Klein III, C. J., & Orlando Jr, S. P. (1994). A spatial framework for water-quality management in the Florida Keys National Marine Sanctuary. Bulletin of Marine Science, **54**:3, 1036–1044.

Kleypas, J. A., McManus J. W., Menez, L. A. B. (1999). Environmental limits to coral reef development: Where do we draw the line? American Zoologist, **39**:146–159

Knies J. L., Kingsolver J. G., Burch C. L. (2009). Hotter is better and broader: Thermal sensitivity of fitness in a population of bacteriophages. Am Nat, **173**:419–430.

Kobluk D. R., Lysenko M. A. (1994). "Ring" bleaching in southern Caribbean Agaricia agaricites during rapid water cooling. Bulletin of Marine Science, **54**:142–150.

Kramer N., Tamir R., Eyal G., Loya Y. (2020). Coral Morphology Portrays the Spatial Distribution and Population Size-Structure Along a 5–100 m Depth Gradient. Front Mar Sci, **7**:

Kramer, P. A. (2003). Synthesis of coral reef health indicators for the western Atlantic: results of the AGRRA program (1997–2000). Atoll Research Bulletin.

Krueger, T., Bodin, J., Horwitz, N., Loussert-Fonta, C., Sakr, A., Escrig, S., Fine, M., & Meibom, A. (2018). Temperature and feeding induce tissue level changes in autotrophic and heterotrophic nutrient allocation in the coral symbiosis – A NanoSIMS study. Scientific Reports 2018, **8**:1, 1–15.

Kuffner, I. B., & Toth, L. T. (2016). A geological perspective on the degradation and conservation of western Atlantic coral reefs. Conservation Biology, **30**:4, 706–715.

Ladd, M. C., Miller, M. W., Hunt, J. H., Sharp, W. C., & Burkepile, D. E. (2018). Harnessing ecological processes to facilitate coral restoration. Frontiers in Ecology and the Environment, **16**:4, 239–247.

Ladd, M. C., Shantz, A. A., Bartels, E., & Burkepile, D. E. (2017). Thermal stress reveals a genotype-specific tradeoff between growth and tissue loss in restored Acropora cervicornis. Marine Ecology Progress Series, **572**:129–139.

Lajeunesse T. C., Parkinson J. E., Gabrielson P. W., Jeong H. J., Reimer J. D. (2018). Systematic Revision of Symbiodiniaceae Highlights the Antiquity and Diversity of Coral Endosymbionts Article Systematic Revision of Symbiodiniaceae Highlights the Antiquity and Diversity of Coral Endosymbionts. Curr Biol, **28**:2570–2580.

Lapointe, B. E., & Clark, M. W. (1992). Nutrient inputs from the watershed and coastal eutrophication in the Florida Keys. Estuaries, **15**:465–476.

Laufkötter, C., Zscheischler, J., & Frölicher, T. L. (2020). High-impact marine heatwaves attributable to human-induced global warming. Science, **369**:6511.

Laverick J. H., Tamir R., Eyal G., Loya Y. (2020). A generalized light-driven model of community transitions along coral reef depth gradients. Global Ecology and Biogeography, **29**:9, 1554–1564.

Leahy, S. M., Kingsford, M. J., & Steinberg, C. R. (2013). Do Clouds Save the Great Barrier Reef? Satellite Imagery Elucidates the Cloud-SST Relationship at the Local Scale. PLOS ONE, **8**:7.

Leggat, W., Gierz, S., Hernandez-Agreda, A., & Ainsworth, T. D. (2019). The Mesophotic Coral Microbial Biosphere (pp. 493–505).

Leichter J. J., Helmuth B., Fischer A. M. (2006). Variation beneath the surface: Quantifying complex thermal environments on coral reefs in the Caribbean, Bahamas and Florida. J Mar Res, **64**:563–588.

Leichter J. J., Stokes M. D., Genovese S. J. (2008). Deep water macroalgal communities adjacent to the Florida Keys reef tract. Mar Ecol Prog Ser, **356**:123–138.

Leichter J. J., Stokes M. D., Hench J. L., Witting J., Washburn L. (2012). The island-scale internal wave climate of Moorea, French Polynesia. J Geophys Res Ocean, **117**:6.

Leichter, J. J., Stewart, H. L., & Miller, S. L. (2003). Episodic nutrient transport to Florida coral reefs. Limnology and Oceanography, **48**:4, 1394–1407.

Lesser M. P., Slattery M., Leichter J. J. (2009). Ecology of mesophotic coral reefs. J Exp Mar Bio Ecol, **375**:1–8.

Levy, O., Fernandes de Barros Marangoni, L., I. C. Benichou, J., Rottier, C., Béraud, E., Grover, R., & Ferrier-Pagès, C. (2020). Artificial light at night (ALAN) alters the physiology and biochemistry of symbiotic reef building corals. Environmental Pollution, **266**, 114987.

Lirman D., Schopmeyer S., Manzello D., Gramer L. J., Precht W. F., Muller-Karger F., Banks K., Barnes B., Bartels E., Bourque A., Byrne J., Donahue S., Duquesnel J., Fisher L.,

Gilliam D., Hendee J., Johnson M., Maxwell K., McDevitt E., Monty J., Rueda D., Ruzicka R., Thanner S. (2011). Severe 2010 cold-water event caused unprecedented mortality to corals of the Florida reef tract and reversed previous survivorship patterns. PLoS One, **6**:

Little, A. F., Van Oppen, M. J., & Willis, B. L. (2004). Flexibility in algal endosymbioses shapes growth in reef corals. Science, **304**:5676, 1492–1494.

Locarnini R. A., Mishonov A. V., Antonov J. I., Boyer T. P., Garcia H. E. (2006). In: Levitus S (ed) World ocean atlas 2005, volume 1: temperature, vol 61, NOAA Atlas NESDIS. US Government Printing Office, Washington, DC.

Logan, C. A., Dunne, J. P., Ryan, J. S., Baskett, M. L., & Donner, S. D. (2021). Quantifying global potential for coral evolutionary response to climate change. Nature Climate Change 2021, **11**:6, 537–542.

Lohr, K. E., & Patterson, J. T. (2017). Intraspecific variation in phenotype among nursery-reared staghorn coral Acropora cervicornis (Lamarck, 1816). Journal of Experimental Marine Biology and Ecology, **486**, 87–92.

Loya Y., Eyal G., Treibitz T., Lesser M. P., Appeldoorn R. (2016). Theme section on mesophotic coral ecosystems: advances in knowledge and future perspectives. Coral Reefs, **35**:1–9.

Lyndby N., Holm J. B., Wangpraseurt D., Grover R., Rottier C., Kühl M., Ferrier-Pagès C. (2018). Effect of feeding and thermal stress on photosynthesis, respiration and the carbon budget of the scleractinian coral Pocillopora damicornis. bioRxiv, **378059**:

Maliao, R. J., Turingan, R. G., & Lin, J. (2008). Phase-shift in coral reef communities in the Florida Keys National Marine Sanctuary (FKNMS), USA. Marine Biology, **154**:5, 841–853.

Manzello D. P. (2015). Rapid Recent Warming of Coral Reefs in the Florida Keys. Sci Rep, **5**:1–10.

Manzello, D. P. (2015). Rapid recent warming of coral reefs in the Florida Keys. Scientific reports, **5**:1, 1–10.

Marshall B., Biscoe P. V. (1980). A model for c3 leaves describing the dependence of net photosynthesis on irradiance: II. Application to the analysis of flag leaf photosynthesis. J Exp Bot, **31**:41–48.

Martell, H. A. (2023). Thermal priming and bleaching hormesis in the staghorn coral, Acropora cervicornis (Lamarck 1816). Journal of Experimental Marine Biology and Ecology, **560**:151820.

Masiri, I., Nunez, M., & Weller, E. (2008). International Journal of Remote Sensing A 10-year climatology of solar radiation for the Great Barrier Reef: implications for recent mass coral bleaching events A 10-year climatology of solar radiation for the Great Barrier Reef: implications for recent mass coral bleaching events.

McClanahan, T. R., Ateweberhan, M., Muhando, C. A., Maina, J., & Mohammed, M. S. (2007). Effects of climate and seawater temperature variation on coral bleaching and mortality. *Ecological monographs*, **77**:4, 503–525.

McClanahan, T. R., Darling, E. S., Maina, J. M., Muthiga, N. A., 'agata, S. D., Jupiter, S. D., ... & Leblond, J. (2019). Temperature patterns and mechanisms influencing coral bleaching during the 2016 El Niño. Nature Climate Change, **9**:11, 845–851.

McClanahan, T., Darling, E., Maina, J., Muthiga, N., D'agata, S., Leblond, J., Arthur, R., Jupiter, S., Wilson, S., Mangubhai, S., Ussi, A., Guillaume, M., Humphries, A., Patankar, V., Shedrawi, G., Pagu, J., & Grimsditch, G. (2020). Highly variable taxa-specific coral bleaching responses to thermal stresses. Marine Ecology Progress Series, **648**:135–151.

McIlroy S. E., Thompson P. D., Yuan F. L., Bonebrake T. C., Baker D. M. (2019). Subtropical thermal variation supports persistence of corals but limits productivity of coral reefs. Proc R Soc B Biol Sci, **286**:

Menza C.O., Kendall M., Rogers C., Miller J. (2007). A deep reef in deep trouble. Continental Shelf Research, **27**:2224–2230.

MEP. (2007). Marine environmental program annual report, 2006–2007. Bermuda Institute of Ocean Sciences, 80pp.

Middlebrook, R., Hoegh-Guldberg, O., & Leggat, W. (2008). The effect of thermal history on the susceptibility of reef-building corals to thermal stress. Journal of Experimental Biology, **211**:7, 1050–1056.

Million, W. C., Ruggeri, M., O'Donnell, S., Bartels, E., Conn, T., Krediet, C. J., & Kenkel, C. D. (2022). Evidence for adaptive morphological plasticity in the Caribbean coral, Acropora cervicornis. Proceedings of the National Academy of Sciences, **119**:49.

Mohamed, H. F., Chen, Y., Abd-Elgawad, A., Cai, R., & Xu, C. (2022). The Unseen Drivers of Coral Health; Coral Microbiome; The Hope for Effective Coral Restoration. Polish Journal of Environmental Studies, **31**:2.

Montefalcone, M., Morri, C., & Bianchi, C. N. (2018). Long-term change in bioconstruction potential of Maldivian coral reefs following extreme climate anomalies. Global change biology, **24**:12, 5629–5641.

Moore, J. A. Y., Bellchambers, L. M., Depczynski, M. R., Evans, R. D., Evans, S. N., Field, S. N., Friedman, K. J., Gilmour, J. P., Holmes, T. H., Middlebrook, R., Radford, B. T., Ridgway, T., Shedrawi, G., Taylor, H., Thomson, D. P., & Wilson, S. K. (2012). Unprecedented mass bleaching and loss of coral across 12° of latitude in Western Australia in 2010–11. PLoS ONE, **7**:12.

Moulding, A., & Ladd, M. (2022). Staghorn coral (Acropora cervicornis), elkhorn coral (Acropora palmata), lobed star coral (Orbicella annularis), mountainous star coral (Orbicella faveolata), boulder star coral (Orbicella franksi), rough cactus coral (Mycetophyllia ferox), and pillar coral (Dendrogyra cylindrus) 5-year review.

Muehllehner, N. (2013). The relationship between carbonate chemistry and calcification on the florida reef tract, and in the symbiotic reef coral, acropora cervicornis. PhD diss., University of Miami.

Muller, E. M., Bartels, E., & Baums, I. B. (2018). Bleaching causes loss of disease resistance within the threatened coral species Acropora cervicornis. Elife, **7**:

Mumby, P. J., Chisholm, J. R. M., Edwards, A. J., Andrefouet, S., & Jaubert, J. (2001). Cloudy weather may have saved Society Island reef corals during the 1998 ENSO event. Marine Ecology Progress Series, **222**:209–216.

Muñiz-Castillo A. I., Rivera-Sosa A., Chollett I., Eakin C. M., Andrade-Gómez L., McField M., Arias-González J. E. (2019). Three decades of heat stress exposure in Caribbean coral reefs: a new regional delineation to enhance conservation. Sci Rep, **9**:

Muñiz-Castillo, A. I., & Arias-González, J. E. (2021). Drivers of coral bleaching in a Marine Protected Area of the Southern Gulf of Mexico during the 2015 event. Marine Pollution Bulletin, **166**:112256.

Murdoch, T. J., & Aronson, R. B. (1999). Scale-dependent spatial variability of coral assemblages along the Florida Reef Tract. Coral Reefs, **18**:341–351.

Muscatine, L., R. McCloskey, L., & E. Marian, R. (1981). Estimating the daily contribution of carbon from zooxanthellae to coral animal respiration1. Limnology and Oceanography, **26**:4, 601–611.

Naumann M. S., Niggl W., Laforsch C., Glaser C., Wild C. (2009). Coral surface area quantification-evaluation of established techniques by comparison with computer tomography. Coral Reefs, **28**:109–117.

Nelson, D. R., Adger, W. N., & Brown, K. (2007). Adaptation to environmental change: contributions of a resilience framework. Annual review of Environment and Resources, **32**:1, 395–419.

O'Donnell, K. E., Lohr, K. E., Bartels, E., Baums, I. B., & Patterson, J. T. (2018). Acropora cervicornis genet performance and symbiont identity throughout the restoration process. Coral Reefs, **37**:4, 1109–1118.

O'Neil, K. (2015). Land-Based Coral Nurseries: A Valuable Tool for Production and Transplantation of Acropora cervicornis. HCNSO Student Theses and Dissertations.

Oksanen, J., Kindt, R., Legendre, P., O'hara, B., Stevens, M. H. H., Oksanen, M. J., & Suggests, M. A. S. S. (2007). The vegan package: community ecology package. R package version, **1**:1–190.

Olito, C., White, C. R., Marshall, D. J., & Barneche, D. R. (2017). Estimating monotonic rates from biological data using local linear regression. The Journal of Experimental Biology, **220**:5, 759–764.

Oliver T. A., Palumbi S. R. (2011). Do fluctuating temperature environments elevate coral thermal tolerance? Coral Reefs, **30**:429–440.

Oliver, E. C. J., Donat, M. G., Burrows, M. T., Moore, P. J., Smale, D. A., Alexander, L. v., Benthuysen, J. A., Feng, M., sen Gupta, A., Hobday, A. J., Holbrook, N. J., Perkins-Kirkpatrick, S. E., Scannell, H. A., Straub, S. C., & Wernberg, T. (2018). Longer and more frequent marine heatwaves over the past century. Nature Communications, **9**:1.

Oliver, J. K., Berkelmans, R., & Eakin, C. M. (2018). Coral bleaching in space and time. Coral bleaching: patterns, processes, causes and consequences. Ecological Studies JM (ed.), 139–158.

Oxenford, H. A., & Vallès, H. (2016). Transient turbid water mass reduces temperature-induced coral bleaching and mortality in Barbados. PeerJ, **4**:6.

Padfield D., Yvon-Durocher G., Buckling A., Jennings S., Yvon-Durocher G. (2016). Rapid evolution of metabolic traits explains thermal adaptation in phytoplankton. Ecol Lett, **19**:133–142.

Padfield, D., O'sullivan, H., & Pawar, S. (2021). rTPC and nls.multstart: a new pipeline to fit thermal performance curves in R. Methods in Ecology and Evolution, **12**:6, 1138–1143.

Padilla-Gamiño, J. L., Roth, M. S., Rodrigues, L. J., Bradley, C. J., Bidigare, R. R., Gates, R. D., Smith, C. M., & Spalding, H. L. (2019). Ecophysiology of mesophotic reef-building corals in Hawai'i is influenced by symbiont–host associations, photoacclimatization, trophic plasticity, and adaptation. Limnology and Oceanography, **64**:5, 1980–1995.

Pausch, R. E., Williams, D. E., & Miller, M. W. (2018). Impacts of fragment genotype, habitat, and size on outplanted elkhorn coral success under thermal stress. Marine Ecology Progress Series, **592**:109–117.

Pigliucci, M. (2005). Evolution of phenotypic plasticity: where are we going now?. Trends in ecology & evolution, **20**:9, 481–486.

Pinheiro H. T., Eyal G., Shepherd B., Rocha L. A. (2019). Ecological insights from environmental disturbances in mesophotic coral ecosystems. Ecosphere, **10**:1–6.

Piniak, G. A. (2002). Effects of symbiotic status, flow speed, and prey type on prey capture by the facultatively symbiotic temperate coral Oculina arbuscula. Marine Biology, **141**:449–455.

Porter, J. W., & Meier, O. W. (1992). Quantification of loss and change in Floridian reef coral populations. American Zoologist, **32**:6, 625–640.

Prasetia R., Sinniger F., Hashizume K., Harii S. (2017). Reproductive biology of the deep brooding coral Seriatopora hystrix: Implications for shallow reef recovery. PLoS One, **12**:

Precht W. F., Aronson R. B., Deslarzes K. J., Robbart M. L., Evans D. J., Zimmer B., & Duncan L. (2008). Long-Term Monitoring at the East and West Flower Garden Banks, 2004–2005-Interim Report, Volume 1: Technical Report.

Precht W. F., Aronson R. B., Gardner T. A., Gill J. A., Hawkins J. P., Hernández-Delgado E. A., Jaap W. C., McClanahan T. R., McField M. D., Murdoch T. J. T., Nugues M. M., Roberts C. M., Schelten C. K., Watkinson A. R., Côté I. M. (2020). The timing and causality of

ecological shifts on Caribbean reefs. Advances in Marine Biology. Academic Press, pp 331–360.

Precht, W. F., & Miller, S. L. (2007). Ecological shifts along the Florida reef tract: the past as a key to the future. Geological approaches to coral reef ecology, 237–312.

Precht, W. F., Gintert, B. E., Robbart, M. L., Fura, R., & Van Woesik, R. (2016). Unprecedented disease-related coral mortality in Southeastern Florida. Scientific reports, **6**:1, 1–11.

Putnam H. M., Gates R. D. (2015). Preconditioning in the reef-building coral Pocillopora damicornis and the potential for trans-generational acclimatization in coral larvae under future climate change conditions. J Exp Biol, **218**:2365–2372.

Putnam, H. M. (2021). Avenues of reef-building coral acclimatization in response to rapid environmental change. Journal of Experimental Biology, **224**:

Putnam, H. M., Barott, K. L., Ainsworth, T. D., & Gates, R. D. (2017). The vulnerability and resilience of reef-building corals. Current Biology, **27**:11, R528–R540.

Randall C. J., Toth L. T., Leichter J. J., Maté J. L., Aronson R. B. (2020). Upwelling buffers climate change impacts on coral reefs of the eastern tropical Pacific. Ecology, **101**:2.

Reich H. G., Robertson D. L., Goodbody-Gringley G. (2017). Do the shuffle: Changes in Symbiodinium consortia throughout juvenile coral development. PLoS One, **12**:

Richmond, R. H., & Hunter, C. L. (1990). Reproduction and recruitment of corals: comparisons among the Caribbean, the tropical Pacific, and the Red Sea. Marine ecology progress series. Oldendorf, **60**:1, 185–203.

Roch, C., Schmidt-Roach, S., & Duarte, C. M. (2023). Coral restoration patents are disconnected from academic research and restoration practitioners.

Rocha L. A., Pinheiro H. T., Shepherd B., Papastamatiou Y. P., Luiz O. J., Pyle R. L., Bongaerts P. (2018). Mesophotic coral ecosystems are threatened and ecologically distinct from shallow water reefs. Science, **361**:281–284.

Rodolfo-Metalpa, R., Huot, Y., & Ferrier-Pagès, C. (2008). Photosynthetic response of the Mediterranean zooxanthellate coral Cladocora caespitosa to the natural range of light and temperature. Journal of Experimental Biology, **211**:10, 1579–1586.

Rogers, C. S. (1979). The effect of shading on coral reef structure and function.

Ruzicka, R. R., Colella, M. A., Porter, J. W., Morrison, J. M., Kidney, J. A., Brinkhuis, V., ... & Colee, J. (2013). Temporal changes in benthic assemblages on Florida Keys reefs 11 years after the 1997/1998 El Niño. Marine Ecology Progress Series, **489**:125–141.

Sangmanee, K., Casareto, B. E., Nguyen, T. D., Sangsawang, L., Toyoda, K., Suzuki, T., & Suzuki, Y. (2020). Influence of thermal stress and bleaching on heterotrophic feeding of two scleractinian corals on pico-nanoplankton. Marine Pollution Bulletin, **158**:111405.

Savage A. M., Trapido-Rosenthal H., Douglas A. E. (2002). On the functional significance of molecular variation in Symbiodinium, the symbiotic algae of Cnidaria: Photosynthetic response to irradiance. Mar Ecol Prog Ser, **244**:27–37.

Sawall Y., Al-Sofyani A., Hohn S., Banguera-Hinestroza E., Voolstra C. R., Wahl M. (2015). Extensive phenotypic plasticity of a Red Sea coral over a strong latitudinal temperature gradient suggests limited acclimatization potential to warming. Sci Rep, **5**:8940.

Scheiner, S. M. (1993). Plasticity as a selectable trait: reply to Via. The American Naturalist, **142**:2, 371–373.

Scheufen T., Krämer W. E., Iglesias-Prieto R., Enriquez S. (2017). Seasonal variation modulates coral sensibility to heat-stress and explains annual changes in coral productivity. Sci Rep, **7**:4937.

Schmidt-Roach, S., Duarte, C. M., Hauser, C. A., & Aranda, M. (2020). Beyond reef restoration: next-generation techniques for coral gardening, landscaping, and outreach. Frontiers in Marine Science, **672**.

Schoepf V., Grottoli A. G., Levas S. J., Aschaffenburg M. D., Baumann J. H., Matsui Y., Warner M. E. (2015). Annual coral bleaching and the long-term recovery capacity of coral. Proceedings of the Royal Society B: Biological Sciences, **282**:1819, 20151887.

Schoolfield R. M., Sharpe P. J. H., Magnuson C. E. (1981). Non-linear regression of biological temperature-dependent rate models based on absolute reaction-rate theory. J Theor Biol, **88**:719–731.

Schopmeyer S. A., Lirman D., Bartels E., Byrne J., Gilliam D. S., Hunt J., Johnson M. E., Larson E. A., Maxwell K., Nedimyer K., Walter C. (2012). In Situ Coral Nurseries Serve as Genetic Repositories for Coral Reef Restoration after an Extreme Cold-Water Event. Restor Ecol, **20**:696–703.

Schulte P. M., Healy T. M., Fangue N.A. (2011). Thermal performance curves, phenotypic plasticity, and the time scales of temperature exposure. Integr Comp Biol, **51**:691–702.

Schutte V. G. W., Selig E. R., Bruno J. F. (2010). Regional spatio-temporal trends in Caribbean coral reef benthic communities. Mar Ecol Prog Ser, **402**:115–122.

Seebacher, F., Holmes, S., Roosen, N. J., Nouvian, M., Wilson, R. S., & Ward, A. J. (2012). Capacity for thermal acclimation differs between populations and phylogenetic lineages within a species. Functional Ecology, **26**:6, 1418–1428.

Seebacher, F., White, C. R., & Franklin, C. E. (2015). Physiological plasticity increases resilience of ectothermic animals to climate change. Nature Climate Change, **5**:1, 61–66.

Selig, E. R., & Bruno, J. F. (2010). A global analysis of the effectiveness of marine protected areas in preventing coral loss. PLos one, **5**:2.

Selig, E. R., Casey, K. S., & Bruno, J. F. (2012). Temperature-driven coral decline: the role of marine protected areas. Global Change Biology, **18**:5, 1561–1570.

sen Gupta, A., Thomsen, M., Benthuysen, J. A., Hobday, A. J., Oliver, E., Alexander, L. v., Burrows, M. T., Donat, M. G., Feng, M., Holbrook, N. J., Perkins-Kirkpatrick, S., Moore, P. J., Rodrigues, R. R., Scannell, H. A., Taschetto, A. S., Ummenhofer, C. C., Wernberg, T., & Smale, D. A. (2020). Drivers and impacts of the most extreme marine heatwaves events. Scientific Reports, **10**:1.

Serrano X. M., Baums I. B., O'Reilly K., Smith T. B., Jones R. J., Shearer T. L., Nunes F. L. D., Baker A. C. (2014). Geographic differences in vertical connectivity in the Caribbean coral Montastraea cavernosa despite high levels of horizontal connectivity at shallow depths. Mol Ecol, **23**:4226–4240.

Serrano X. M., Baums I. B., Smith T. B., Jones R. J., Shearer T. L., Baker A. C. (2016). Long distance dispersal and vertical gene flow in the Caribbean brooding coral Porites astreoides. Sci Rep, **6**:21619.

Sharpe P. J. H., DeMichele D. W. (1977). Reaction kinetics of poikilotherm development. J Theor Biol, **64**:649–670.

Sheppard C., Sheppard A., Fenner D. (2020). Coral mass mortalities in the Chagos Archipelago over 40 years: Regional species and assemblage extinctions and indications of positive feedbacks. Mar Pollut Bull, **154**:111075.

Shinn, E. (1963). Spur and groove formation on the Florida reef tract. Journal of Sedimentary Research, **33**:2, 291–303.

Shinn, E. A., Hudson, J. H., Robbin, D. M., & Lidz, B. H. (1982). Spurs and grooves revisited: construction versus erosion, Looe Key Reef, Florida.

Shinn, E. A., Reich, C. D., Hickey, T. D., & Lidz, B. H. (2003). Staghorn tempestites in the Florida Keys. Coral Reefs, **22**:91–97.

Silbiger N. J., Goodbody-Gringley G., Bruno J. F., Putnam H. M. (2019). Comparative thermal performance of the reef-building coral Orbicella franksi at its latitudinal range limits. Mar Biol, **166**:1–14.

Simpson, G. G. (1953). The baldwin effect. Evolution, **7**:2, 110–117.

Sinclair, B. J., Marshall, K. E., Sewell, M. A., Levesque, D. L., Willett, C. S., Slotsbo, S., Dong, Y., Harley, C. D. G., Marshall, D. J., Helmuth, B. S., & Huey, R. B. (2016). Can we predict ectotherm responses to climate change using thermal performance curves and body temperatures? Ecology Letters, **19**:11, 1372–1385.

Slattery, M., Lesser, M. P., Brazeau, D., Stokes, M. D., & Leichter, J. J. (2011). Connectivity and stability of mesophotic coral reefs. *Journal of Experimental Marine Biology and Ecology*, **408**:1–2, 32–41.

Smale, D. A., Wernberg, T., Oliver, E. C. J., Thomsen, M., Harvey, B. P., Straub, S. C., Burrows, M. T., Alexander, L. v., Benthuysen, J. A., Donat, M. G., Feng, M., Hobday, A. J., Holbrook, N. J., Perkins-Kirkpatrick, S. E., Scannell, H. A., sen Gupta, A., Payne, B. L., & Moore, P. J. (2019). Marine heatwaves threaten global biodiversity and the provision of ecosystem services. Nature Climate Change 2019, **9**:4, 306–312.

Smith S., Sarkis S., Murdoch T., Weil E., Croquer A., Bates N., Johnson R., de Putron S., Andersson A. (2013a). Threats to Coral Reefs of Bermuda. In: Sheppard C, editor. Coral Reefs of the United Kingdom Overseas Territories. Dordrecht: Springer Science+Business Media; pp. 173–188.

Smith T. B., Brandt M. E., Calnan J. M., Nemeth R. S., Blondeau J., Kadison E., Taylor M., Rothenberger P. (2013b). Convergent mortality responses of Caribbean coral species to seawater warming. Ecosphere, **4**:87.

Smith T. B., Gyory J., Brandt M. E., Miller W. J., Jossart J., Nemeth R. S. (2016) Caribbean mesophotic coral ecosystems are unlikely climate change refugia. Glob Chang Biol, **22**:2756–2765.

Smith T. B., Nemeth R. S., Blondeau J., Calnan J. M., Kadison E., Herzlieb S. (2008). Assessing coral reef health across onshore to offshore stress gradients in the US Virgin Islands. Mar Pollut Bull, **56**:1983–1991.

Smith, E. G., Hazzouri, K. M., Choi, J. Y., Delaney, P., Al-Kharafi, M., Howells, E. J., Aranda, M., & Burt, J. A. (2022). Signatures of selection underpinning rapid coral adaptation to the world's warmest reefs. In Sci. Adv, **8**:

Smith, K. E., Burrows, M. T., Hobday, A. J., Gupta, A. sen, Moore, P. J., Thomsen, M., Wernberg, T., & Smale, D. A. (2021). Socioeconomic impacts of marine heatwaves: Global issues and opportunities. Science, **374**:6566.

Smith, L. W., Barshis, D., & Birkeland, C. (2007). Phenotypic plasticity for skeletal growth, density and calcification of Porites lobata in response to habitat type. Coral Reefs, **26**:559–567.

Smith, T. B., Glynn, P. W., Maté, J. L., Toth, L. T., & Gyory, J. (2014). A depth refugium from catastrophic coral bleaching prevents regional extinction. Ecology, **95**:6, 1663–1673.

Solé-Cava, A. D., & Thorpe, J. P. (1991). High levels of genetic variation in natural populations of marine lower invertebrates. Biological Journal of the Linnean Society, **44**:1, 65–80.

Somerfield, P. J., Jaap, W. C., Clarke, K. R., Callahan, M., Hackett, K., Porter, J., ... & Yanev, G. (2008). Changes in coral reef communities among the Florida Keys, 1996–2003. Coral Reefs, **27**:951–965.

Sorokin, Y. (2013). Coral Reef Ecology - Yuri I. Sorokin - Google Books. Springer Science & Business Media.

Spalding, M., Burke, L., Wood, S. A., Ashpole, J., Hutchison, J., & zu Ermgassen, P. (2017). Mapping the global value and distribution of coral reef tourism. Marine Policy, **82**:104–113.

Spitze, K., & Sadler, T. D. (1996). Evolution of a generalist genotype: multivariate analysis of the adaptiveness of phenotypic plasticity. The American Naturalist, 148, S108–S123.Smith, L. W., Barshis, D., & Birkeland, C. (2007). Phenotypic plasticity for skeletal growth, density and calcification of Porites lobata in response to habitat type. Coral Reefs, **26**: 559–567.

Stefanoudis, Paris V., Molly Rivers, Struan R. Smith, Craig W. Schneider, Daniel Wagner, Helen Ford, Alex D. Rogers, and Lucy C. Woodall. "Low connectivity between shallow, mesophotic and rariphotic zone benthos." *Royal Society Open Science*, **6**:9.

Studivan M. (2018) Genetic Connectivity and Phenotypic Plasticity of Shallow and Mesophotic Coral Ecosystems in the Gulf of Mexico. ProQuest Diss Theses 256Titlyanov EA, Titlyanova TV, Yamazato K, van Woesik R (2001). Photo- acclimation dynamics of the coral Stylophora pistillata to low and extremely low light. J Exp Mar Biol Ecol, **263**:211–225.

Sweet, M. J., & Brown, B. E. (2016). Coral responses to anthropogenic stress in the twenty-first century: an ecophysiological perspective. Oceanography and Marine Biology, 279–322.

Szmant, A. M., & Forrester, A. (1996). Water column and sediment nitrogen and phosphorus distribution patterns in the Florida Keys, USA. Coral Reefs, **15**: 21–41.

Takahashi, S., Nakamura, T., Sakamizu, M., van Woesik, R., & Yamasaki, H. (2004). Repair Machinery of Symbiotic Photosynthesis as the Primary Target of Heat Stress for Reef-Building Corals. Plant and Cell Physiology, **45**:2, 251–255.

Tanzil, J. T., Brown, B. E., Dunne, R. P., Lee, J. N., Kaandorp, J. A., & Todd, P. A. (2013). Regional decline in growth rates of massive Porites corals in Southeast Asia. Global change biology, **19**:10, 3011–3023.

Therneau, T., & Lumley, T. (2010). Survival: survival analysis, including penalized likelihood. R package version 2.35–4. R Found, Stat. Comput.

Thomas L., Rose N. H., Bay R. A., López E. H., Morikawa M. K., Ruiz-Jones L., Palumbi S. R. (2018). Mechanisms of Thermal Tolerance in Reef-Building Corals across a Fine-Grained Environmental Mosaic: Lessons from Ofu, American Samoa. Front Mar Sci, **4**:434.

Thomas, L., Kennington, W. J., Evans, R. D., Kendrick, G. A., & Stat, M. (2017). Restricted gene flow and local adaptation highlight the vulnerability of high-latitude reefs to rapid environmental change. Global Change Biology, **23**:6, 2197–2205.

Thompson, D. M., & Van Woesik, R. (2009). Corals escape bleaching in regions that recently and historically experienced frequent thermal stress. *Proceedings of the Royal Society B: Biological Sciences*, **276**:1669, 2893–2901.

Thornhill, D. J., LaJeunesse, T. C., Kemp, D. W., Fitt, W. K., & Schmidt, G. W. (2006). Multi-year, seasonal genotypic surveys of coral-algal symbioses reveal prevalent stability or post-bleaching reversion. Marine Biology, **148**:711–722.

Thornhill, D. J., Xiang, Y. U., Fitt, W. K., & Santos, S. R. (2009). Reef endemism, host specificity and temporal stability in populations of symbiotic dinoflagellates from two ecologically dominant Caribbean corals. PloS one, **4**:7.

Todd, P. A. (2008). Morphological plasticity in scleractinian corals. Biological reviews, **83**:3, 315–337.

Toth, L. T., Kuffner, I. B., Stathakopoulos, A., & Shinn, E. A. (2018). A 3,000-year lag between the geological and ecological shutdown of Florida's coral reefs. Global change biology, **24**:11, 5471–5483.

Toth, L. T., Stathakopoulos, A., Kuffner, I. B., Ruzicka, R. R., Colella, M. A., & Shinn, E. A. (2019). The unprecedented loss of Florida's reef-building corals and the emergence of a novel coral-reef assemblage. Ecology, **100**:9.

Turner J. A., Andradi-Brown D. A., Gori A., Bongaerts P., Burdett H. L., Ferrier-Pagès C., Voolstra C. R., Weinstein D. K., Bridge T. C. L., Costantini F., Gress E., Laverick J., Loya Y., Goodbody-Gringley G., Rossi S., Taylor M. L., Viladrich N., Voss J. D., Williams J., Woodall L. C., Eyal G. (2019). Key Questions for Research and Conservation of Mesophotic Coral Ecosystems and Temperate Mesophotic Ecosystems. Coral Reefs of the World. pp 989–1003.

Turner J. A., Thomson D. P., Cresswell A. K., Trapon M., Babcock R. C. (2018). Depth-related patterns in coral recruitment across a shallow to mesophotic gradient. Coral Reefs, **37**:711–722.

Valladares, F., Matesanz, S., Guilhaumon, F., Araújo, M. B., Balaguer, L., Benito-Garzón, M., ... & Zavala, M. A. (2014). The effects of phenotypic plasticity and local adaptation on forecasts of species range shifts under climate change. Ecology letters, **17**:11, 1351–1364.

van Oppen, M. J. H., Oliver, J. K., Putnam, H. M., & Gates, R. D. (2015). Building coral reef resilience through assisted evolution. In Proceedings of the National Academy of Sciences of the United States of America (Vol. 112, Issue 8, pp. 2307–2313). National Academy of Sciences.

van Oppen, M. J., Bongaerts, P. I. M., Underwood, J. N., Peplow, L. M., & Cooper, T. F. (2011). The role of deep reefs in shallow reef recovery: an assessment of vertical connectivity in a brooding coral from west and east Australia. *Molecular ecology*, *20*(8), 1647-1660. Bridge, Tom CL, Terry P. Hughes, John M. Guinotte, and Pim Bongaerts. "Call to protect all coral reefs." *Nature Climate Change*, **3**:6, 528–530.

van Oppen, M. J., Gates, R. D., Blackall, L. L., Cantin, N., Chakravarti, L. J., Chan, W. Y., ... & Putnam, H. M. (2017). Shifting paradigms in restoration of the world's coral reefs. Global change biology, **23**:9, 3437–3448.

van Os, N., Massé, L. M., Séré, M. G., Sara, J. R., Schoeman, D. S., & Smit, A. J. (2011). Influence of heterotrophic feeding on the survival and tissue growth rates of Galaxea fascicularis (Octocorralia: Occulinidae) in aquaria. Aquaculture, **330**:156–161.

van Woesik, R., & Kratochwill, C. (2022). A global coral-bleaching database, 1980–2020. Scientific Data, **9**:1, 1–7.

van Woesik, R., Banister, R. B., Bartels, E., Gilliam, D. S., Goergen, E. A., Lustic, C., ... & Lirman, D. (2021). Differential survival of nursery-reared Acropora cervicornis outplants along the Florida reef tract. Restoration ecology, **29**:1.

Veal, C. J., Carmi, M., Dishon, G., Sharon, Y., Michael, K., Tchernov, D., Hoegh-Guldberg, O., & Fine, M. (2010). Shallow-water wave lensing in coral reefs: a physical and biological case study. Journal of Experimental Biology, **213**:24, 4304–4312.

Vermeij, M. J., Sandin, S. A., & Samhouri, J. F. (2007). Local habitat distribution determines the relative frequency and interbreeding potential for two Caribbean coral morphospecies. Evolutionary Ecology, **21**: 27–47.

Voolstra, C. R., Suggett, D. J., Peixoto, R. S., Parkinson, J. E., Quigley, K. M., Silveira, C. B., ... & Aranda, M. (2021). Extending the natural adaptive capacity of coral holobionts. Nature Reviews Earth & Environment, **2**:11, 747–762.

Wall, C. (2016). Symbiodinium counts in coral tissue protocol. In Dr. Ruth Gates' Laboratory Hawaii Institute of Marine Biology.

Wall, C. B., Fan, T.-Y., & Edmunds, P J. (2014). Ocean acidification has no effect on thermal bleaching in the coral Seriatopora caliendrum. Coral Reefs, **33**:119–130.

Walton, C. J., Hayes, N. K., & Gilliam, D. S. (2018). Impacts of a regional, multi-year, multi-species coral disease outbreak in Southeast Florida. Frontiers in Marine Science, **5**:323.

Ware, M. (2015). Assessment of Nursery-Raised Acropora cervicornis Transplants in the Upper Florida Keys. 380.

Warner, M. E., Fitt, W. K., & Schmidt, G. W. (1999). Damage to photosystem II in symbiotic dinoflagellates: A determinant of coral bleaching. Proceedings of the National Academy of Sciences, **96**:14, 8007–8012.

Warner, R. R. (1997). Evolutionary ecology: how to reconcile pelagic dispersal with local adaptation. Coral Reefs, **16**:S115–S120.

West J. M., Salm R. V. (2003). Resistance and Resilience to Coral Bleaching: Implications for Coral Reef Conservation and Management. Conserv Biol, **17**:956–967.

West-Eberhard, M. J. (1989). Phenotypic plasticity and the origins of diversity. Annual review of Ecology and Systematics, **20**:1, 249–278.

Westoby, R., Becken, S., & Laria, A. P. (2020). Perspectives on the human dimensions of coral restoration. Regional Environmental Change, **20**:4, 1–13.

Wijgerde, T., Diantari, R., Lewaru, M. W., Verreth, J. A. J., & Osinga, R. (2011). Extracoelenteric zooplankton feeding is a key mechanism of nutrient acquisition for the scleractinian coral Galaxea fascicularis. Journal of Experimental Biology, **214**:20, 3351–3357.

Wijgerde, T., Spijkers, P., Karruppannan, E., Verreth, J. A. J., & Osinga, R. (2012). Water Flow Affects Zooplankton Feeding by the Scleractinian Coral Galaxea fascicularis on a Polyp and Colony Level. Journal of Marine Biology, **2012**:1–7.

Williams, G. J., Knapp, I. S., Maragos, J. E., & Davy, S. K. (2010). Modeling patterns of coral bleaching at a remote Central Pacific atoll. *Marine Pollution Bulletin*, **60**:9, 1467–1476.

Woodhead, A. J., Hicks, C. C., Norström, A. v, Gareth, |, Williams, J., & Graham, N. A. J. (2019). Coral reef ecosystem services in the Anthropocene. Functional Ecology, **33**:1023–1034.

Wooldridge, S. A. (2014). Formalising a mechanistic linkage between heterotrophic feeding and thermal bleaching resistance.

Wyatt A. S. J., Leichter J. J., Toth L. T., Miyajima T., Aronson R. B., Nagata T. (2019). Heat accumulation on coral reefs mitigated by internal waves. Nat Geosci, **18**:1–7.

Yetsko, K., Ross, M., Bellantuono, A., Merselis, D., Lanetty, M. R., & Gilg, M. R. (2020). Genetic differences in thermal tolerance among colonies of threatened coral Acropora cervicornis: potential for adaptation to increasing temperature. Marine Ecology Progress Series, **646**:45–68.

Yost D. M., Jones R., Rowe C. L., Mitchelmore C. L. (2012). Quantification of total and particulate dimethylsulfoniopropionate (DMSP) in five Bermudian coral species across a depth gradient. Coral Reefs, **31**:561–570.

Young, C. N., Schopmeyer, S. A., & Lirman, D. (2012). A review of reef restoration and Coral propagation using the threatened genus Acropora in the Caribbean and western Atlantic. Bulletin of Marine Science, **88**:4,1075–1098.

Zepp, R. G., Shank, G. C., Stabenau, E., Patterson, K. W., Cyterski, M., Fisher, W., Bartels, E., & Anderson, S. L. (2008). Spatial and temporal variability of solar ultraviolet exposure of coral assemblages in the Florida Keys: Importance of colored dissolved organic matter. Limnology and Oceanography, **53**:5, 1909–1922.